EFFECT OF 5α-REDUCTASE INHIBITORS ON LNCaP CELLS, SYRIAN HAMSTER FLANK ORGANS, AND TRAMP MICE PROSTATE CANCER

by

ALEXANDER BOADU OPOKU-ACHEAMPONG

B.Sc., University of Ghana, 2005
M.S., Kansas State University, 2011

AN ABSTRACT OF A DISSERTATION

submitted in partial fulfillment of the requirements for the degree

DOCTOR OF PHILOSOPHY

Department of Human Nutrition
College of Human Ecology

KANSAS STATE UNIVERSITY
Manhattan, Kansas

2015

Abstract

The growth-inhibitory effect of saw palmetto supplements (SPS) with high long-chain fatty acids (FA)-low phytosterols (HLLP), high long-chain FA-high phytosterols (HLHP), and high medium-chain FA-low phytosterols (HMLP) was determined using androgen-sensitive LNCaP prostate cancer (PCa) cells and Syrian hamster flank organs. *In vitro*, all three SPS at high concentrations significantly decreased dihydrotestosterone-stimulated LNCaP cell number. HMLP and HLLP at high concentrations significantly decreased, but HLHP which significantly increased testosterone-stimulated LNCaP cell number. In Syrian hamsters, all three SPS treatments caused notable, but nonsignificant reduction in the difference between the left and right flank organ growth in the testosterone-, but not dihydrotestosterone-treated SPS groups. Results suggest SPS might be a mild 5-alpha-reductase (5-alpha-R) inhibitor.

The pharmaceuticals finasteride inhibits 5-alpha-R2, and dutasteride inhibits 5-alpha-R1 and 5-alpha-R2 isoenzymes. Because finasteride inhibits only 5-alpha-R2, we hypothesized that it would not be as efficacious in preventing PCa development and/or progression in TRAMP mice as dutasteride. Six-week-old C57BL/6 TRAMP x FVB male mice were randomized to control, pre- and post- finasteride and dutasteride diet groups that began at 6 and 12 weeks of age, respectively, and terminated at 20 weeks of age. Pre and post groups received drugs before and after mice were expected to develop PCa, respectively. Post-Dutasteride treatment was significantly more effective than Pre-Dutasteride; and dutasteride treatments significantly more effective than finasteride treatments in decreasing prostatic intraepithelial neoplasia progression and PCa development. The finasteride groups and the Pre-Dutasteride group had significantly increased incidence of poorly differentiated PCa versus control. Androgen receptor and Ki-67 protein, DNA fragmentation from apoptosis, 5-alpha-R1 and 5-alpha-R2 mRNA levels were

determined in mice with genitourinary weight less than 1 gram and greater than 1 gram to elucidate the discordant response in Pre-Dutasteride and finasteride groups, and Post-Dutasteride's efficacy. Results suggest the difference in genitourinary weights is influenced more by proliferation, rather than androgen receptor and apoptosis in tumor. Mice age may not be significantly important in regulating proliferation, androgen receptor and apoptosis to promote tumor growth. In conclusion, the results with 5-alpha-reductase inhibitors may support the therapeutic use of dutasteride, but not finasteride, or saw palmetto supplements.

EFFECT OF 5α-REDUCTASE INHIBITORS ON LNCaP CELLS, SYRIAN HAMSTER FLANK ORGANS, AND TRAMP MICE PROSTATE CANCER

by

ALEXANDER BOADU OPOKU-ACHEAMPONG

B.Sc., University of Ghana, 2005
M.S., Kansas State University, 2011

A DISSERTATION

submitted in partial fulfillment of the requirements for the degree

DOCTOR OF PHILOSOPHY

Department of Human Nutrition
College of Human Ecology

KANSAS STATE UNIVERSITY
Manhattan, Kansas

2015

Approved by:

Major Professor
Dr. Brian L. Lindshield

Copyright

Abstract

The growth-inhibitory effect of saw palmetto supplements (SPS) with high long-chain fatty acids (FA)-low phytosterols (HLLP), high long-chain FA-high phytosterols (HLHP), and high medium-chain FA-low phytosterols (HMLP) was determined using androgen-sensitive LNCaP prostate cancer (PCa) cells and Syrian hamster flank organs. *In vitro*, all three SPS at high concentrations significantly decreased dihydrotestosterone-stimulated LNCaP cell number. HMLP and HLLP at high concentrations significantly decreased, but HLHP which significantly increased testosterone-stimulated LNCaP cell number. In Syrian hamsters, all three SPS treatments caused notable, but nonsignificant reduction in the difference between the left and right flank organ growth in the testosterone-, but not dihydrotestosterone-treated SPS groups. Results suggest SPS might be a mild 5-alpha-reductase (5-alpha-R) inhibitor.

The pharmaceuticals finasteride inhibits 5-alpha-R2, and dutasteride inhibits 5-alpha-R1 and 5-alpha-R2 isoenzymes. Because finasteride inhibits only 5-alpha-R2, we hypothesized that it would not be as efficacious in preventing PCa development and/or progression in TRAMP mice as dutasteride. Six-week-old C57BL/6 TRAMP x FVB male mice were randomized to control, pre- and post- finasteride and dutasteride diet groups that began at 6 and 12 weeks of age, respectively, and terminated at 20 weeks of age. Pre and post groups received drugs before and after mice were expected to develop PCa, respectively. Post-Dutasteride treatment was significantly more effective than Pre-Dutasteride; and dutasteride treatments significantly more effective than finasteride treatments in decreasing prostatic intraepithelial neoplasia progression and PCa development. The finasteride groups and the Pre-Dutasteride group had significantly increased incidence of poorly differentiated PCa versus control. Androgen receptor and Ki-67 protein, DNA fragmentation from apoptosis, 5-alpha-R1 and 5-alpha-R2 mRNA levels were

determined in mice with genitourinary weight less than 1 gram and greater than 1 gram to elucidate the discordant response in Pre-Dutasteride and finasteride groups, and Post-Dutasteride's efficacy. Results suggest the difference in genitourinary weights is influenced more by proliferation, rather than androgen receptor and apoptosis in tumor. Mice age may not be significantly important in regulating proliferation, androgen receptor and apoptosis to promote tumor growth. In conclusion, the results with 5-alpha-reductase inhibitors may support the therapeutic use of dutasteride, but not finasteride, or saw palmetto supplements.

Table of Contents

List of Figures

List of Tables

Acknowledgements

First, I would like to express my sincere gratitude to my advisor Dr. Brian Lindshield for the continuous support of my doctoral study and related research, for his patience, constructive criticism, and immense knowledge. His commitment to the highest standards inspired and motivated me. His guidance helped me in all the time of research and writing of this dissertation. I appreciate his commitment to see me succeed in life, and his mentorship which provided me with a well-rounded experience consistent with my long-term career goal. Aside academics, I enjoyed the basketball and football games we attended together. I could not have imagined having a better advisor and mentor for my doctoral study.

Next, I would like to thank my other committee members, Dr. Jamie Henningson, Dr. Mark Haub, Dr. Weiqun (George) Wang, and Dr. Robin Denell. I am grateful to Dr. Henningson for the histopathological examination and scoring of mice prostate tissues, training me on immunohistochemistry, and providing access to the Kansas State Histology and Immunohistochemistry laboratory for research. I appreciate Dr. Haub's immense advice in the writing process, and his approachability which allowed me to walk up to his office anytime I had any concerns ranging from academic to personal matters. My sincere thanks goes to Dr. Wang for providing insightful comments which incented me to widen my dissertation write-up from various perspectives. My sincere appreciation goes to Dr. Robin Denell for serving as the outside chair on my committee, and for providing constructive criticism and suggestions on how to improve my dissertation.

Third, I would like to thank members of the Kansas State Histology and Immunohistochemistry laboratory, especially Jennifer Hill, for providing resources and assistance to complete my research.

Fourth, I would like to thank fellow members in Dr. Lindshield's laboratory including Kavitha Penugonda, Dave Unis, Nicole Delimont, Kristen Noriega, and Nicole Fiorentino for their contribution to the projects and the many proofreading of abstracts, Powerpoints, oral presentations and dissertation.

Last but not the least, I would like to thank my wife Audrey Anima Opoku-Acheampong for proof-reading and support, and my son Sean Nkansah Opoku-Acheampong (Seannie) for being considerate and giving me the time to complete this dissertation. To my siblings, Dora Opoku-Acheampong and Alexander Yaw Okae-Acheampong, thank you for encouraging me to reach higher academic success.

Dedication

I dedicate this dissertation to my mum, Mrs. Faustina Felicity Opoku-Acheampong who has been very pivotal in my educational career. You have dedicated your whole life to giving me the best education possible no matter the financial constraints, and I am extremely happy that you have lived to see this day. God bless you for your sacrifice, time and support.

Preface

Chapter 1 will review benign prostatic hyperplasia, prostatic intraepithelial neoplasia and prostate cancer development, clinical trials, animal and cell culture studies that have been carried out with 5α-reductase inhibitors (finasteride, dutasteride and saw palmetto supplements), major prostate cancer signaling pathways, key prostate cancer biomarkers, immunohistochemistry and *in situ* hybridization techniques for determining and quantifying biomarkers in prostate cancer. Chapters 2, 3 and 4 were written in a format intended to be submitted for publication. Chapter 2 is an investigation of the growth-inhibitory effect of saw palmetto supplements on LNCaP cell number and Syrian hamster androgen-sensitive flank organ growth. Chapter 3 is a published manuscript which investigated the preventive and therapeutic efficacy of finasteride and dutasteride in transgenic adenocarcinoma of the mouse prostate (TRAMP) mice. Chapter 4 is an investigation of the molecular changes due to finasteride and dutasteride treatment in TRAMP mice prostate cancer; and in 8, 12, 16 and 20-week-old AIN-93G-fed TRAMP mice prostate cancer. Chapter 5 is a summary of the major findings in all chapters and recommendations to improve the outcome of these research findings.

Chapter 1 - Literature Review

Introduction

Prostate cancer is the most commonly diagnosed non-skin neoplasm in men, and is projected to account for 26% of US male cancer cases in 2015. It is estimated that 1 in 7 US men will develop prostate cancer in their lifetime [1]. In the prostate, the main circulating androgen, testosterone, is converted to dihydrotestosterone (DHT) by 5α-reductase 1, 5α-reductase 2 and 5α-reductase 3 isoenzymes. DHT is a more potent androgen because it binds with up to 2-5 times greater affinity to the androgen receptor than testosterone, and 10-fold higher potency of inducing androgen receptor signaling than testosterone [2-4]. DHT also plays an important role in the development of normal prostate and prostate cancer [5,6]. 5α-reductase 2 is predominantly expressed in benign/normal prostate [7], although others [8-12], but not all, [13,14] studies, have reported increased 5α-reductase 1 and/or decreased 5α-reductase 2 mRNA expression or activity in prostate cancer compared with nonmalignant prostate tissue. Recently, 5α-reductase 3 has been identified as a new isoenzyme and found to be overexpressed in hormone-refractory prostate cancer cells and tissues [4].

Most prostate cancers rely on androgens for growth at the initial stages of development, and are therefore described as androgen-dependent or sensitive. Thus, inhibiting androgen production or blocking its action can be useful in the early treatment or prevention of prostate cancer [13,15,16]. Finasteride (5α-reductase 2 inhibitor) and dutasteride (5α-reductase 1 and 5α-reductase 2 inhibitor) are two chemopreventive drugs commonly used to treat benign prostatic hyperplasia (BPH), a nonmalignant enlargement of the prostate. The potential of these inhibitors to decrease prostate cancer development and/or progression through their antiandrogen action has been examined in several clinical trials, however, the reduction in prostate cancer risk was coupled with an increased risk of more aggressive prostate cancer [17,18]. As a result of this increased aggressiveness of prostate cancer associated with the use of finasteride and dutasteride, non-pharmaceutical, mild inhibitors of 5α-reductase enzyme(s) might be alternatives to reduce prostate cancer risk without increasing aggressive prostate cancer risk.

These alternative options to decrease prostate cancer risk have increased consumer interest in dietary supplements such as saw palmetto supplements (SPS). While not well understood, it has been suggested that phytosterols and fatty acids, particularly saturated, medium-chain fatty acids laurate and myristate, are at least partially responsible for the supplements' antiandrogenic activity [19].

This chapter will review the development of benign prostatic hyperplasia, prostatic intraepithelial neoplasia and prostate cancer, clinical trials, animal and cell culture studies that have been performed with 5α-reductase inhibitors (finasteride, dutasteride and saw palmetto supplements), major prostate cancer signaling pathways, key prostate cancer biomarkers, immunohistochemistry and *in situ* hybridization techniques for determining and quantifying prostate cancer biomarkers.

Anatomy and histology of the human and mouse prostate

The human prostate constitutes the largest accessory gland of the male reproductive system. It is located posterior to the symphysis pubis, anterior to the rectum, and inferior to the urinary bladder [20]. It is composed of 70% glandular tissue (secretory ducts and acini) and 30% stromal tissue (collagen and smooth muscle) [21]. The prostate secretes a thin, slightly alkaline fluid that provides approximately 30% of the volume of seminal fluid [22]. The human prostate is divided into four regions, the central zone, transition zone, peripheral zone, and anterior fibromuscular stroma. The peripheral, central and transition zones comprise approximately 70%, 25% and 5% of the glandular tissue, respectively. The anterior fibromuscular stroma is composed of fibrous and smooth muscular elements [23,24]. The human prostate has two cell types: epithelial and stromal [25]. The epithelial cell layer is composed of four differentiated cell types known as basal, secretory luminal, neuroendocrine, and transit-amplifying cells [26]. The stromal cell layer consists of several types of cells that include smooth muscle cells, fibroblasts, and myofibroblasts [27]. The luminal cells are the major cell type of the prostate and constitute the gland's exocrine component, secreting prostate specific antigen (PSA), and prostatic acid phosphatase (PAP) into the lumen. The luminal epithelial cells express high levels of androgen receptor [28,29]. PSA, a glycoprotein, is used as a biomarker for prostate cancer screening [30]. The expression of androgen

receptor is low or undetectable in the basal cells, thus the basal cells are independent of androgens for their survival [31,32].

The mice prostate has a lobular structure with four lobes-anterior, ventral, dorsal and lateral. The latter two are commonly referred to as dorsolateral lobe, which has been described as the most similar to the human prostate peripheral zone because of their histological similarities [33,34]. Histologically, the mouse prostate is similar to humans in that both types of prostate contain a pseudostratified epithelium with differentiated epithelial cell types: luminal, basal, and neuroendocrine [35-39].

Diagnostic criteria for benign prostatic hyperplasia, prostatic intraepithelial neoplasia, and prostate cancer

Benign prostatic hyperplasia (BPH) is a nonmalignant growth of the prostate found in over 50% of men aged 60 or over [40,41]. The increase in prostate cell number may be due to epithelial and stromal proliferation or to impaired programmed cell death or apoptosis leading to cellular proliferation [42]. This cellular proliferation leads to increased prostate volume and increased stromal smooth muscle tone [43]. BPH mainly develops in the transition zone of the human prostate [44].

Prostatic intraepithelial neoplasia (PIN) is characterized by cellular proliferation within the lining of the prostatic ducts and acini, loss of markers of secretory differentiation, progressive basal cell layer disruption, nuclear and nucleolar abnormalities, increasing proliferative potential, increasing microvessel density, variation in deoxyribonucleic acid (DNA) content, and allelic loss [45,46]. PIN usually involves an acinus or a small cluster of acini. The partial involvement of an acinus helps to distinguish PIN from adenocarcinoma [46]. PIN is an established precursor to prostate cancer. Prostate cancer is characterized by the abnormal proliferation of the glandular structure, invasion of the basement membrane, and progressive loss of basal cells (<1%) [47-49]. Androgen receptor positive luminal cells increase and contribute substantially to prostate mass (>99%) in prostate cancer [50]. In prostate cancer, there is a loss of constraints on cell proliferation along with dysregulation of apoptosis which leads to an imbalance between cell division and cell death [51]. PIN and most prostate cancers mainly develop

in the peripheral zone of the human prostate [52]. Fewer cancer lesions occur in the transition zone, and almost none arise in the central zone [53]. Cancer in the peripheral zone tends to be high-grade, and thus are poorly differentiated or undifferentiated, faster growing and metastasize rapidly. Cancer in the transition zone tends to be low-grade, and are therefore well differentiated and slow growing [52].

In normal cells, the layers of epithelial cells are arranged in a uniform and ordered manner, but in cancer cells, the epithelial cells are arranged in an irregular manner. Normal cells reproduce at a normal rate to restore lost cells, but in cancer, a greater number of cells are produced than are needed to restore lost cells [54,55]. Actin fibers which constitute the cytoskeleton of normal cells are arranged in an orderly manner, but in cancer cells, the actin fibers are either lost or disorganized [56]. Cancer cells are either much larger than normal cells within the same tissue or smaller and less developed than normal cells. Cancer cells are characterized by large nucleus, and constitute a greater portion of the total volume of the cell. There is frequent cell division and greater number of mitoses in cancer cells compared with normal cells [57,58].

Androgens and androgen receptor in prostate cancer development

Androgens are male steroid hormones that control the development and differentiation of the male reproductive system [59]. Testosterone, the main circulating androgen, is synthesized by the Leydig cells of the testes (90-95%) under the influence of the hypothalamus and anterior pituitary gland. The remaining 5-10% is produced from dehydroepiandrosterone (DHEA), which is synthesized by the zona reticularis of the adrenal cortex [60-62]. Approximately 97% of testosterone is bound to albumin and sex hormone-binding globulin (SHBG) and the remaining 3% is free and biologically active. Testosterone stimulates the differentiation of the Wolffian duct into male internal genitalia (epididymis, vas deferens, and seminal vesicles) in male fetuses. It is also involved in the development of libido, enlargement of the vocal cords, skeletal muscles, penis, and scrotum and the initiation of spermatogenesis at puberty [63,64]. Intracellular testosterone is converted by 5α-reductase isoenzymes to DHT, the preferred ligand for androgen receptor transactivation [65]. Twenty-percent of DHT comes

from the testes, while 80% comes from the conversion in the peripheral tissues facilitated by 5α-reductase isoenzymes [66]. DHT is important for *in utero* differentiation and growth of the prostate gland, male external genitalia (penis and scrotum), and pubertal growth of facial and body hair. DHT plays an important role in several human diseases such as BPH and prostate cancer [67]. The prostate gland depends on androgen stimulation for its growth, development, and function [68].

The androgen receptor (AR) is a nuclear steroid receptor, composed of 919 amino acids, with a molecular weight of 98.8 kilodaltons (kDa). The AR gene is composed of 8 exons separated by large intron segments. It has four functional domains: the amino-terminal transcription activation (transactivation) domain (*N*-terminal domain), the DNA-binding domain (DBD), a hinge region, and the carboxy-terminal ligand-binding domain (LBD) [69]. The amino-terminal domain contains a transactivation domain, activation function 1 (AF1), which is the primary transcriptional regulatory region, and the LBD contains the secondary transcriptional regulatory region, activation function 2 (AF2). The DBD is composed of two zinc fingers that are critical to DNA recognition and binding. The hinge domain contains the nuclear localization signal that regulates translocation of the AR into the nucleus, which indirectly affects transcriptional activity [70-72]. The androgen receptor is cytoplasmic in its unbound state, forming a circulating complex with heat-shock-protein (HSP)-90. Inactive AR binds DHT, causing a conformational change that frees it from its cytoplasmic chaperone proteins [73]. Upon ligand binding, the DHT-AR complex translocates from cytoplasm to nucleus, where it binds to a homodimer to canonical nuclear receptor inverted repeat DNA response elements to stimulate target gene transcription, which in turn leads to DNA synthesis and cellular proliferation in androgen-dependent cancerous tissues. The androgen-AR complex homodimerizes, translocates to the nucleus to bind androgen response elements, and recruits co-activators and co-repressors, which then stimulates transcription of androgen-dependent proteins [3,74-77]. Androgen receptor expression is present in prostate stroma and tumors at all developmental stages of the disease [78,79].

5α-reductase enzyme structure and biochemical properties

5α-reductase 1, 5α-reductase 2 and 5α-reductase 3 isoenzymes are nicotinamide adenine dinucleotide phosphate (NADPH)-dependent, microsomal membrane-associated enzymes, comprised of 259, 254 and 318 amino acids (mainly hydrophobic), and have molecular weights of 29.5, 28.4 and 36.5 kDa respectively. The enzymes are also encoded by 5α-R1, 5α-R2 and 5α-R3 genes respectively [7,80]. The isoenzymes 5α-reductase 1, 5α-reductase 2 and 5α-reductase 3 are potential targets because they convert testosterone to the more potent DHT for androgen receptor transactivation [3,4,81,82]. 5α-reductase 1 has a broad pH optimum (6.0-8.5), while 5α-reductase 2 has a sharp pH optimum (5.0-5.5) [83], although evidence suggests that inside intact human cells, 5α-reductase 2 isoenzyme functions optimally at a more neutral pH (6.0-7.0) [7]. In humans, 5α-reductase 1 isoenzyme occurs in tissues such as liver and non-genital skin, while 5α-reductase 2 occurs in tissues such as liver, prostate, epididymis, seminal vesicle and genital skin. 5α-reductase 1 isoenzyme is present in the liver of the mouse [7]. Majority of published literature indicates that the expression of 5α-reductase 1 increases and 5α-reductase 2 decreases in prostate cancer compared to benign prostate and BPH [8-11,84]. Also, 5α-reductase 1 and 5α-reductase 2 expression is increased in recurrent and metastatic prostate cancers, and 5α-reductase 3 isoenzyme is overexpressed in hormone-refractory prostate cancer cells and tissues suggesting that these enzymes may be important in the development and progression of prostate cancer [4,85].

5α-reductase inhibitors and their mechanism of inhibition

5α-reductase inhibitors function by inhibiting 5α-reductase isoenzymes, thereby blocking the enzymatic conversion of testosterone to the more potent androgen dihydrotestosterone (DHT). This leads to a reduction in the epithelial components of the prostate, and ultimately prostate size [86]. Finasteride and dutasteride are two pharmaceuticals commonly used to treat BPH [7]. Finasteride inhibits 5α-reductase 2 isoenzyme, while dutasteride inhibits 5α-reductase 1 and 5α-reductase 2 isoenzymes. Dutasteride lowers serum DHT by 90% compared to a 70% reduction with finasteride [9,87]. A

structural modification in dutasteride increases its serum half-life and inhibition potency [88]. This dual inhibition may offer an advantage over finasteride and is approximately 60 times more potent than finasteride in reducing 5α-reductase activity [89,90]. The potential of these inhibitors to decrease prostate cancer development and/or progression through their antiandrogen action has been studied in several clinical trials [17,18]. Saw palmetto extracts are commonly used by men to combat BPH, a nonmalignant enlargement of the prostate. These supplements are also used by men with prostate cancer [91]. The antiandrogen action of SPS has been attributed to the phytosterols and fatty acids that they contain, particularly the medium-chain saturated fatty acids laurate (C12:0) and myristate (C14:0) [19].

5α-reductase inhibition involves a stereospecific, irreversible breakage of the double bond between carbon atoms 4 and 5 with the aid of cofactor (nicotinamide adenine dinucleotide phosphate) NADPH and the insertion of a hydride ion to the α face at carbon C-5 and a proton to the β face at position C-4, leading to the formation of DHT, ultimately leaving the enzyme-$NADP^+$ complex. $NADP^+$ departs last and the 5α-reductase enzyme becomes free for further catalytic cycles. The mechanism of inhibition of 5α-reductase isoenzymes is divided into three types:

a. Competitive inhibition with NADPH and substrate: 5α-reductase inhibitor binds 5α-reductase enzyme.
b. Competitive inhibition with testosterone: 5α-reductase inhibitor binds the enzyme-NADPH complex (e.g. finasteride, dutasteride).
c. Uncompetitive inhibition with the enzyme-$NADP^+$ complex: 5α-reductase inhibitor binds the enzyme-$NADP^+$ complex after the product (DHT) leaves [92].

Finasteride and dutasteride in prostate cancer clinical trials

The Prostate Cancer Prevention Trial (PCPT) was a multicenter, randomized, double blind, placebo-controlled clinical trial designed to compare finasteride with placebo in the prevention of prostate cancer in men at low risk for the disease. A total of 18,882 men over the age of 55, with a PSA level of 3 ng/ml or lower and a normal digital rectal examination (DRE) were randomized to receive 7

years of finasteride (5 mg) or placebo daily. Of the 9,060 men included in the final statistical analysis, 18.4% of men in the finasteride group were diagnosed with prostate cancer, compared with 24.4% in the placebo group; a 24.8% relative risk reduction [17]. In another study, a total of 28 untreated patients with asymptomatic, stage D prostate cancer were randomized in a double-blinded fashion to receive finasteride (10 mg/day), or placebo. Finasteride had no effect upon PAP, serum testosterone, prostatic volume or appearance of metastasis in bone scans. There was a decrease in serum PSA in the finasteride treatment group suggesting that finasteride was causing a minor effect in patients with prostate cancer [93].

The Reduction by Dutasteride of Prostate Cancer Events (REDUCE) was a multicenter, randomized, double blind, placebo-controlled clinical trial designed to compare dutasteride with placebo in the prevention of prostate cancer in men at low risk for the disease. A total of 6,729 men between 50 and 75 years, with a PSA level of 2.5 to 10 ng/ml, and had had one negative prostate biopsy within 6 months before were randomized to receive 4 years of dutasteride (0.5 mg) or placebo daily. After the final statistical analysis, 19.9% of men in the dutasteride group were diagnosed with prostate cancer, compared with 25.1% in the placebo group; a 22.8% relative risk reduction [18].

The Reduction by Dutasteride of Clinical Progression Events in Expectant Management (REDEEM) trial assessed the efficacy of dutasteride in preventing disease progression in men with low-risk prostate cancer on active surveillance. Three hundred and two participants were randomized to receive dutasteride 0.5 mg once daily or placebo. The inclusion criteria were clinical stage T2a or lower PSA ≤11 ng/ml, and Gleason 6 cancer diagnosed in <4 cores of a minimum 10-core biopsy with <50% of any core positive. By the third year, 38% and 48% of the dutasteride and control participants, respectively, had progressed by pathologic or therapeutic criteria, a risk reduction of 38% for dutasteride. However, there were 14% of higher-grade cancers with dutasteride and 16% with placebo [94].

In the ARIA series studies, four thousand three hundred and twenty five participants were randomized to receive dutasteride 0.5 mg once daily or placebo for 2 years. Analysis of pooled data from

all three phase 3 BPH monotherapy studies (ARIA3001, ARIA3002, ARIB3003) found the incidence for detectable prostate cancer in the dutasteride group to be 50% less compared to the placebo group at 27 months [95]. In the Combination of Avodart and Tamsulosin (CombAT) study, four thousand eight hundred and forty four participants were randomized to receive 0.5 mg dutasteride or 0.4 mg tamsulosin, or a combination (0.5 mg dutasteride and 0.4 mg tamsulosin) daily for 4 years. Dutasteride, alone or in combination with tamsulosin, caused a relative reduction of 40% in the risk of detectable prostate cancers compared to tamsulosin monotherapy, as well as a 40% reduction in biopsies. Fewer Gleason score 7–10 and Gleason score 8–10 tumors were detected in the dutasteride groups combined, compared with the tamsulosin group. Low- and high-grade Gleason score cancers were reduced by 40% [96].

Finasteride, dutasteride and saw palmetto extracts in prostate cancer animal studies

Administration of finasteride (160 mg/kg/day) to male Sprague-Dawley rats for 15 days resulted in a significant reduction in circulating DHT levels, dorsolateral and ventral prostate DHT levels and weights [97]. Treatment of young adult male Sprague-Dawley rats with finasteride (5 and 20 mg/kg/day) for 28 days significantly reduced ventral prostate, epididymal, and seminal vesicle weights [98]. Similarly, finasteride (25 mg/kg/day) administered to young adult male rats for 7 days significantly reduced ventral prostate weight and prostatic concentrations of the mRNA for both 5α-reductase and 5α-reductase activity [99]. Administration of finasteride (0.7, 7 or 72 mg/kg/day) to intact adult male Copenhagen rats for 55 days resulted in a significant reduction in normal ventral prostate weight and DHT content but did not inhibit R-3327H prostate cancer growth or DHT content [88]. Finasteride significantly reduced the weights of the androgen-sensitive tissues, seminal vesicles and prostate, but did not decrease Dunning R-3327H tumor areas or weights [100].

Administration of dutasteride (2 mg/kg every 2 days) to 6-7 week-old heterozygous male large probasin-large T antigen (LPB-Tag) mice for 4 weeks caused a significant reduction in ventral prostate, dorsolateral prostate, coagulating gland and seminal vesicle weights. Dutasteride at a lower dose (0.2

mg/kg every 2 days); or when treatment was extended to 8 weeks, dutasteride (1 mg/kg/day) significantly reduced all except ventral prostate weights [101]. Administration of dutasteride (1, 10 or 100 mg/kg/day) to intact adult male Copenhagen rats for 55 days reduced normal ventral prostate and R-3327H tumor DHT content and weight in intact mice [88]. Treatment of 4-week-old heterozygous male probasin-Tag transgene (TRAMP) mice with saw palmetto extracts (300 mg/kg/day) for 8 or 20 weeks significantly decreased the concentration of DHT in the prostate and resulted in a significant increase in apoptosis and significant decrease in pathological tumor grade and frank tumor incidence. Saw palmetto extracts at a lower dose (50 mg/kg/day) did not significantly change ventral prostate DHT levels [102].

Finasteride, dutasteride and saw palmetto extracts in prostate cancer *in vitro* studies

Treatment of LNCaP cells with finasteride (4 μM and 13 μM) significantly reduced cell viability. In RWPE-1 cells, growth was significantly inhibited at concentrations between 35 μM and 50 μM. In PC3 cells, cell viability was reduced noticeably at concentrations between 4 μM and 50 μM. Treatment of LNCaP cells with dutasteride (1 μM and 25 μM) significantly reduced cell viability. In RWPE-1 cells, dutasteride was effective in inhibiting cell growth at concentrations between 0.5 μM and 50 μM. PC3 cell number was reduced at dutasteride concentration of 0.5 μM. No statistical differences were observed between the two 5α-reductase inhibitors in LNCaP-treated cells [103], although Lazier and colleagues found dutasteride to be more effective at inhibiting LNCaP cell growth compared with finasteride [104]. Dutasteride was also found to be significantly more effective in inhibiting PC3 and RWPE-1 cell growth than finasteride [103].

Saw palmetto (Permixon) inhibited LNCaP and PC3 cell growth at concentrations of 44 μg/ml and 88 μg/ml [105]. Treatment of DU-145 and PC-3 cells with 100 CH saw palmetto (*Sabal serrulata*) significantly decreased cell proliferation after 24 and 72 hour-recovery periods, respectively [106]. Saw palmetto extract (Prostasan) significantly induced suppression of growth in concentrations above 100 μg/ml (MCF-7 and LNCaP), 200 μg/ml (MDA MB231, DU-145, HCT 116, J82, Caki-1) and 333 μg/ml

(A549) [107]. Saw palmetto (Permixon; 10 μg/ml) markedly inhibited 5α-reductase activity in the prostate, without suppressing PSA secretion [108].

In vitro culture systems

In vitro cell culture systems can be classified into two types: primary and immortalized cell cultures. Primary cell cultures are derived directly from tumors and are more representative of their original tissue. The disadvantages are the limited access, finite lifespan and specific culturing techniques for maintaining these cells. Immortalized cell lines are derived from normal or cancer tissues and have an unlimited proliferation capacity. They offer the advantage of having an unlimited lifespan. The disadvantage of these lines is that they are not as representative of the original tissues [109,110]. The three most widely used immortalized cancer cell lines are LNCaP, DU-145, and PC-3 cells, which are all derived from human metastasized prostate cancer [111]. LNCaP cells were derived from lymph node metastasis and are androgen-sensitive meaning androgens stimulate their growth [112-114]. DU-145 cells were isolated from brain metastasis while PC-3 cells were derived from bone metastasis; both lines are androgen-insensitive [115,116]. RWPE-1 prostate epithelial cells are derived from the peripheral zone of a histologically normal adult human prostate and immortalized using human papilloma virus-18 (HPV-18) [117]. To produce cancerous cells, RWPE-1 cells were transformed using the carcinogen *N*-methyl-*N*-nitrosourea and subcutaneously injected into nude mice to form tumors. Second generation tumors were then cultured, progressively, to create WPE1-NA22, WPE1-NB14, WPE1-NB11 and WPE1-NB26 cell lines [118]. Another cell line, the PC-346C cells are human, androgen-sensitive cells derived from the transurethral resection of a primary prostate tumor [119]. Previously, we examined the effect of finasteride and dutasteride, pre- and post-tumor injection on the growth of WPE1-NA22 xenografts in nude mice. There were no differences in final tumor areas or tumor weights between groups, likely due to poor tumor growth. We found proliferation of WPE1-NA22 and RWPE-1 cells were unaltered by treatment with testosterone, DHT or mibolerone, suggesting that these cell lines are not androgen-sensitive [120].

Prostate Cancer Animal Models

Xenograft models

Nude/athymic mice

The nude or athymic mouse lacks mature T-cells due to the absence of a thymus, hence cannot initiate an immunologic response to foreign tissue. This enables them to readily accept subcutaneous xenografts of human tumor. Prostate cancer cells can be subcutaneously injected into flanks or shoulders, orthotopically injected into the prostate, or implanted into the sub-renal capsule of immunocompromised animal models [121]. The benefits of subcutaneous tumor models are their ease of tumor establishment, management and reproducibility. Currently, only 25-35% of human tumors have been successfully transplanted into athymic mice and their use is hampered by the high natural killer (NK) cell activity. There is no metastasis seen in conventional subcutaneous xenograft [122,123].

SCID mice

The severe combined immunodeficiency (SCID) mouse lacks B and T lymphocytes and is unable to initiate an immunologic response to foreign tissue [124-126]. The presence of NK cell and myeloid function is capable of promoting initial tumor growth and metastatic spread after xenograft implantation [127]. SCID mice readily accept xenografts of human tumor and develop spontaneous metastasis from human xenografts at an increased rate than do nude mice [128-132]. HER-2/neu overexpressing human LNCaP cells were subcutaneously injected into this model to demonstrate that HER-2/neu stimulates androgen-independent tumor growth via regulation of the androgen receptor signaling pathway [133].

NOD-SCID mice

The non-obese diabetic (NOD)-SCID mice is defined by a functional deficit in NK cells, an absence of circulating complement and defects in the differentiation and function of antigen-presenting cells [134]. This model can be used for subcutaneous and orthotopic implantation of human prostate cancer cells. The tumor take rate was 100% for subcutaneous implantation and 83% for orthotopic implantation when PC-3 and DU-145 cells, respectively were injected to animals. NOD/SCID mice have

been shown to have a better growth rate compared to the nude or SCID mice. There is an increased incidence of metastatic sites in comparison to other metastatic mouse models [135]. The disadvantages of SCID and NOD-SCID mice include the frequent occurrence of thymic lymphoma and the leakiness, in which T and B cells develop in aged mice [136,137].

NOG-NSG mice

The NOG-NSG mouse is a cross between the NOD-SCID mouse and interleukin 2 receptor γ (IL2Rγ) null mouse which completely lack B, T, and NK cells. This model readily accepts humanized tissue and human cell engraftment than the NOD/SCID mice [138-141], and are a more valuable model, particularly for long-term studies because they survive longer than NOD-SCID mice [141]. NOG-NSG mice readily accept subcutaneous cancer cells efficiently compared to nude mice. NOG-NSG mice were subcutaneously injected with E006AA prostate cancer cells to characterize the androgen responsiveness and phenotypic expression of these cells [142].

RAG mice

RAG mice lack the recombination activating gene, RAG1 and RAG2, which are responsible for activation of V(D)J recombination during the development of T cells [143,144]. The inactivation of these proteins causes mice to be deficient in both B and T cells, similar to SCID mice [145,146]. The RAG mice have an inflammatory response and NK cell activity [147]. RAG mice deficient in RAG 2 have been reported to have a higher tumor growth rate than SCID mice [148]. TRAMP-C2 prostate cancer cells were subcutaneously injected into RAG1 null mice to understand the effectiveness of an antitumor treatment [147].

Transgenic models

TRAMP mice

In transgenic mouse models (TRAMP), the rat prostate-specific promoter probasin directs expression of the simian virus 40 (SV40) large and small T antigen to the prostate epithelium to cause

cell transformation. As a result, TRAMP mice develop progressive forms of prostate cancer with lesions ranging from mild PIN through well-differentiated (WD) adenocarcinoma, to invasive poorly differentiated (PD) adenocarcinoma with distant site metastasis to pelvic lymph nodes and lungs [149,150]. In TRAMP mice, the transgene is detected as early as 3 weeks of age [151], with pathological features similar to low-grade PIN developing as early as 4-6 weeks of age [152]. TRAMP mice develop high-grade PIN and well-differentiated adenocarcinoma at 12 weeks old with poorly differentiated and invasive carcinoma appearing between 18-30 weeks and metastasizing into lymph nodes and lungs and occasionally kidney, bone and adrenal glands [152,153]. By 30 weeks of age, TRAMP mice on an FVB background (TRAMP/FVB) display 100% metastasis to lungs and lymph nodes along with bone metastasis [150,154]. TRAMP mice develop neuroendocrine carcinoma, a rare occurrence in human prostate cancer. Majority of human prostate cancer are acinar adenocarcinoma, with neuroendocrine prostate cancers making up less than 2% of cancer cases. The limitation of using TRAMP mice for prostate cancer studies is that results are applicable to only a small subpopulation of prostate cancer patients [155-158].

LADY mice

The large probasin promoter directs the expression of the large-T antigen that results in the development of glandular hyperplasia and PIN by 10 weeks of age, followed by high-grade epithelial dysplasia and poorly undifferentiated adenocarcinoma by 20 weeks. There is accelerated rate of disease progression and frequency of neuroendocrine differentiation of tumor cells [159,160].

Syrian hamster androgen-sensitive flank organs

Syrian hamsters have a pair of flank organs, each located on either side of the costovertebral angle, and are sensitive to androgen stimulation [161]. The androgen-sensitive components of the flank organ include dermal melanocytes, sebaceous glands, and hair follicles [162]. The advantage of using this animal model is that a test compound can be applied topically to only one of the flank organs leaving

the other flank organ as a control. Flank organ growth is dependent on the local conversion of testosterone to DHT as is prostate growth in humans [163]. This animal model has been used widely for testing androgenic [161,162] and antiandrogenic compounds [164,165]. This serves as a good model for testing inhibitor of 5α-reductase that is topically active and inactive systemically for treatment of androgen-dependent flank organ growth [166].

Other animal models that can be used for anti-androgenic studies

The fuzzy rat expresses androgen-dependent hypersecretion of sebum and hyperplastic sebaceous glands [167]. The ear of Syrian hamsters is also useful for anti-androgenic studies [168].

Grading of human prostate cancer and TRAMP mice prostatic lesions

Gleason grading uses five basic grade patterns ranging from 1 to 5 to grade prostate cancer in humans. A histologic score is obtained by the summation of the primary grade pattern and the secondary grade pattern to give a range from 2 to 10, with 2 representing the most well-differentiated tumors and 10 the least-differentiated tumors. Where there is only one grade pattern present, it is multiplied by 2 to give the histologic score [169]. The Gleason score was not used to evaluate TRAMP mice prostate pathology because it is based on clinical-pathological relationships in human samples. The mouse prostate has features which differ anatomically from human prostate. Also, prostate cancer in TRAMP mice differ clinically from humans because TRAMP mice will develop prostate cancer with a 100% incidence and progress to poorly differentiated carcinoma [153]. Additionally, the Gleason grading system evaluates only prostate cancer not PIN, and therefore cannot be used for grading in TRAMP mice where there is assessment and differentiation of PIN and prostate cancer. This grading scheme is also limited in determining the distribution of lesion in prostate lobes since it accounts for only the common lesion, and not the severity of the lesion. As a result, a refined grading system developed by Berman-Booty and colleagues has several advantages for grading prostate cancer in TRAMP mice. First, it is able to distinguish low-, moderate-, and high-grade PIN, and thus makes it possible to establish whether

a drug changes the severity of PIN. Second, it is able to differentiate high-grade PIN, a preneoplastic lesion, from well-differentiated adenocarcinoma, a neoplastic lesion, which can determine if a drug treatment is able to prevent progression to neoplasia. Third, this is a numerical grading system that accounts for lesion type and its distribution to promote the evaluation of lesion severity and allow statistical assessment. The anterior, dorsal, lateral and ventral lobes of C57BL/6 TRAMP × FVB mice are assigned two grades each between 0-7. The first grade is the most severe lesion within the lobe [normal prostate as least severe (grade 0), and poorly differentiated as most severe (grade 7)]. The second grade is the most common lesion within the lobe [normal prostate as least common (grade 0), and poorly differentiated as most common (grade 7)] [170]. Evaluating both the severe and common lesions in TRAMP mice prostate cancer paints a better picture of the disease and represents closely the Gleason system used for grading prostate cancer in humans [171].

1. Grade 1, Low-grade PIN: There is focal hyperplasia of prostate epithelial cells resulting in stratification of cells. Hyperplastic cells have increased basophilia and increased nuclear to cytoplasmic ratios. Cytoplasmic and nuclear atypia are minimal.
2. Grade 2, Moderate-grade PIN: Hyperplastic epithelial cells form increased numbers of short and tall papillary projections that extend into the glandular lumen. There may be mild hyperplasia of smooth muscle surrounding the glands.
3. Grade 3, High-grade PIN: There is loss of prostate glandular lumina due to the presence of numerous hyperplastic prostate epithelial cells that project into the lumen and form cribiform pattern. Hyperplastic cells do not invade the connective tissue that separates the glands into distinct lobules.
4. Grade 4. Phyllodes-like tumor: These lesions are commonly found in the dorsal or anterior lobes. The main component of a phyllodes-like tumor is stroma. They consist of papillary projections of loose stroma with loosely arranged stellate mesenchymal cells.

5. Grade 5, Well-differentiated adenocarcinoma: Well-differentiated neoplastic cells form tubular or glandular like structures that have obliterated lobular architecture by invasion of the basement membrane, which is a key feature for distinguishing PIN from carcinoma. Necrosis of neoplastic cells is absent.
6. Grade 6, Moderately differentiated adenocarcinoma: Neoplastic prostate epithelial cells are attempting to form glandular structures. Glandular structures vary in size and shape. Cellular atypia is increased and necrosis is present.
7. Grade 7, Poorly differentiated carcinoma: Neoplastic cells have marked nuclear and cytoplasmic atypia and arranged in polygonal or elongated sheets with no attempt at forming glandular or tubular structures [170,172].

Molecular pathways in prostate cancer

Androgen receptor signaling pathway

The androgen receptor (AR) signaling pathway is important for prostate cancer cell proliferation [173]. The AR signaling pathway begins with the translocation of testosterone to the cytoplasm, where it is converted to DHT by 5α-reductase isoenzymes. DHT binds to the androgen receptor as a homodimer, undergoes a conformational change which results in dissociation of cytoplasmic chaperones, AR dimerization, and translocation to the nucleus [174-177]. Inside the nucleus, AR binds to androgen response elements (ARE) on the promoter/enhancer regions, recruits coregulators, and forms the transcriptional machinery for AR-regulated gene expression. This is termed as genomic signaling pathway [173,178].

Nongenomic steroid activity normally involves activated AR in the cytoplasm interacting with several signaling molecules including the phosphatidyl-inositol 3-kinase (PI3K)/Akt, Src, Ras-Raf-1, and protein kinase C (PKC), which then converge on mitogen activated protein kinase (MAPK)/extracellular signal-regulated kinase (ERK) activation, resulting in cell proliferation. The

MAPK/ERK signaling cascade is important in controlling diverse biological functions such as cell survival, motility, and proliferation which are important to prostate carcinogenesis [173].

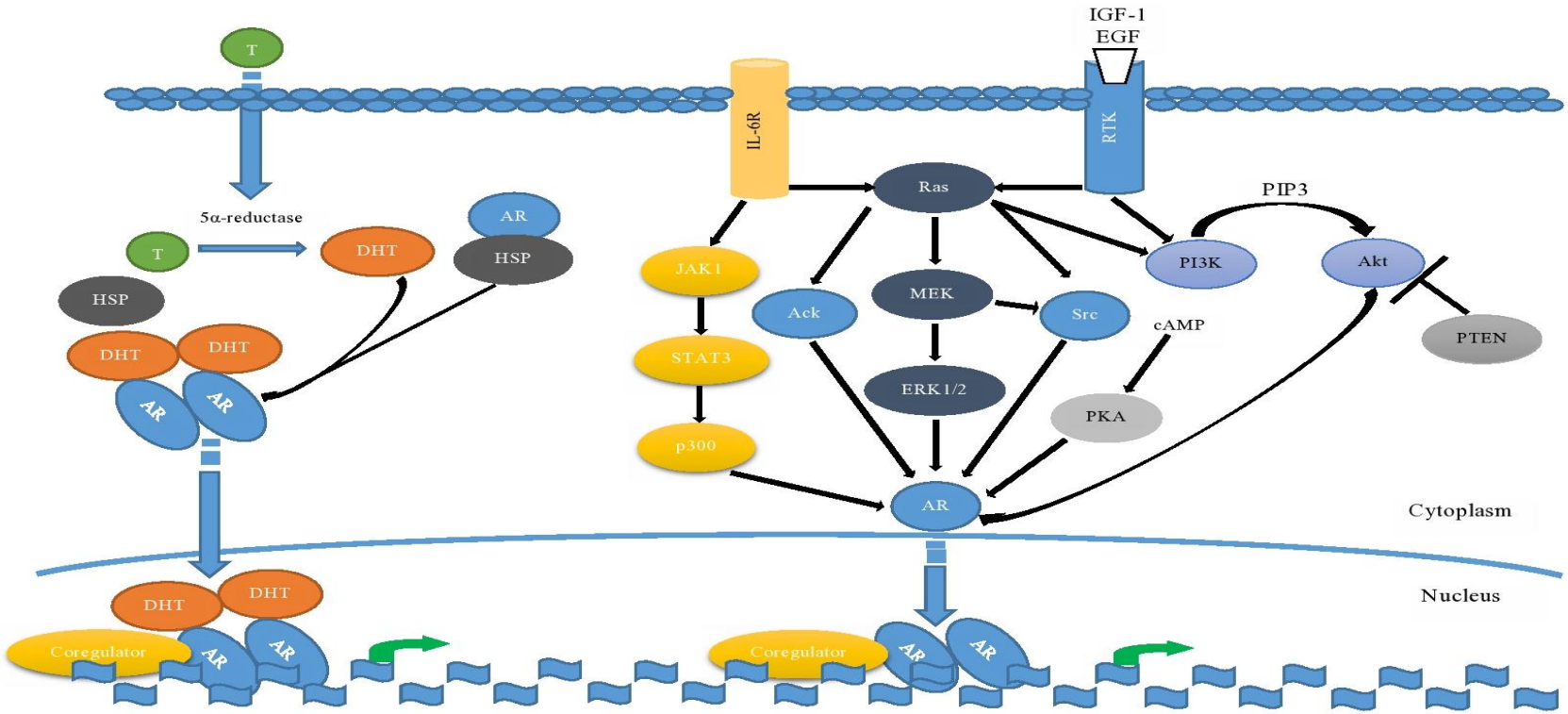

Figure 1.1 Summary of the androgen receptor signaling pathways in prostate cancer. Adapted from Lonergan et al, 2011 [179].
T = testosterone; DHT = dihydrotestosterone; AR = androgen receptor; HSP = heat shock protein; JAK-1 = Janus kinase 1; STAT3 = signal transducer and activator of transcription 3; PTEN = phosphatase and tensin homolog deleted on chromosome 10; PIP3= phosphatidylinositol 3,5-triphosphate; cAMP = cyclic adenosine monophosphate; ERK1/2 = extracellular-signal-regulated kinases 1/2; PKA = protein kinase A; Akt = serine/threonine protein kinase; Src = sarcoma-related kinase; P13K = phosphatidylinositol-3 kinase; MEK = MAPK extracellular kinase; RTK = receptor tyrosine kinases; Ack = acetate kinase; Ras = membrane-associated guanine nucleotide-binding protein; p300 = histone acetyltransferase; EGF = epidermal growth factor; IGF-1 = insulin-like growth factor 1; IL-6R = interleukin-6 receptor.

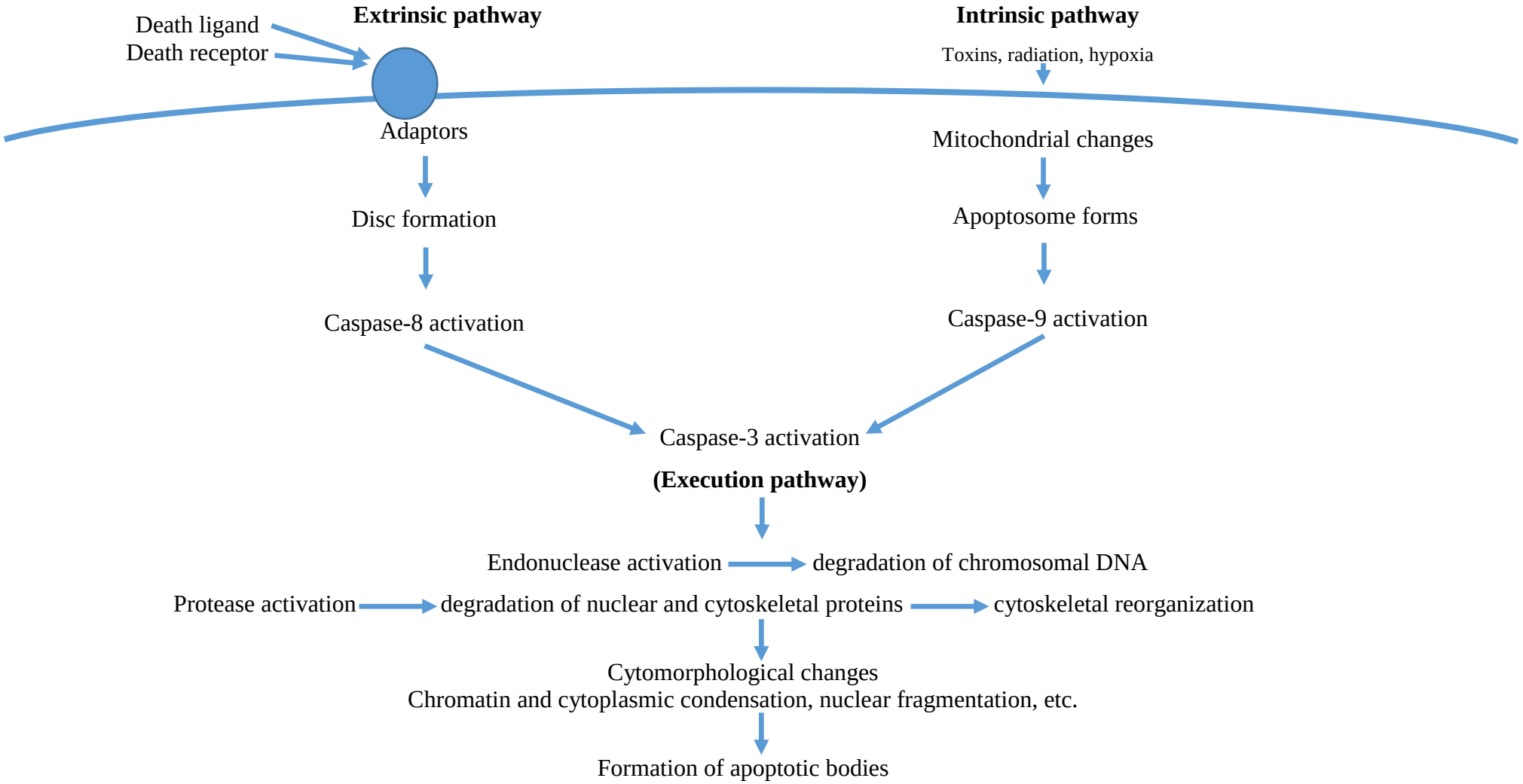

Figure 1.2. Summary of the apoptosis signaling pathways. Adapted from Elmore et al, 2007 [180]. The two main pathways of apoptosis are extrinsic and intrinsic pathway. Specific triggering signals trigger each pathway to begin an energy-dependent cascade of molecular events. Each pathway is activated by its own initiator caspase (8, 9) which then activate the executioner caspase-3. The execution pathway results in characteristic cytomorphological features such as cell shrinkage, chromatin condensation, formation of cytoplasmic blebs and apoptotic bodies and finally phagocytosis of the apoptotic bodies by adjacent parenchymal cells, neoplastic cells or macrophages.

Apoptosis signaling pathway

Pathological and physiological triggers of apoptosis

The apoptosis signaling pathway is involved in the genetically determined destruction of cells, a homeostatic mechanism to conserve cell populations in tissues [181-184]. Apoptosis can be triggered pathologically by stimuli such as heat, free radicals, ultra violet light, ionizing radiation, alkylating agents; and physiologically by stimuli such as steroid hormones, interleukins, and cytokines [185]. The most common described initiation pathways are the intrinsic (or mitochondrial) and extrinsic (or death receptor) pathways of apoptosis. Caspases are essential in the initiation and execution of apoptosis [186,187].

Extrinsic pathway of apoptosis

The extrinsic pathway is initiated through ligation of transmembrane death receptors (FasL/FasR, TNF-α/TNFR1, Apo3L/DR3, Apo2L/DR4 and Apo2L/DR5) [188-192]. Fas ligand binds to Fas receptor, and this results in the binding of the adapter protein FADD and the binding of TNF ligand to TNF receptor. This leads to the binding of the adapter protein TRADD with enrolment of FADD and RIP [193,194]. FADD binds with procaspase-8 to form a death-inducing signaling complex (DISC) which catalyzes the proteolytic cleavage and transactivation of procaspase-8 to produce caspase-8 [195]. Activated caspase-8 is released from DISC to cytoplasm to initiate downstream cleavage of caspase-3 through direct or mitochondrial-dependent mechanisms, which activates the execution phase of apoptosis [196-198].

Intrinsic pathway of apoptosis

The intrinsic pathway of caspase activation is caused by events such as irreparable genetic damage, growth factor withdrawal, loss of contact with the extracellular matrix, extremely high concentrations of cytosolic Ca^{2+} and hypoxia. These stimuli initiate changes in the inner mitochondrial membrane that leads to the opening of the mitochondrial permeability transition (MPT) pore, loss of the

mitochondrial transmembrane potential and release of two main groups of pro-apoptotic proteins from the intermembrane space into the cytosol [199]. The first group consists of cytochrome *c*, Smac/DIABLO, and the serine protease HtrA2/Omi [200-203]. These proteins activate the caspase-dependent mitochondrial pathway. Cytochrome *c* binds and activates Apaf-1 and procaspase-9, leading to caspase-9 activation [204,205]. Smac/DIABLO and HtrA2/Omi promote apoptosis through the inhibition of inhibitors of apoptosis proteins (IAP) activity. The second group of pro-apoptotic proteins consists of AIF, endonuclease G and CAD. AIF translocates to the nucleus to initiate DNA fragmentation and condensation of peripheral nuclear chromatin [206]. Endonuclease G also translocates to the nucleus to cleave nuclear chromatin to produce oligonucleosomal DNA fragments [207]. CAD is released from the mitochondria and translocates to the nucleus, and cleaved by caspase-3, resulting in oligonucleosomal DNA fragmentation and chromatin condensation [208].

Execution pathway of apoptosis

Both intrinsic and extrinsic pathways eventually lead to the execution phase of apoptosis. Cytoplasmic endonuclease are activated by execution caspases, which degrade nuclear material, and proteases that degrade the cytoskeletal and nuclear and proteins [209]. Substrates such as PARP, cytokeratins, nuclear protein NuMA are cleaved by caspase-3, caspase-6 and caspase-7, resulting in DNA fragmentation, degeneration of cytoskeletal and nuclear proteins, cross-linking of proteins, generation of apoptotic bodies, expression of ligands for phagocytic cell receptors, and finally the phagocytic uptake of apoptotic cells [210]. Caspase-3 is the primary executioner caspase and is activated by caspases-8, caspases-9 or caspases-10 [211]. Caspase-3 stimulates endonuclease CAD to degrade DNA and proteases and initiates chromatin condensation [212,213]. Caspase-3 induces cytoskeletal reorganization and fragmentation of the cell into apoptotic bodies. Caspase-3 also cleaves gelsolin, followed by cleavage of actin filaments which results in disruption of the cytoskeleton, intracellular transport, cell division, and signal transduction [180,214].

The MAPK pathway

Mitogen-activated protein kinases (MAPKs) regulate intracellular signaling involved in cellular activities such as cell proliferation, differentiation, survival, death, and transformation [215,216]. The three main members that integrate the MAPK family in mammalian cells are stress-activated protein kinase c-Jun NH2-terminal kinase (JNK), stress-activated protein kinase 2 (SAPK2, p38), and the extracellular signal-regulated protein kinases (ERK1/2, p44/p42). JNK and p38 normally mediate cell death and tumor suppression, while ERK mediates cell survival and tumor promotion in response to stimuli such as cytokines and growth factors [217]. The full activation of JNK requires dual phosphorylation of threonine and tyrosine residues [218-222]. JNKs phosphorylate different substrates, including transcription factors (ATF-2, c-Myc, p53) and members of the Bcl-2 family, in addition to those involved in proliferation, inflammation and apoptosis [223-225]. p38 is activated in cells in response to stress signals, proinflammatory or anti-inflammatory cytokines [226,227]. Activated p38 phosphorylates and regulates many transcription factors including ATF-2, NF-κB, Elk-1, Max, MEF-2, Mac, p53, or Stat1 [227-229] and other cell cycle and apoptotic mediators (e.g., Cdc25A, Bcl-2) [230]. ERK is activated by cytokines and phosphorylates a series of transcription factors including Elk1, c-Fos, p53, Ets1/2, and c-Jun, each one involved in regulation of cell proliferation, differentiation, and morphogenesis [177]. ERK can stimulate the phosphorylation of apoptotic regulatory molecules including bcl-2 family members and caspase-9 [231].

The TGF-β/SMAD signaling pathway

The TGF-β/SMAD signaling pathway regulates many cellular activities including cell growth, adhesion, migration, cell differentiation, embryonic development, and apoptosis [232]. TGF-β ligand binds to a specific set of type 1 and type 2 receptors which then results in signal transduction by SMAD proteins and formation of heterotetrameric receptor complex. The active type 2 receptor phosphorylates the type 1 receptor, which then promotes a signal by phosphorylating the receptor-specific SMADs (R-

SMADs) [233,234]. When R-SMADs are activated, they form complexes with SMAD4, which are translocated to the nucleus where SMAD complexes interact with nuclear proteins to initiate or suppress target genes transcription. TGF-β can initiate androgen receptor (AR) translocation into the nucleus and AR-dependent gene transcription. Androgen receptor can combine with SMAD4 to stimulate TGF-β-mediated apoptosis. In early stage-cancer cells, TGF-β functions as a tumor suppressor by inhibiting cell growth, invasiveness, and motility and promoting apoptosis. In advanced-stage cancer cells, TGF-β is involved in proliferation, invasion, motility of cells and inhibition of apoptosis [177].

Prognostic molecular markers of prostate cancer

Cell-proliferation nuclear markers

The Ki-67 antigen is a prototypic cell cycle-related protein expressed by proliferating cells. It is a reliable marker of cell proliferation in malignant tissues because it is expressed in all phases of the active cell cycle (G1, S, G2 and M) and absent in resting (G0) cells [235]. High Ki-67 index is associated with poor prognosis of prostate cancer [236]. Abnormal Ki-67 expression in prostate tumor is associated with higher Gleason scores and more aggressive cancers as well as higher rates of recurrence and metastases. An increase in Ki-67 expression indicates a rise of mitotic activity and cell proliferation. Ki-67 is well recognized to be a useful factor to evaluate the proliferative activity of various neoplastic tissues, and considered the gold standard for cell proliferation [237]. Proliferating cell nuclear antigen (PCNA) is another useful marker of cells with proliferative potential and for identifying the status of proliferation in tumor tissue. PCNA is expressed in the nuclei of cells during the DNA-synthesis (S) phase only, and therefore not proliferative specific. Many studies have found a weak correlation between PCNA and other proliferation markers [238].

Apoptosis markers

During apoptosis, cells reduce their volume, contract their reorganized cytoskeleton and disintegrate into many small apoptotic bodies in order to promote engulfment. This shrinkage results in

nuclear condensation and internucelosomal DNA-fragmentation [239]. Degraded DNA can be detected enzymatically and quantified using *in situ* nick translation (ISNT), *in situ* nick end labeling (ISNT), and terminal deoxynucleotidyl transferase end labelling (TUNEL) [240]. *In situ* nick end labelling is 10 times more specific and can detect cells undergoing DNA repair, therefore it is more specific than TUNEL [241]. During TUNEL assay, single and double stranded DNA strand breaks are detected by enzymatically labeling the free 3'-OH termini with modified nucleotides. These new DNA ends that are generated upon DNA fragmentation are typically localized in morphologically identifiable nuclei and apoptotic bodies [242,243]. The caspase-cascade system plays significant roles in the induction, transduction and amplification of intracellular apoptotic signals. To date, fourteen caspases have been identified. Caspase-3 is activated in apoptosis and is essential for DNA fragmentation and morphological changes of apoptosis. Cell death is enhanced in the presence of caspase-3, which is the primary executioner of apoptotic death [244]. Other apoptotic executioners include caspase-6 and caspase-7 [245]. Caspase-3 is commonly used to measure apoptosis because it is the major activator of apoptotic DNA fragmentation [246], and provides greater sensitivity than TUNEL staining [213].

Androgen receptor markers

Androgen receptor plays a significant role in the development and progression of prostatic carcinoma and androgen receptor expression is maintained throughout prostate carcinoma progression [247,248]. Androgen receptor expression is a potential marker of prognosis and hormonal responsiveness in prostate cancer [249]. High levels of androgen receptor are associated with increased proliferation and markers of aggressive disease [250]. Androgen regulated genes such as CAMKK2, MiR-125b RNA, ARFGAP3 and APP could also be used as biomarkers of prostate cancer [251].

5α-reductase enzyme assays

Several methods have been developed for measuring 5α-reductase activities. In one method, tritiated testosterone is incubated with tissue homogenates and the radiolabeled steroid metabolites are separated by thin layer chromatography or reverse phase chromatography [252,253]. A nonradioactive assay for measuring 5α-reductase activities is performed by incubation of cell homogenates with tritiated testosterone, and then steroid metabolites separated by reverse phase chromatography [254]. Immunohistochemistry using 5α -reductase 1 and 5α -reductase 2 antibodies have also been employed to quantify the expression of the isoenzymes in hyperplastic and prostatic tissues [255,256].

Immunohistochemistry

Immunohistochemistry is a method for localizing specific antigens in tissues based on the binding of antibodies (immunoglobulins) to specific antigens in tissue sections [257]. An antigen is any molecule that stimulates an immune response by stimulating the B-lymphocytes to produce antibodies (immunoglobulin) against it [258]. Immunoglobulins are glycoprotein molecules which are produced by plasma cells. There are five classes of immunoglobulins but the most frequently used immunoglobulin in immunohistochemistry is IgG; IgM is less commonly used [259]. All immunoglobulins have a four chain structure as their basic unit. Immunoglobulins are Y-shaped and are composed of two identical light chains (κ and λ) (23kDa) and two identical heavy chains (α, δ, ε, γ and μ) (50-75kDa) that are encoded by different segments of DNA, and held together by interchain disulfide bonds and by non-covalent interactions [260]. The disulfide bonds are positioned within a flexible region called the hinge region, which separates the lobes of the antibody from one another and provides ample flexibility to bind antigens effectively [261]. Antibodies (Abs) are made by immunizing animals with purified antigen. The animal responds by producing antibodies that specifically recognize and bind to the antigen. Antibodies are referred to as polyclonal when they are secreted by different B cell lineages. Monoclonal antibodies come from a single cell lineage. Polyclonal antibodies have a higher affinity and wide reactivity but

lower specificity when compared with monoclonal antibodies [262]. Polyclonal antibodies have the advantage over monoclonal antibodies in that they are more likely to identify multiple isoforms (epitopes) of the target protein [263]. The bonds between antigen and antibody are weak (mostly hydrophobic and electrostatic) [264]. The paratope is the part of an antibody which recognizes an antigen. Antibodies recognize specific areas of antigens called epitopes [262]. Epitopes are normally 5-21 amino acids long [265].

Immunohistochemistry techniques

Immunohistochemical techniques utilize antibodies to detect and visualize antigens in cells and tissue using chromogenic or fluorescent methods. The direct method uses an antibody labeled with an enzyme, which can be visualized by the addition of a chromogenic substrate at the site of antigen-antibody interaction. Indirect methods increase the number of assay steps, but amplifies antibody-antigen signal for greater sensitivity [259].

Direct method

The direct method is a one-step staining method, and involves only one labeled antibody reacting directly with the antigen in tissue sections [266]. The antibody against the target antigen is conjugated to an enzyme (biotin, horseradish peroxidase, alkaline phosphatase) [267-269], and then activated by adding a substrate (hydrogen peroxidase substrate) [270]. Addition of a chromogenic substrate [3,3'-diaminobenzidine (DAB), nitro blue tetrazolium chloride (NBT), 5-bromo-4-chloro-3-indoyl-β-D-galactopyranoside] to the enzyme allows for the immediate visualization of the antigen using a light microscope [271-273]. Direct methods are suitable when labeled primary antibodies are available or when the target molecule is present at levels that do not require amplification. This method is quick because only one antibody is utilized, and also nonspecific reactions are minimized. However, this technique is insensitive because only one antibody is used and no amplification occurs [259].

Indirect method

The indirect method involves an unlabeled primary antibody (first layer) which reacts with tissue antigen, and a labeled secondary antibody (second layer) binds to the primary antibody to amplify the primary signal. The secondary antibody must be against the immunoglobulin of the animal species from which the primary antibody is raised [266,274]. The second layer antibody may be labeled with an enzyme such as biotin, horseradish peroxidase, alkaline phosphatase [267-269]. Increased signal amplification occurs due to the binding of secondary antibodies to multiple epitopes on the primary antibody. Chromogenic substrate is added to provide visualization of the antigen [275]. An advantage of this method is the capacity to use a variety of primary antibodies from the same species with the same labeled secondary antibody. Secondary antibody can cross-react with endogenous immunoglobulins in the specimen to yield undesired reactions. Using secondary antibodies which are preabsorbed with immunoglobulin from the species from which the specimen is obtained can eliminate this cross-reactivity [276,277].

Avidin-Biotin Complex (ABC) method

Avidin is a glycoprotein naturally found in egg whites, can be labelled with peroxidase or fluorescein, and binds with high affinity and specificity to biotin. Biotin, a low molecular weight vitamin, can be conjugated to antibodies. There are three layers involved in this method. The first layer is an unlabeled primary antibody. The second layer is a biotinylated secondary antibody. The third layer is a complex of avidin-biotin peroxidase. The enzyme is then visualized by application of the chromogenic substrate [259,275,278].

Labeled Streptavidin Biotin (LSAB) method

This method is a buildup on the ABC method, and uses streptavidin, derived from *streptococcus avidini*, in place of avidin. There are three layers involved in this method. The first layer is unlabeled primary antibody. The second layer is biotinylated secondary antibody. The third layer is

enzyme-streptavidin conjugates (HRP-Streptavidin or AP-Streptavidin) to replace the avidin-biotin peroxidase complex. The enzyme is then visualized by application of the chromogenic substrate. LSAB can increase the sensitivity of detection 8-fold over ABC detection [259,278].

Peroxidase anti-peroxidase (PAP) method

An unconjugated secondary antibody is added to the primary antibody, leading to multiple secondary antibodies reacting with each primary antibody. A tertiary antibody complexed with peroxidase is then added to react with each secondary antibody to increase the level of amplification [275,278]. The tertiary antibody upon addition of chromogenic substrate is 100 to 1000 times greater than just secondary antibody amplification. Less primary antibody can be used for each sample staining, thus eliminating most unwanted antibodies and decreasing non-specific background staining [259,274,279,280].

Polymer-based immunohistochemistry

Significant background staining can result due to the presence of endogenous biotin in tissues. When using the heat-induced antigen retrieval method, the retrieval of biotin may appear as unwanted side effect. Residual activity is still found in tissues such as liver and kidney after formalin fixation and paraffin embedding. Also, frozen tissues have higher levels of endogenous biotin than those found in paraffin-embedded specimens. Although there are methods which can partially block endogenous biotin activity, they make the immunohistochemistry procedure cumbersome. The polymer-based immunohistochemical method does not rely on biotin, but rather relies on a technology based on a polymer backbone to which multiple antibodies and enzyme molecules are conjugated. The whole immunohistochemical staining procedure, from primary antibody to enzyme, can be done in a single step [281-283].

Antigen retrieval

Fixation of tissues causes protein cross-linking, resulting in the inability of some protein epitopes to react with complementary antibodies. Pretreating the tissues with antigen retrieval reagent or procedures can significantly re-open the cross-linked epitopes for antibodies to easily bind to target antigens [284]. Heat-retrieval and enzyme-retrieval are the most commonly used antigen-retrieval methods [259]. Heating unmasks epitopes by hydrolysis of methylene cross-links, extraction of diffusible blocking proteins, precipitation of proteins, rehydration of the tissue section allowing greater penetration of antibody, and heat mobilization of trace paraffin. The enzyme-retrieval functions by digestion of proteins in the tissues [285,286]. The effect of enzyme retrieval depends on the concentration and type of enzyme, time, temperature, and pH, and the duration of fixation. Examples of enzymes used in this method are proteinase K, trypsin, chymotrypsin, and pepsin [287-289].

In situ hybridization

This technique allows for precise localization of a specific segment of nucleic acid within a histologic section [290]. A series of target probes are designed to hybridize to the target RNA molecule. Probes are complementary sequences of nucleotide bases to the specific mRNA sequence of interest. The probes can be as small as 20-40 bases or up to a 1000 base pairs. Each target probe contains an 18- to 25 base region complementary to the target RNA, a spacer, and a 14-base tail sequence. A pair of double probes, each possessing a different type of tail sequence, hybridizes contiguously to a target region (~50 bases). The two tail sequences together form a 28-base hybridization site for the preamplifier, which contains 20 binding sites for the preamplifier, which in turn contains 20 binding sites for the label probe. After hybridization, the tissue is washed to remove unbound probe or probe which has loosely bound to imperfectly matched sequences. The label probe can be conjugated to an alkaline phosphatase or horseradish peroxidase (HRP) molecule for chromogenic reactions [291]. Controls are used to ensure that the hybridization reaction is specific and that the probe is binding

selectively to the target mRNA sequence and not to other components or other closely related mRNA sequences.

References

1. American Cancer Society. Cancer facts and figures 2015.

2. Saartok T, Dahlberg E, Gustafsson JÅ. Relative binding affinity of anabolic-androgenic steroids: Comparison of the binding to the androgen receptors in skeletal muscle and in prostate, as well as to sex hormone-binding globulin. Endocrinology. 1984;114(6):2100-2106.

3. Grossmann ME, Huang H, Tindall DJ. Androgen receptor signaling in androgen-refractory prostate cancer. J Natl Cancer Inst. 2001;93(22):1687–1697.

4. Uemura M, Tamura K, Chung S, Honma S, Okuyama A, et al. Novel 5α-steroid reductase (SRD5A3, type-3) is overexpressed in hormone-refractory prostate cancer. Cancer Sci. 2008;99(1):81-86.

5. Berger R, Febbo PG, Majumder PK, Zhao JJ, Mukherjee S, et al. Androgen-induced differentiation and tumorigenicity of human prostate epithelial cells. Cancer Res. 2004;64(24):8867-8875.

6. Voigt KD, Bartsch W. Intratissular androgens in benign prostatic hyperplasia and prostatic cancer. J Steroid Biochem. 1986;25(5B):749-757.

7. Russell DW, Wilson JD. Steroid 5α-reductase: Two genes/two enzymes. Annu Rev Biochem. 1994;63(1):25-61.

8. Luo J, Dunn TA, Ewing CM, Walsh PC, Isaacs WB. Decreased gene expression of steroid 5α-reductase 2 in human prostate cancer: implications for finasteride therapy of prostate carcinoma. Prostate. 2003;57(2):134-139.

9. Titus MA, Gregory CW, Ford OH, Schell MJ, Maygarden SJ, et al. Steroid 5α-reductase isozymes I and II in recurrent prostate cancer. Clin Cancer Res. 2005;11(12):4365-4371.

10. Söderström TG, Bjelfman C, Brekkan E, Ask B, Egevad L, et al. Messenger ribonucleic acid levels of steroid 5α-reductase 2 in human prostate predict the enzyme activity. J Clin Endocrinol Metab. 2001;86(2):855-858.

11. Bjelfman C, Söderström TG, Brekkan E, Norlén BJ, Egevad L, et al. Differential gene expression of steroid 5α-reductase 2 in core needle biopsies from malignant and benign prostatic tissue. J Clin Endocrinol Metab. 1997;82(7):2210-2214.

12. Iehlé C, Radvanyi F, de Medina SGD, Ouafik LH, Gérard H, et al. Differences in steroid 5α-reductase iso-enzymes expression between normal and pathological human prostate tissue. J Steroid Biochem Mol Biol.1999;68(5):189-195.

13. Nakamura Y, Suzuki T, Nakabayashi M, Endoh M, Sakamoto K, et al. In situ androgen producing enzymes in human prostate cancer. Endocr Relat Cancer. 2005;12(1):101-107.

14. Habib FK, Ross M, Bayne CW, Bollina P, Grigor K, et al. The loss of 5α-reductase type I and type II mRNA expression in metastatic prostate cancer to bone and lymph node metastasis. Clin Cancer Res. 2003;9(5):1815-1819.

15. Tien AH, Sadar MD. Androgen-responsive gene expression in prostate cancer progression. In: Androgen-responsive genes in prostate cancer. Springer. 2013;135-153.

16. Feldman BJ, Feldman D. The development of androgen-independent prostate cancer. Nat Rev Cancer. 2001;1(1):34-45.

17. Thompson IM, Goodman PJ, Tangen CM, Lucia MS, Miller GJ, et al. The influence of finasteride on the development of prostate cancer. N Engl J Med. 2003;349(3):215-224.

18. Andriole GL, Bostwick DG, Brawley OW, Gomella LG, Marberger M, et al. Effect of dutasteride on the risk of prostate cancer. N Engl J Med. 2010;362(13):1192-1202.

19. Schantz MM, Bedner M, Long SE, Molloy JL, Murphy KE, et al. Development of saw palmetto (Serenoa repens) fruit and extract standard reference materials. Anal Bioanal Chem. 2008;392(3):427-438.

20. Lee CH, Akin-Olugbade O, Kirschenbaum A. Overview of prostate anatomy, histology, and pathology. Endocrinol Metab Clin North Am. 2011;40(3):565-575.

21. Djavan B, Bostanci Y, Kazzazi A. Epidemiology, screening, pathology and pathogenesis. In: Urol Oncol. Springer (Lond). 2015;677-695.

22. Lilja H, Ahrahamsson PA, Lundwall A. Semenogelin, the predominant protein in human semen. Primary structure and identification of closely related proteins in the male accessory sex glands and on the spermatozoa. J Biol Chem. 1989;264(3):1894-1900.

23. Janus C, Lippert M. Benign prostatic hyperplasia: Appearance on magnetic resonance imaging. Urology. 1992;40(6):539-541.

24. Pollack HM. Imaging of the prostate gland. Eur Urol. 1991;20 Suppl 1:50-58.

25. Cunha GR, Hayward SW, Dahiya R, Foster BA. Smooth muscle-epithelial interactions in normal and neoplastic prostatic development. Acta Anat (Basel). 1996;155(1):63-72.

26. Long RM, Morrissey C, Fitzpatrick JM, Watson RW. Prostate epithelial cell differentiation and its relevance to the understanding of prostate cancer therapies. Clin Sci (Lond). 2005;108(1):1-11.

27. Takao T, Tsujimura A. Prostate stem cells: The niche and cell markers. Int J Urol. 2008;15(4):289-294.

28. El-Alfy M, Luu-The V, Huang XF, Berger L, Labrie F, et al. Localization of type 5 17beta-hydroxysteroid dehydrogenase, 3beta-hydroxysteroid dehydrogenase, and androgen receptor in the human prostate by in situ hybridization and immunocytochemistry. Endocrinology. 1999;140(3):1481-1491.

29. Sar M, Lubahn DB, French FS, Wilson EM. Immunohistochemical localization of the androgen receptor in rat and human tissues. Endocrinology. 1990;127(6):3180-3186.

30. Barry MJ. Prostate-specific-antigen testing for early diagnosis of prostate cancer. N Engl J Med. 2001;344(18):1373-1377.

31. Bonkhoff H, Remberger K. Widespread distribution of nuclear androgen receptors in the basal cell layer of the normal and hyperplastic human prostate. Virchows Arch A Pathol Anat Histopathol. 1993;422(1):35-38.

32. Wang Y, Hayward SW, Cao M, Thayer KA, Cunha GR. Cell differentiation lineage in the prostate. Differentiation. 2001;68(4-5):270-279.

33. Abate-Shen C, Shen MM. Mouse models of prostate carcinogenesis. Trends Genet. 2002;18(5):S1-S5.

34. Powell WC, Cardiff RD, Cohen MB, Miller GJ, Roy-Burman P. Mouse strains for prostate tumorigenesis based on genes altered in human prostate cancer. Curr Drug Targets. 2003;4(3):263-279.

35. Foster BA, Evangelou A, Gingrich JR, Kaplan PJ, DeMayo F, et al. Enforced expression of FGF-7 promotes epithelial hyperplasia whereas a dominant negative FGFR2iiib promotes the emergence of neuroendocrine phenotype in prostate glands of transgenic mice. Differentiation. 2002;70(9-10):624-632.

36. van Leenders GJ, Schalken JA. Epithelial cell differentiation in the human prostate epithelium: Implications for the pathogenesis and therapy of prostate cancer. Crit Rev Oncol Hematology. 2003;46 Suppl:S3-S10.

37. Hudson DL. Epithelial stem cells in human prostate growth and disease. Prostate Cancer Prostatic Dis. 2004;7(3):188-194.

38. Shappell SB, Thomas GV, Roberts RL, Herbert R, Ittmann MM, et al. Prostate pathology of genetically engineered mice: definitions and classification. The consensus report from the Bar Harbor meeting of the Mouse Models of Human Cancer Consortium Prostate Pathology Committee. Cancer Res. 2004;64(6):2270-2305.

39. Peehl DM. Primary cell cultures as models of prostate cancer development. Endocr Relat Cancer. 2005;12(1):19-47.

40. Abate-Shen C, Shen MM. Molecular genetics of prostate cancer. Genes Dev. 2000;14(19):2410-2434.

41. Thorpe A, Neal D. Benign prostatic hyperplasia. Lancet. 2003;361(9366):1359-1367.

42. Roehrborn CG. Pathology of benign prostatic hyperplasia. Int J Impot Res. 2008;20 Suppl 3:S11-S18.

43. McNeal J. Pathology of benign prostatic hyperplasia. Insight into etiology. Urol Clin North Am. 1990;17(3):477-486.

44. McNeal JE. Origin and evolution of benign prostatic enlargement. Invest Urol. 1978;15(4):340-345.

45. Argani P, Epstein JI. Inverted (hobnail) high-grade prostatic intraepithelial neoplasia (PIN): report of 15 cases of a previously undescribed pattern of high-grade PIN. Am J Surg Pathol. 2001;25(12):1534-1539.

46. Ayala AG, Ro JY. Prostatic intraepithelial neoplasia: Recent advances. Arch Pathol Lab Med. 2007;131(8):1257-1266.

47. Brawer MK. Prostatic intraepithelial neoplasia: An overview. Rev Urol. 2005;7 Suppl 3:S11-S8.

48. Maitland NJ, Frame FM, Polson ES, Lewis JL, Collins AT. Prostate cancer stem cells: Do they have a basal or luminal phenotype? Horm Cancer. 2011;2(1):47-61.

49. Gleason DF. Classification of prostatic carcinomas. Cancer Chemother Rep. 1966;50(3):125-128.

50. Grisanzio C, Signoretti S. p63 in prostate biology and pathology. J Cell Biochem. 2008;103(5):1354-1368.

51. Andreeff M, Goodrich DW, Pardee AB. Cell proliferation, differentiation, and apoptosis. Holland-Frei Cancer Medicine. 2000:17-32.

52. De Marzo AM, Platz EA, Sutcliffe S, Xu J, Grönberg H, et al. Inflammation in prostate carcinogenesis. Nat Rev Cancer. 2007;7(4):256-269.

53. McNeal JE, Redwine EA, Freiha FS, Stamey TA. Zonal distribution of prostatic adenocarcinoma: Correlation with histologic pattern and direction of spread. Am J Surg Pathol. 1988;12(12):897-906.

54. Vasioukhin V. Hepsin paradox reveals unexpected complexity of metastatic process. Cell Cycle. 2004;3(11):1394-1397.

55. Franks LM, Teich NM. Introduction to the cellular and molecular biology of cancer. Introduction to the cellular and molecular biology of cancer. Oxford University Press. 1997.

56. Varmus H, Weinberg RA. Genes and the biology of cancer. Scientific American Library. 1993

57. Baba AI, Câtoi C. Tumor cell morphology. 2007.

58. Cotran RS, Kumar V, Robbins SL. Robbins SL Pathologic basis of disease. Philadelphia PA, Saunders. 1994;8.

59. Dohle GR, Smit M, Weber RF. Androgens and male fertility. World J Urol. 2003;21(5):341-345.

60. Lamb AD, Neal DE. Role of the androgen receptor in prostate cancer. Trends in Urology & Men's Health. 2013;4(3):26-30.

61. Vasaitis TS, Bruno RD, Njar VC. CYP17 inhibitors for prostate cancer therapy. J Steroid Biochem Mol Biol. 2011;125(1-2):23-31.

62. Labrie F. Adrenal androgens and intracrinology. Semin Reprod Med. 2004;22(4):299-309.

63. Siiteri PK, Wilson JD. Testosterone formation and metabolism during male sexual differentiation in the human embryo. J Clin Endocrinol Metab. 1974;38(1):113-125.

64. Imperato-McGinley J, Zhu YS. Androgens and male physiology the syndrome of 5α-reductase-2 deficiency. Mol Cell Endocrinol. 2002;198(1-2):51-59.

65. Azzouni F, Mohler J. Role of 5α-reductase inhibitors in prostate cancer prevention and treatment. Urology. 2012;79(6):1197-1205.

66. Zylicz Z. Opoid-induced hypogonadsim: the role of androgens in the well-being and pain thresholds in men and women with advanced disease. Adv Pall Med. 2009;8(2):57-62.

67. Cilotti A, Danza G, Serio M. Clinical application of 5α-reductase inhibitors. J Endocrinol Invest. 2001;24(3):199-203.

68. Steers WD. 5α-reductase activity in the prostate. Urology. 2001;58(6):17-24.

69. Culig Z, Hobisch A, Bartsch G, Klocker H. Androgen receptor-an update of mechanisms of action in prostate cancer. Urol Res. 2000;28(4):211-219.

70. Egan A, Dong Y, Zhang H, Qi Y, Balk SP, et al. Castration-resistant prostate cancer: Adaptive responses in the androgen axis. Cancer Treat Rev. 2014;40(3):426-433.

71. Tanner TM, Denayer S, Geverts B, Van Tilborgh N, Kerkhofs S, et al. A 629RKLKK633 motif in the hinge region controls the androgen receptor at multiple levels. Cell Mol Life Sci. 2010;67(11):1919-1927.

72. Clinckemalie L, Vanderschueren D, Boonen S, Claessens F. The hinge region in androgen receptor control. Mol Cell Endocrinol. 2012;358(1):1-8.

73. Chen Y, Clegg NJ, Scher HI. Anti-androgens and androgen-depleting therapies in prostate cancer: new agents for an established target. Lancet Oncol. 2009;10(10):981-991.

74. Attar RM, Takimoto CH, Gottardis MM. Castration-resistant prostate cancer: locking up the molecular escape routes. Clin Cancer Res. 2009;15(10):3251-3255.

75. Sharifi N, Auchus RJ. Steroid biosynthesis and prostate cancer. Steroids. 2012;77(7):719-726.

76. Shang Y, Myers M, Brown M. Formation of the androgen receptor transcription complex. Mol Cell. 2002;9(3):601-610.

77. Dehm SM, Tindall DJ. Androgen receptor structural and functional elements: Role and regulation in prostate cancer. Mol Endocrinol. 2007;21(12):2855-2863.

78. Prins GS, Birch L, Greene GL. Androgen receptor localization in different cell types of the adult rat prostate. Endocrinology. 1991;129(6):3187-3199.

79. Prins GS, Birch LY. Immunocytochemical analysis of androgen receptor along the ducts of the separate rat prostate lobes after androgen withdrawal and replacement. Endocrinology. 1993;132(1):169-178.

80. Langlois VS, Zhang D, Cooke GM, Trudeau VL. Evolution of steroid-5α-reductases and comparison of their function with with 5β-reductase. Gen Comp Endocrinol. 2010;166(3):489-497.

81. Andriole GL, Kirby R. Safety and tolerability of the dual 5α-reductase inhibitor dutasteride in the treatment of benign prostatic hyperplasia. Eur Urol. 2003;44(1):82-88.

82. Stiles AR, Russell DW. SRD5A3: A surprising role in glycosylation. Cell. 2010;142(2):196-198.

83. Chang CY. Androgen and androgen receptor. MA Kluwer Academic Publishers (Boston). 2002.

84. Thomas LN, Douglas RC, Lazier CB, Too CK, Rittmaster RS, et al. Type 1 and type 2 5α-reductase expression in the development and progression of prostate cancer. Eur Urol. 2008;53(2):244-252.

85. Thomas LN, Lazier CB, Gupta R, Norman RW, Troyer DA, et al. Differential alterations in 5α-reductase type 1 and type 2 levels during development and progression of prostate cancer. Prostate. 2005;63(3):231-239.

86. Thiruchelvam N. Benign prostatic hyperplasia. Surgery (Oxford). 2014;32(6):314-322.

87. Frye SV. Discovery and clinical development of dutasteride, a potent dual 5α-reductase inhibitor. Curr Top Med Chem. 2006;6(5):405-421.

88. Xu Y, Dalrymple SL, Becker RE, Denmeade SR, Isaacs JT. Pharmacologic basis for the enhanced efficacy of dutasteride against prostatic cancers. Clin Cancer Res. 2006;12(13):4072-4079.

89. Aggarwal S, Thareja S, Verma A, Bhardwaj TR, Kumar M. An overview on 5α-reductase inhibitors. Steroids. 2010;75(2):109-153.

90. Lee C. Role of androgen in prostate growth and regression: Stromal-epithelial interaction. Prostate. 1996;29 Suppl 6:52-56.

91. Barnes PM, Bloom B, Nahin RL. Complementary and alternative medicine use among adults and children: United States, 2007. Natl Health Stat Report. 2008;(12):1-23.

92. Occhiato EG, Guarna A, Danza G, Serio M. Selective non-steroidal inhibitors of 5α-reductase type 1. J Steroid Biochem Mol Biol. 2004;88(1):1-16.

93. Presti JC Jr, Fair WR, Andriole G, Sogani PC, Seidmon EJ, et al. Multicenter, randomized, double-blind, placebo controlled study to investigate the effect of finasteride (MK-906) on stage D prostate cancer. J Urol. 1992;148(4):1201-1204.

94. Fleshner NE. Dutasteride and active surveillance of low-risk prostate cancer. Lancet. 2012;379(9826):1590.

95. Andriole GL, Roehrborn C, Schulman C, Slawin KM, Somerville M, et al. Effect of dutasteride on the detection of prostate cancer in men with benign prostatic hyperplasia. Urology. 2004;64(3):537-541.

96. Roehrborn CG, Andriole GL, Wilson TH, Castro R, Rittmaster RS. Effect of dutasteride on prostate biopsy rates and the diagnosis of prostate cancer in men with lower urinary tract symptoms and enlarged prostates in the Combination of Avodart and Tamsulosin trial. Eur Urol. 2011;59(2):244-249.

97. Prahalada S, Rhodes L, Grossman SJ, Heggan D, Keenan KP, et al. Morphological and hormonal changes in the ventral and dorsolateral prostatic lobes of rats treated with finasteride, a 5α-reductase inhibitor. Prostate. 1998;35(3):157-164.

98. Shao TC, Kong A, Marafelia P, Cunningham GR. Effects of finasteride on the rat ventral prostate. J Androl. 1993;14(2):79-86.

99. George FW, Russell DW, Wilson JD. Feed-forward control of prostate growth: dihydrotestosterone induces expression of its own biosynthetic enzyme, steroid 5α-reductase. Proc Natl Acad Sci U S A. 1991;88(18):8044-8047.

100. Canene-Adams K, Lindshield BL, Wang S, Jeffery EH, Clinton SK, et al. Combinations of tomato and broccoli enhance antitumor activity in Dunning R3327-H prostate adenocarcinomas. Cancer Res. 2007;67(2):836-843.

101. Shao TC, Li H, Ittmann M, Cunningham GR. Effects of dutasteride on prostate growth in the large probasin-large T antigen mouse model of prostate cancer. J Urol. 2007;178(4 pt 1):1521-1527.

102. Wadsworth TL, Worstell TR, Greenberg NM, Roselli CE. Effects of dietary saw palmetto on the prostate of transgenic adenocarcinoma of the mouse prostate model (TRAMP). Prostate. 2007;67(6):661-673.

103. Das K, Lorena PD, Ng LK, Lim D, Shen L, et al. Differential expression of steroid 5α-reductase isozymes and association with disease severity and angiogenic genes predict their biological role in prostate cancer. Endocr Relat Cancer. 2010;17(3):757-770.

104. Lazier CB, Thomas LN, Douglas RC, Vessey JP, Rittmaster RS. Dutasteride, the dual 5α-reductase inhibitor, inhibits androgen action and promotes cell death in the LNCaP prostate cancer cell line. Prostate. 2004;58(2):130-144.

105. Silvestri I, Catarrino S, Aglianò A, Nicolazzo C, Scarpa S, et al. Effect of Serenoa repens (Permixon) on the expression of inflammation-related genes: Analysis in primary cell cultures of human prostate carcinoma. J Inflamm (Lond). 2013;10:11.

106. MacLaughlin BW, Gutsmuths B, Pretner E, Jonas WB, Ives J, et al. Effects of homeopathic preparations on human prostate cancer growth in cellular and animal models. Integr Cancer Ther. 2006;5(4):362-372.

107. Hostanska K, Suter A, Melzer J, Saller R. Evaluation of cell death caused by an ethanolic extract of Serenoae repentis fructus (Prostasan) on human carcinoma cell lines. Anticancer Res. 2007;27(2):873-881.

108. Habib FK, Ross M, Ho CK, Lyons V, Chapman K. Serenoa repens (Permixon) inhibits the 5α-reductase activity of human prostate cancer cell lines without interfering with PSA expression. Int J Cancer. 2005;114(2):190-194.

109. Peehl DM. Are primary cultures realistic models of prostate cancer? J Cell Biochem. 2004;91(1):185-195.

110. Sandhu C, Peehl DM, Slingerland J. p16INK4A mediates cyclin dependent kinase 4 and 6 inhibition in senescent prostatic epithelial cells. Cancer Res. 2000;60(10):2616-2622.

111. Sobel RE, Sadar MD. Cell lines used in prostate cancer research: A compendium of old and new lines--part 2. J Urol. 2005;173(2):360-372.

112. Igawa T, Lin FF, Lee MS, Karan D, Batra SK, et al. Establishment and characterization of androgen-independent human prostate cancer LNCaP cell model. Prostate. 2002;50(4):222-235.

113. Horoszewicz JS, Leong SS, Chu TM, Wajsman ZL, Friedman M, et al. The LNCaP cell line--a new model for studies on human prostatic carcinoma. Prog Clin Biol Res. 1980;37:115-132.

114. Horoszewicz JS, Leong SS, Kawinski E, Karr JP, Rosenthal H, et al. LNCaP model of human prostatic carcinoma. Cancer Res. 1983;43(4):1809-1818.

115. Stone KR, Mickey DD, Wunderli H, Mickey GH, Paulson DF. Isolation of a human prostate carcinoma cell line (DU-145). Int J Cancer. 1978;21(3):274-281.

116. Kaighn ME, Narayan KS, Ohnuki Y, Lechner JF, Jones LW. Establishment and characterization of a human prostatic carcinoma cell line (PC-3). Invest Urol. 1979;17(1):16-23.

117. Bello D, Webber MM, Kleinman HK, Wartinger DD, Rhim JS. Androgen responsive adult human prostatic epithelial cell lines immortalized by human papillomavirus 18. Carcinogenesis. 1997;18(6):1215-1223.

118. Webber MM, Quader ST, Kleinman HK, Bello-DeOcampo D, Storto PD, et al. Human cell lines as an in vitro/in vivo model for prostate carcinogenesis and progression. Prostate. 2001;47(1):1-13.

119. Marques RB, Erkens-Schulze S, de Ridder CM, Hermans KG, Waltering K, et al. Androgen receptor modifications in prostate cancer cells upon long-term androgen ablation and antiandrogen treatment. Int J Cancer. 2005;117(2):221-229.

120. Opoku-Acheampong AB, Nelsen MK, Unis D, Lindshield BL. The effect of finasteride and dutasteride on the growth of WPE1-NA22 prostate cancer xenografts in nude mice. PLoS One. 2012;7(1):e29068.

121. Corey E, Vessella RL. Xenograft models of human prostate cancer. Prostate Cancer. Humana Press. 2007;3-31.

122. Kariya R, Matsuda K, Gotoh K, Vaeteewoottacharn K, Hattori S, et al. Establishment of nude mice with complete loss of lymphocytes and NK cells and application for in vivo bio-imaging. In Vivo. 2014;28(5):779-784.

123. Kerbel RS. Human tumor xenografts as predictive preclinical models for anticancer drug activity in humans: 18 better than commonly perceived-but they can be improved. Cancer Biol Ther. 2003;2(4 Suppl 1):S134-S139.

124. Giblett ER, Anderson JE, Cohen F, Pollara B, Meuwissen HJ. Adenosine-deaminase deficiency in two patients with severely impaired cellular immunity. Lancet. 1972;2(7786):1067-1069.

125. Hirschhorn R, Vawter GF, Kirkpatrick JA, Rosen FS. Adenosine deaminase deficiency: Frequency and comparative pathology in autosomally recessive severe combined immunodeficiency. Clin Immunol Immunopathol. 1979;14(1):107-120.

126. McKusick VA. Mendelian inheritance in man. Catalogs of autosomal dominant, autosomal recessive, and X-Linked phenotypes. The Johns Hopkins University Press, Baltimore. 1990;20-26, 1015.

127. Fidler IJ. Rationale and methods for the use of nude mice to study the biology and therapy of human cancer metastasis. Cancer Metastasis Rev. 1986;5(1):29-49.

128. Huang P, Allam A, Taghian A, Freeman J, Duffy M, et al. Growth and metastatic behavior of five human glioblastomas compared with nine other histological types of human tumor xenografts in SCID mice. J Neurosurg. 1995;83(2):308-315.

129. Huang P, Taghian A, Hsu DW, Perez LA, Allam A, et al. Spontaneous metastasis, proliferation characteristics and radiation sensitivity of fractionated irradiation recurrent and unirradiated human xenografts. Radiother Oncol. 1996;41(1):73-81.

130. Nomura T, Takahama Y, Hongyo T, Inohara H, Takatera H, et al. SCID (severe combined immunodeficiency) mice as a new system to investigate metastasis of human tumors. J Radiat Res. 1990;31(3):288-292.

131. Taghian A, Budach W, Zietman A, Freeman J, Gioioso D, et al. Quantitative comparison between the transplantability of human and murine tumors into the subcutaneous tissue of NCr/Sed-nu/nu nude and severe combined immunodeficient mice. Cancer Res. 1993;53(20):5012-5017.

132. Xie X, Brünner N, Jensen G, Albrectsen J, Gotthardsen B, et al. Comparative studies between nude and scid mice on the growth and metastatic behavior of xenografted human tumors. Clin Exp Metastasis. 1992;10(3):201-210.

133. Craft N, Shostak Y, Carey M, Sawyers CL. A mechanism for hormone-independent prostate cancer through modulation of androgen receptor signaling by the HER-2/neu tyrosine kinase. Nat Med. 1999;5(3):280-285.

134. Hudson WA, Li Q, Le C, Kersey JH. Xenotransplantation of human lymphoid malignancies is optimized in mice with multiple immunologic defects. Leukemia. 1998;12(12):2029-2033.

135. Bastide C, Bagnis C, Mannoni P, Hassoun J, Bladou F. A Nod Scid mouse model to study human prostate cancer. Prostate Cancer Prostatic Dis. 2002;5(4):311-315.

136. Custer RP, Bosma GC, Bosma MJ. Severe combined immunodeficiency (SCID) in the mouse. Pathology, reconstitution, neoplasms. Am J Pathol. 1985;120(3):464-477.

137. Bosma MJ. B and T cell leakiness in the scid mouse mutant, Immunodefic Rev. 1992;3(4):261-276.

138. Ohbo K, Suda T, Hashiyama M, Mantani A, Ikebe M, et al. Modulation of hematopoiesis in mice with a truncated mutant of the interleukin-2 receptor gamma chain. Blood. 1996;87(3):956-967.

139. Cao X, Shores EW, Hu-Li J, Anver MR, Kelsail BL, et al. Defective lymphoid development in mice lacking expression of the common cytokine receptor γ chain. Immunity. 1995;2(3):223-238.

140. DiSanto JP, Müller W, Guy-Grand D, Fischer A, Rajewsky K. Lymphoid development in mice with a targeted deletion of the interleukin 2 receptor gamma chain. Proc Natl Acad Sci U S A. 1995;92(2):377-381.

141. Shultz LD, Lyons BL, Burzenski LM, Gott B, Chen X, et al. Human lymphoid and myeloid cell development in NOD/LtSz-scid IL2Rγnull mice engrafted with mobilized human hemopoietic stem cells. J Immunol. 2005;174(10):6477-6489.

142. D'Antonio JM, Vander Griend DJ, Antony L, Ndikuyeze G, Dalrymple SL, et al. Loss of androgen receptor-dependent growth suppression by prostate cancer cells can occur independently from acquiring oncogenic addiction to androgen receptor signaling. PLoS One. 2010;5(7):e11475.

143. Oettinger MA, Schatz DG, Gorka C, Baltimore D. RAG-1 and RAG-2, adjacent genes that synergistically activate V(D)J recombination. Science. 1990;248(4962):1517-1523.

144. Schatz DG, Oettinger MA, Baltimore D. The V(D)J recombination activating gene, RAG-1. Cell. 1989;59(6):1035-1048.

145. Mombaerts P, Iacomini J, Johnson RS, Herrup K, Tonegawa S, et al. RAG-1-deficient mice have no mature B and T lymphocytes. Cell. 1992;68(5):869-877.

146. Shinkai Y, Rathbun G, Lam KP, Oltz EM, Stewart V, et al. RAG-2-deficient mice lack mature lymphocytes owing to inability to initiate V(D)J rearrangement. Cell. 1992;68(5):855-867.

147. Zhang Q, Yang XJ, Kundu SD, Pins M, Javonovic B, et al. Blockade of transforming growth factor-{beta} signaling in tumor-reactive CD8+ T cells activates the antitumor immune response cycle. Mol Cancer Ther. 2006;5(7):1733-1743.

148. Reuther T, Kübler AC, Staff CJ, Flechtenmacher C, Haase T, et al. The RAG 2 mouse model for xenografted human oral squamous cell carcinoma. Contemp Top Lab Anim Sci. 2002;41(2):31-35.

149. Greenberg NM, DeMayo F, Finegold MJ, Medina D, Tilley WD, et al. Prostate cancer in a transgenic mouse. Proc Natl Acad Sci U S A. 1995;92(8):3439-3443.

150. Gingrich JR, Barrios RJ, Morton RA, Boyce BF, DeMayo FJ, et al. Metastatic prostate cancer in a transgenic mouse. Cancer Res. 1996;56(18):4096-4102.

151. Hurwitz AA, Foster BA, Allison JP, Greenberg NM, Kwon ED. The TRAMP mouse as a model for prostate cancer. Curr Protoc Immunol. 2001;20-25.

152. Gingrich JR, Barrios RJ, Foster BA, Greenberg NM. Pathologic progression of autochthonous prostate cancer in the TRAMP model. Prostate Cancer Prostatic Dis. 1999;2(2):70-75.

153. Kaplan-Lefko PJ, Chen TM, Ittmann MM, Barrios RJ, Ayala GE, et al. Pathobiology of autochthonous prostate cancer in a pre-clinical transgenic mouse model. Prostate. 2003;55(3):219-237.

154. Wang F. Modeling human prostate cancer in genetically engineered mice. Prog Mol Biol Transl Sci. 2011;100:1-49.

155. Ahmad I, Sansom OJ, Leung HY. Advances in mouse models of prostate cancer. Expert Rev Mol Med. 2008;10:e16.

156. Kasper S, Smth JA Jr. Genetically modified mice and their use in developing therapeutic strategies for prostate cancer. J Urol. 2004;172(1):12-19.

157. Klein RD. The use of genetically engineered mouse models of prostate cancer for nutrition and cancer chemoprevention research. Mutat Res. 2005;576(1-2):111-119.

158. Grignon DJ. Unusual subtypes of prostate cancer. Mod Pathol. 2004;17(3):316-327.

159. Ishii K, Shappell SB, Matusik RJ, Hayward SW. Use of tissue recombination to predict phenotypes of transgenic mouse models of prostate carcinoma. Lab Invest. 2005;85(9):1086-1103.

160. Kasper S. Survey of genetically engineered mouse models for prostate cancer: Analyzing the molecular basis of prostate cancer development, progression, and metastasis. J Cell Biochem. 2005;94(2):279-297.

161. Hamilton JB, Montagna W. The sebaceous glands of the hamster; morphological effects of androgens on integumentary structures. Am J Anat. 1950;86(2):191-233.

162. Frost P, Giegel JL, Weinstein GD, Gomez EC. Biodynamic studies of hamster flank organ growth: Hormonal influences. J Invest Dermatol. 1973;61(3):159-167.

163. Liang T, Liao S. Growth suppression of hamster flank organs by topical application of gamma-linolenic and other fatty acid inhibitors of 5α-reductase. J Invest Dermatol. 1997;109(2):152-157.

164. Voigt W, Hsia SL. The antiandrogenic action of 4–androsten–3–one–17β–carboxylic acid and its methyl ester on hamster flank organ. Endocrinology. 1973;92(4):1216-1222.

165. Weissmann A, Bowden J, Frank B, Horwitz SN, Frost P. Morphometric studies of the hamster flank organ: an improved model to evaluate pharmacologic effects on sebaceous glands. J Invest Dermatol. 1984;82(5):522-525.

166. Liao S, Hiipakka R. Method and compositions for regulation of 5α-reductase activity U.S. 2004. Patent No. 6,696,484. Washington, DC: U.S. Patent and Trademark Office.

167. Ye F, Imamura K, Imanishi N, Rhodes L, Uno H. Effects of topical antiandrogen and 5α-reductase inhibitors on sebaceous glands in male fuzzy rats. Skin Pharmacol. 1997;10(5-6):288-297.

168. Matias JR, Malloy VL, Orentreich N. Synergistic antiandrogenic effects of topical combinations of 5α-reductase and androgen receptor inhibitors in the hamster sebaceous glands. J Invest Dermatol. 1988;91(5):429-433.

169. Humphrey PA. Gleason grading and prognostic factors in carcinoma of the prostate. Mod Pathol. 2004;17(3):292-306.

170. Berman-Booty LD, Sargeant AM, Rosol TJ, Rengel RC, Clinton SK, et al. A review of the existing grading schemes and a proposal for a modified grading scheme for prostatic lesions in TRAMP mice. Toxicol Pathol. 2012;40(1):5-17.

171. Kumar V, Abbas AK, Fausto N, Aster JC. Pathologic basis of disease. 2005:1525.

172. Opoku-Acheampong AB, Unis D, Henningson JN, Beck AP, Lindshield BL. Preventive and therapeutic efficacy of finasteride and dutasteride in TRAMP Mice. 2013;8:e77738.

173. Liao RS, Ma S, Miao L, Li R, Yin Y, et al. Androgen receptor-mediated non-genomic regulation of prostate cancer cell proliferation. Transl Androl Urol. 2013;2(3):187-196.

174. Langley E, Zhou ZX, Wilson EM. Evidence for an anti-parallel orientation of the ligand-activated human androgen receptor dimer. J Biol Chem. 1995;270:29983-29990.

175. Wong CI, Zhou ZX, Sar M, Wilson EM. Steroid requirement for androgen receptor dimerization and DNA binding. Modulation by intramolecular interactions between the NH_2-terminal and steroid-binding domains. J Biol Chem. 1993;268(25):19004-19012.

176. Kim J, Coetzee GA. Prostate specific antigen gene regulation by androgen receptor. J Cell Biochem. 2004;93(2):233-241.

177. da Silva HB, Amaral EP, Nolasco EL, de Victo NC, Atique R, et al. Dissecting major signaling pathways throughout the development of prostate cancer. Prostate Cancer. 2013;920612.

178. Beato M. Gene regulation by steroid hormones. Cell. 1989;56(3):335-344.

179. Lonergan PE, Tindall DJ. Androgen receptor signaling in prostate cancer development and progression. J Carcinog. 2011;10:20.

180. Elmore S. Apoptosis: A review of programmed cell death. Toxicol Pathol. 2007;35(4):495-516.

181. Formigli L, Papucci L, Tani A, Schiavone N, Tempestini A, et al. Aponecrosis: Morphological and biochemical exploration of a syncretic process of cell death sharing apoptosis and necrosis. J Cell Physiol. 2000;182(1):41-49.

182. Sperandio S, de Belle I, Bredesen DE. An alternative, nonapoptotic form of programmed cell death. Proc Natl Acad Sci U S A. 2000;97(26):14376-14381.

183. Debnath J, Baehrecke EH, Kroemer G. Does autophagy contribute to cell death? Autophagy. 2005;1(2):66-74.

184. Norbury CJ, Hickson ID. Cellular responses to DNA damage. Annu Rev Pharmacol Toxicol. 2001;41:367-401.

185. Saunders M. Apoptosis and cell death. Scott-Brown's Otorhinolaryngology: Head and Neck Surgery (7th ed.). 2008:156.

186. Igney FH, Krammer PH. Death and anti-death: Tumour resistance to apoptosis. Nat Rev Cancer. 2002;2(4):277-288.

187. O'Brien MA, Kirby R. Apoptosis: A review of pro-apoptotic and anti-apoptotic pathways and dysregulation in disease. J Vet Emerg Crit Care. 2008;18(6):572-585.

188. Chicheportiche Y, Bourdon PR, Xu H, Hsu YM, Scott H, et al. TWEAK, a new secreted ligand in the tumor necrosis factor family that weakly induces apoptosis. J Biol Chem. 1997;272(51):32401-32410.

189. Ashkenazi A, Dixit VM. Death receptors: Signaling and modulation. Science. 1998;281(5381): 1305-1308.

190. Peter ME, Krammer PH. Mechanisms of CD95 (APO-1/Fas)-mediated apoptosis. Curr Opin Immunol. 1998;10(5):545-551.

191. Suliman A, Lam A, Datta R, Srivastava RK. Intracellular mechanisms of TRAIL: Apoptosis through mitochondrial-dependent and -independent pathways. Oncogene. 2001;20(17):2122-2133.

192. Rubio-Moscardo F, Blesa D, Mestre C, Siebert R, Balasas T, et al. Characterization of 8p21.3 chromosomal deletions in B-cell lymphoma: TRAIL-R1 and TRAIL-R2 as candidate dosage-dependent tumor suppressor genes. Blood. 2005;106(9):3214-3222.

193. Hsu H, Xiong J, Goeddel DV. The TNF receptor 1-associated protein TRADD signals cell death and NF-kappa B activation. Cell. 1995;81(4):495-504.

194. Wajant H. The Fas signaling pathway: More than a paradigm. Science. 2002;296(5573):1635-1636.

195. Love S. Apoptosis and brain ischaemia. Prog Neuropsychopharmacol Biol Psychiatry. 2003;27(2):267-282.

196. Klionsky DJ, Emr SD. Autophagy as a regulated pathway of cellular degradation. Science. 2000;290(5497):1717-1721.

197. Kischkel FC, Hellbardt S, Behrmann I, Germer M, Pawlita M, et al. Cytotoxicity-dependent APO-1 (Fas/CD95)-associated proteins form a death-inducing signaling complex (DISC) with the receptor. EMBO J. 1995;14(22):5579-5588.

198. Broughton BR, Reutens DC, Sobey CG. Apoptotic mechanisms after cerebral ischemia. Stroke. 2009;40(5):e331-e339.

199. Saelens X, Festjens N, Vande Walle L, van Gurp M, van Loo G, et al. Toxic proteins released from mitochondria in cell death. Oncogene. 2004;23(16):2861-2874.

200. Cai J, Yang J, Jones DP. Mitochondrial control of apoptosis: The role of cytochrome c. Biochim Biophys Acta. 1998;1366(1-2):139-149.

201. Du C, Fang M, Li Y, Li L, Wang X. Smac, a mitochondrial protein that promotes cytochrome c-dependent caspase activation by eliminating IAP inhibition. Cell. 2000;102(1):33-42.

202. van Loo G, Saelens X, van Gurp M, MacFarlane M, Martin SJ, et al. The role of mitochondrial factors in apoptosis: A Russian roulette with more than one bullet. Cell Death Differ. 2002;9(10):1031-1042.

203. Garrido C, Galluzzi L, Brunet M, Puig PE, Didelot C, et al. Mechanisms of cytochrome c release from mitochondria. Cell Death Differ. 2006;13(9):1423-1433.

204. Chinnaiyan AM. The apoptosome: Heart and soul of the cell death machine. Neoplasia. 1999;1(1):5-15.

205. Hill MM, Adrain C, Duriez PJ, Creagh EM, Martin SJ. Analysis of the composition, assembly kinetics and activity of native Apaf-1 apoptosomes. EMBO J. 2004;23(10):2134-2145.

206. Joza N, Susin SA, Daugas E, Stanford WL, Cho SK, et al. Essential role of the mitochondrial apoptosis-inducing factor in programmed cell death. Nature. 2001;410(6828):549-554.

207. Li LY, Luo X, Wang X. Endonuclease G is an apoptotic DNase when released from mitochondria. Nature. 2001;412(6842):95-99.

208. Enari M, Sakahira H, Yokoyama H, Okawa K, Iwamatsu A, et al. A caspase-activated DNase that degrades DNA during apoptosis, and its inhibitor ICAD. Nature. 1998;391(6662):43-50.

209. Slee EA, Adrain C, Martin SJ. Executioner caspase-3, -6, and -7 perform distinct, non-redundant roles during the demolition phase of apoptosis. J Biol Chem. 2001;276(10):7320-7326.

210. Rai NK, Tripathi K, Sharma D, Shukla VK. Apoptosis: A basic physiologic process in wound healing. Int J Low Extrem Wounds. 2005;4(3):138-144.

211. Cohen GM. Caspases: The executioners of apoptosis. Biochem J. 1997;326(Pt 1):1-16.

212. Sakahira H, Enari M, Nagata S. Cleavage of CAD inhibitor in CAD activation and DNA degradation during apoptosis. Nature. 1998;391(6662):96-99.

213. Duan WR, Garner DS, Williams SD, Funckes-Shippy CL, Spath IS, et al. Comparison of immunohistochemistry for activated caspase-3 and cleaved cytokeratin 18 with the TUNEL method for quantification of apoptosis in histological sections of PC-3 subcutaneous xenografts. J Pathol. 2003;199(2):221-228.

214. Kothakota S, Azuma T, Reinhard C, Klippel A, Tang J, et al. Caspase-3-generated fragment of gelsolin: effector of morphological change in apoptosis. Science. 1997;278(5336):294-298.

215. McCubrey JA, LaHair MM, Franklin RA. Reactive oxygen species-induced activation of the MAP kinase signaling pathways. Antioxid Redox Signal. 2006;8(9-10):1775-1789.

216. Kholodenko BN, Birtwistle MR. Four-dimensional dynamics of MAPK information-processing systems. Wiley Interdiscip Rev Syst Biol Med. 2009;1(1):28-44.

217. Rodríguez-Berriguete G, Fraile B, Martínez-Onsurbe P, Olmedilla G, Paniagua R, et al. MAP kinases and prostate cancer. J Signal Transduct. 2012:169170.

218. Sánchez I, Hughes RT, Mayer BJ, Yee K, Woodgett JR, et al. Role of SAPK/ERK kinase-1 in the stress-activated pathway regulating transcription factor c-Jun. Nature. 1994;372(6508):794-798.

219. Lawler S, Fleming Y, Goedert M, Cohen P. Synergistic activation of SAPK1/JNK1 by two MAP kinase kinases in vitro. Curr Biol. 1998;8(25):1387-1390.

220. Fleming Y, Armstrong CG, Morrice N, Paterson A, Goedert M, et al. Synergistic activation of stress-activated protein kinase 1/c-Jun N-terminal kinase (SAPK1/JNK) isoforms by mitogen-activated protein kinase kinase 4 (MKK4) and MKK7. Biochem J. 2000;352 Pt 1:145-154.

221. Wada T, Nakagawa K, Watanabe T, Nishitai G, Seo J, et al. Impaired synergistic activation of stress-activated protein kinase SAPK/JNK in mouse embryonic stem cells lacking SEK1/MKK4:

different contribution of SEK2/MKK7 isoforms to the synergistic activation. J Biol Chem. 2001;276(33):30892-30897.

222. Wang X, Nadarajah B, Robinson AC, McColl BW, Jin JW, et al. Targeted deletion of the mitogen-activated protein kinase kinase 4 gene in the nervous system causes severe brain developmental defects and premature death. Mol Cell Biol. 2007;27(22):7935-7946.

223. Heasley LE, Han SY. JNK regulation of oncogenesis. Mol Cells. 2006;21(2):167-173.

224. Bode AM, Dong Z. The functional contrariety of JNK. Mol Carcinog. 2007;46(8):591-598.

225. Turjanski AG, Vaqué JP, Gutkind JS. MAP kinases and the control of nuclear events. Oncogene. 2007;26(22):3240-3253.

226. Raingeaud J, Gupta S, Rogers JS, Dickens M, Han J, et al. Pro-inflammatory cytokines and environmental stress cause p38 mitogen-activated protein kinase activation by dual phosphorylation on tyrosine and threonine. J Biol Chem. 1995;270(13):7420-7426.

227. Whyte J, Bergin O, Bianchi A, McNally S, Martin F. Mitogen-activated protein kinase signaling in experimental models of breast cancer progression and in mammary gland development. Breast Cancer Res. 2009:11(5):209.

228. Zhao M, New L, Kravchenko VV, Kato Y, Gram H, et al. Regulation of the MEF2 family of transcription factors by p38. Mol Cell Biol. 1999;19(1):21-30.

229. Royuela M, Rodríguez-Berriguete G, Fraile B, Paniagua R. TNF-α/IL-1/NF-kappaB transduction pathway in human cancer prostate. Histol Histopathol. 2008;23(10):1279-1290.

230. Thornton TM, Rincon M. Non-classical p38 map kinase functions: Cell cycle checkpoints and survival. Int J Biol Sci. 2009;5(1):44-51.

231. Thakur N, Sorrentino A, Heldin CH, Landström M. TGF-beta uses the E3-ligase TRAF6 to turn on the kinase TAK1 to kill prostate cancer cells. Future Oncol. 2009;5(1):1-3.

232. Blobe GC, Schiemann WP, Lodish HF. Role of transforming growth factor beta in human disease. N Engl J Med. 2000;342(18):1350-1358.

233. Massagué J. How cells read TGF-β signals. Nat Rev Mol Cell Biol. 2000;1(3):169-178.

234. Massagué J, Seoane J, Wotton D. Smad transcription factors. Genes Dev. 2005;19(23):2783-2810.

235. Ihmann T, Liu J, Schwabe W, Häusler P, Behnke D, et al. High-level mRNA quantification of proliferation marker pKi-67 is correlated with favorable prognosis in colorectal carcinoma. J Cancer Res Clin Oncol. 2004;130(12):749-756.

236. Brown DC, Gatter KC. Ki-67 protein: The immaculate deception? Histopathology. 2002;40(1):2-11.

237. Bologna-Molina R, Mosqueda-Taylor A, Molina-Frechero N, Mori-Estevez AD, Sánchez-Acuña G. Comparison of the value of PCNA and Ki-67 as markers of cell proliferation in ameloblastic tumors. Med Oral Patol Oral Cir Bucal. 2013;18(2):e174-e179.

238. Buchwalow IB, Böcker W. Immunohistochemistry: Basics and methods. Springer Science & Business Media. 2010.

239. Woo M, Hakem R, Soengas MS, Duncan GS, Shahinian A, et al. Essential contribution of caspase 3/CPP32 to apoptosis and its associated nuclear changes. Genes Dev. 1998;12(6):806-819.

240. Boyce BF, Xing L, Jilka RL, Bellido T, Weinstein RS, et al. Apoptosis and bone cells. In: Bilezikian JP, Raisz LG, Rodan GA, eds. Principles of bone biology. Academic Press. 2002;2:151-168.

241. Gold R, Schmied M, Giegerich G, Breitschopf H, Hartung HP, et al. Differentiation between cellular apoptosis and necrosis by the combined use of in situ tailing and nick translation techniques. Lab Invest. 1994;71(2):219-225.

242. McGahon A, Bissonnette R, Schmitt M, Cotter KM, Green DR, et al. BCR-ABL maintains resistance of chronic myelogenous leukemia cells to apoptotic cell death. Blood. 1994;83(5):1179-1187.

243. Gavrieli Y, Sherman Y, Ben-Sasson SA. Identification of programmed cell death in situ via specific labeling of nuclear DNA fragmentation. J Cell Biol. 1992;119(3):493-501.

244. Jänicke RU, Sprengart ML, Wati MR, Porter AG. Caspase-3 is required for DNA fragmentation and morphological changes associated with apoptosis. J Biol Chem. 1998;273(16):9357-9360.

245. Fan TJ, Han LH, Cong RS, Liang J. Caspase family proteases and apoptosis. Acta Biochim Biophys Sin (Shanghai). 2005;37(11):719-727.

246. Wolf BB, Schuler M, Echeverri F, Green DR. Caspase-3 is the primary activator of apoptotic DNA fragmentation via DNA fragmentation factor-45/inhibitor of caspase-activated DNase inactivation. J Biol Chem. 1999;274(43):30651-30656.

247. Chodak GW, Kranc DM, Puy LA, Takeda H, Johnson K, et al. Nuclear localization of androgen receptor in heterogeneous samples of normal, hyperplastic and neoplastic human prostate. J Urol. 1992;147(3 Pt 2):798-803.

248. Heinlein CA, Chang C. Androgen receptor in prostate cancer. Endocr Rev. 2004;25(2):276-308.

249. Osman WM, Abd El Atti RM, Abou Gabal HH. DJ-1 and androgen receptor immunohistochemical expression in prostatic carcinoma: A possible role in carcinogenesis. J Egypt Natl Canc Inst. 2013;25(4):223-230.

250. Li R, Wheeler T, Dai H, Frolov A, Thompson T, et al. High level of androgen receptor is associated with aggressive clinicopathologic features and decreased biochemical recurrence-free survival in prostate: cancer patients treated with radical prostatectomy. Am J Surg Pathol. 2004;28(7):928-934.

251. Takayama K, Inoue S. Transcriptional network of androgen receptor in prostate cancer progression. Int J Urol. 2013;20(8):756-768.

252. Maudelonde T, Rosenfield RL, Shuler CF, Schwartz SA. Studies of androgen metabolism and action in cultured hair and skin cells. J Steroid Biochem. 1986;24(5):1053-1060.

253. Tamura M, Sueishi T, Sugibayashi K, Morimoto Y, Juni K, et al. Metabolism of testosterone and its ester derivatives in organotypic coculture of human dermal fibroblasts with differentiated epidermis. Int J Pharm. 1996;131(2):263-271.

254. Condac E, Georgescu SE, Dinischiotu A, Iordachescu D, Costache M. A Non-radioactive FPLC method for measuring steroid 5α-reductase activity in cultured cells. Rom Biotechnol Lett. 2004;9:1517-1522.

255. Levine AC, Wang JP, Ren M, Eliashvili E, Russell DW, et al. Immunohistochemical localization of steroid 5α-reductase 2 in the human male fetal reproductive tract and adult prostate. J Clin Endocrinol Metab. 1996;81(1):384-389.

256. Silver RI, Wiley EL, Davis DL, Thigpen AE, Russell DW, et al. Expression and regulation of steroid 5α-reductase 2 in prostate disease. J Urol. 1994;152(2 Pt 1):433-437.

257. Taylor CR, Burns J. The demonstration of plasma cells and other immunoglobulin-containing cells in formalin-fixed, paraffin-embedded tissues using peroxidase-labelled antibody. J Clin Pathol. 1974;27(1):14-20.

258. Engel P, Gómez-Puerta JA, Ramos-Casals M, Lozano F, Bosch X. Therapeutic targeting of B cells for rheumatic autoimmune diseases. Pharmacol Rev. 2011;63(1):127-156.

259. Ramos-Vara JA. Technical aspects of immunohistochemistry. Vet Pathol. 2005;42(4):405-426.

260. Chailyan A, Tramontano A, Marcatili P. A database of immunoglobulins with integrated tools: DIGIT. Nucleic Acids Res. 2012;40:D1230-D1234.

261. Huang GS, Chen YS, Yeh HW. Measuring the flexibility of immunoglobulin by gold nanoparticles. Nano Lett. 2006;6(11):2467-2471.

262. Hayat MA. Antigens and antibodies. In: Hayat MA, ed. Microscopy, Immunohistochemistry, and antigen retrieval methods for light and electron microscopy. Kluwer Academic. 2002:31–51

263. Mighell AJ, Hume WJ, Robinson PA. An overview of the complexities and subtleties of immunohistochemistry. Oral Dis. 1998;4(3):217-223.

264. Boenisch T, Farmilo AJ. Handbook on immunochemical staining methods. 2001. Gostrup, Denmark: DAKO.

265. Taylor KB, Roitt IM, Doniach D, Couchman KG, Shapland C. Autoimmune phenomena in pernicious anaemia: Gastric antibodies. Br Med J. 1962;2(5316):1347-1352.

266. Coons AH, Kaplan MH. Localization of antigen in tissue cells; improvements in a method for the detection of antigen by means of fluorescent antibody. J Exp Med. 1950;91(1):1-13.

267. Hsu SM, Raine L. Protein A, avidin, and biotin in immunohistochemistry. J Histochem Cytochem. 1981;29(11):1349-1353.

268. Ormanns W, Schäffer R. An alkaline-phosphatase staining method in avidin-biotin immunohistochemistry. Histochemistry. 1985;82(5):421-424.

269. Ludwin SK, Kosek JC, Eng LF. The topographical distribution of S-100 and GFA proteins in the adult rat brain: An immunohistochemical study using horseradish peroxidase-labelled antibodies. J Comp Neurol. 1976;165(2):197-207.

270. Malik SN, Brattain M, Ghosh PM, Troyer DA, Prihoda T, et al. Immunohistochemical demonstration of phospho-Akt in high Gleason grade prostate cancer. Clin Cancer Res. 2002;8(4):1168-1171.

271. Siegel D, Franklin WA, Ross D. Immunohistochemical detection of NAD(P)H:quinone oxidoreductase in human lung and lung tumors. Clin Cancer Res. 1998;4(9):2065-2070.

272. Gorski JA, Talley T, Qiu M, Puelles L, Rubenstein JL, et al. Cortical excitatory neurons and glia, but not GABAergic neurons, are produced in the Emx1-expressing lineage. J Neurosci. 2002;22(15):6309-6314.

273. Kriegsmann J, Keyszer G, Geiler T, Gay RE, Gay S. A new double labeling technique for combined in situ hybridization and immunohistochemical analysis. Lab Invest. 1994;71(6):911-917.

274. Polak JM, Van Noorden S. Introduction to immunocytochemistry; 1997. Introduction to immunocytochemistry (2nd ed.). Oxford: Bios Scientific Publishers.

275. Davidoff M, Schulze W. Combination of the peroxidase anti-peroxidase (PAP)-and avidin-biotin-peroxidase complex (ABC)-techniques: An amplification alternative in immunocytochemical staining. Histochemistry. 1990;93(5):531-536.

276. Russo J, Russo IH. Techniques and methodological approaches in breast cancer research. Springer. 2014.

277. Lu QL, Partridge TA. A new blocking method for application of murine monoclonal antibody to mouse tissue sections. J Histochem Cytochem. 1998;46(8):977-984.

278. Elias JM, Margiotta M, Gaborc D. Sensitivity and detection efficiency of the peroxidase antiperoxidase (PAP), avidin-biotin peroxidase complex (ABC), and peroxidase-labeled avidin-biotin (LAB) methods. Am J Clin Pathol. 1989;92(1):62-67.

279. Sternberger LA, Hardy PH Jr, Cuculis JJ, Meyer HG. The unlabeled antibody enzyme method of immunohistochemistry: preparation and properties of soluble antigen-antibody complex (horseradish

peroxidase-antihorseradish peroxidase) and its use in identification of spirochetes. J Histochem Cytochem. 1970;18(5):315-333.

280. Taylor CR, Shi SR, Barr NJ, Wu N. Techniques of immunohistochemistry: principles, pitfalls, and standardization. Diagnostic immunohistochemistry. 2001;2:3-44.

281. Key M. Immunohistochemistry Staining Methods. Education Guide (4th ed.). 2006;47.

282. Heras A, Roach CM, Key ME. Enhanced polymer detection system for immunohistochemistry. Lab Invest 1995;72:165.

283. Chilosi M, Lestani M, Pedron S, Montagna L, Benedetti A, et al. A rapid immunostaining method for frozen sections. Biotech Histochem 1994;69:235.

284. Hayat MA. Microscopy, immunohistochemistry, and antigen retreival methods. For light and electron microscopy. Springer. 2002.

285. Sompuram SR, Vani K, Messana E, Bogen SA. A molecular mechanism of formalin fixation and antigen retrieval. Am J Clin Pathol. 2004;121(2):190-199.

286. Hecke DV. Routine immunohistochemical staining today: Choices to make, challenges to take. J Histotechnol. 2002;25:45–54.

287. Battifora H, Kopinski M. The influence of protease digestion and duration of fixation on the immunostaining of keratins. A comparison of formalin and ethanol fixation. J Histochem Cytochem. 1986;34(8):1095-1100.

288. Jacobsen M, Clausen PP, Smidth S. The effect of fixation and trypsinization on the immunohistochemical demonstration of intracellular immunoglobulin in paraffin embedded material. Acta Pathol Microbiol Scand A. 1980;88(6):369-376.

289. Pinkus GS, O'Connor EM, Etheridge CL, Corson JM. Optimal immunoreactivity of keratin proteins in formalin-fixed, paraffin-embedded tissue requires preliminary trypsinization. An immunoperoxidase study of various tumours using polyclonal and monoclonal antibodies. J Histochem Cytochem. 1985;33(5):465-473.

290. Brown C. In situ hybridization with riboprobes: An overview for veterinary pathologists. Vet Pathol. 1998;35(3):159-167.

291. Wang F, Flanagan J, Su N, Wang LC, Bui S, et al. RNAscope: A novel in situ RNA analysis platform for formalin-fixed, paraffin-embedded tissues. J Mol Diagn. 2012;14(1):22-29.

Chapter 2 - Effect of Saw Palmetto Supplements on Androgen-Sensitive LNCaP Human Prostate Cancer Cell Number and Syrian Hamster Androgen-Sensitive Flank Organ Growth

Abstract

Background: Saw palmetto supplements (SPS) are consumed by men with prostate cancer. SPS' antiandrogen action may be related to their ability to inhibit 5α-reductase enzymes, which convert testosterone to the more potent dihydrotestosterone (DHT). SPS contain phytosterols and fatty acids, with the saturated medium-chain fatty acids laurate and myristate thought to be bioactive components. We investigated whether SPS fatty acid and phytosterol concentrations determine their growth-inhibitory action in androgen-sensitive LNCaP human prostate cancer cells and androgen-sensitive Syrian hamster flank organs.

Method/Principal findings: LNCaP cells were treated with high long-chain fatty acids (FA)-low phytosterols (HLLP), high long-chain FA-high phytosterols (HLHP) or high medium-chain FA-low phytosterols (HMLP) SPS with and without 10 nM testosterone or 1 nM DHT. HMLP SPS above 750 nM or with androgens, and HLHP SPS above 500 nM with DHT significantly decreased LNCaP cell number. HLLP SPS above 750 nM with testosterone significantly increased or above 500 nM with DHT significantly decreased LNCaP cell number. In animal studies, five to six-week-old, castrated male Syrian hamsters treated with testosterone or DHT (0.5 μg each) were randomized to control, HLLP, HLHP and HMLP groups. Testosterone or DHT was applied topically daily for 21 days to the right flank organ; the control left flank organ was treated with ethanol. Thirty minutes later, SPS or ethanol was applied to each flank organ in treatment and control groups, respectively. SPS treatments caused notable, but nonsignificant reduction in the difference between the left and right flank organ growth in the

testosterone-treated SPS groups. The same level of inhibition was not seen in the DHT-treated SPS groups.

Conclusion: The results suggest saw palmetto supplements may be better at inhibiting the conversion of testosterone to DHT to prevent Syrian hamster androgen-sensitive flank organ growth. SPS with longer-chain fatty acids were more effective in decreasing Syrian-hamster androgen-sensitive flank organ growth.

Contributors to study

Conceived and designed the experiments: Alexander B. Opoku-Acheampong, Brian L. Lindshield. Performed the experiments: Alexander B. Opoku-Acheampong, Kavitha Penugonda. Analyzed the data: Alexander B. Opoku-Acheampong, Brian L. Lindshield. Contributed reagents/materials/analysis tools: Alexander B. Opoku-Acheampong. Wrote the manuscript: Alexander B. Opoku-Acheampong.

Introduction

Prostate cancer is the most common non-skin cancer in men and is projected to account for 26% of US male cancer cases in 2015 [1]. Androgens stimulate growth of most prostate cancers, thus inhibiting androgen metabolism or action is a common approach to combating this malignancy. 5α-reductase 1, 5α-reductase 2 and 5α-reductase 3 isoenzymes are potential targets because they convert testosterone to the more potent androgen, dihydrotestosterone (DHT), which binds with up to 10-fold higher affinity to the androgen receptor than testosterone [2-5]. The 5α-reductase inhibitors finasteride (Proscar and Propecia) and dutasteride (Avodart) are commonly used by men diagnosed with benign prostatic hyperplasia (BPH) to help alleviate the nonmalignant enlargement of the prostate that occurs in this condition [6]. Both finasteride and dutasteride have been shown to reduce prostate cancer risk in large clinical trials, however, this reduction in risk was coupled with an increased risk of more aggressive

prostate cancer [7,8]. Non-pharmaceutical, mild inhibitors of 5α-reductase enzymes may therefore reduce prostate cancer risk without increasing aggressive prostate cancer risk.

Saw palmetto extract inhibited 5α-reductase and decreased growth of human prostatic cells *in vitro* [9-11], decreased prostate tumor progression and prostate DHT concentrations in transgenic adenocarcinoma of the mouse prostate (TRAMP) mice [12], and prostate growth and hyperplasia in castrated, DHT-implanted, and sulpiride-treated rats [13]. Saw palmetto extract decreased testosterone-stimulated prostate growth to about the same size as in non-castrated rats [14]. SPS may have antiandrogen action as demonstrated by the ability of the lipidosterolic extract of these supplements to decrease testosterone-induced prostate hyperplasia [15] and decrease prostate specific antigen (PSA) levels in men with enlarged prostates [16]. PSA is an androgen-sensitive, prostate-specific gene that is commonly used for prostate cancer screening [17].

The antiandrogen action of SPS has been attributed to the fatty acids and phytosterols that they contain. In particular, what is relatively unique about SPS is that they are a rich source of the medium-chain saturated fatty acids laurate (C12:0) and myristate (C14:0) [18]. Multiple studies [19-21] suggest that fatty acids in SPS are responsible for their ability to inhibit 5α-reductase enzymes. However, the specific fatty acid(s) purported to be responsible for this inhibition differs between publications. For example, Liang and colleagues found that γ-linolenic acid inhibited testosterone-treated but not DHT-treated growth of hamster androgen-sensitive flank organs [22]. Oleate and laurate have also been found to be responsible for the pharmacological effects of SPS as shown by their inhibitory effect on 5α-reductase in rats [23]. Laurate and myristate have been shown to inhibit epithelial and stromal 5α-reductase activity in human BPH [24].

There are also multiple studies that suggest that SPS phytosterols (β-sitosterol, campesterol, and stigmasterol) inhibit 5α-reductase [25], prostate cancer cell/tumor growth [26-28], and/or BPH symptoms [29]. Most prostate cancers rely on androgens for growth at the initial stages of development,

thus inhibiting androgen production or blocking its action can be useful in the early treatment or prevention of prostate cancer [30-32]. There is growing evidence to suggest that single-agent interventions identified using a reductionist approach are not an effective strategy for decreasing cancer risk [33]. Rather than taking a reductionist approach to try to identify the bioactive compound(s) in SPS, we set out to determine the efficacy of supplements with different fatty acid and phytosterol profiles (high long-chain FA-low phytosterols, high long-chain FA-high phytosterols and high medium-chain FA-low phytosterols) in decreasing androgen-sensitive LNCaP human prostate cancer cell number and Syrian hamster androgen-sensitive flank organ growth.

The cell culture studies tested which concentration of total fatty acids in SPS is capable of decreasing androgen-sensitive LNCaP human prostate cancer cell [34-36] number without inducing cytotoxicity with and without androgen stimulation. The Syrian hamster was selected for animal studies because their flank organs have sebaceous glands and hair follicles that are highly dependent on androgens [37,38]. Application of SPS to the flank organs of the Syrian hamsters is a way to topically determine whether SPS potentially have antiandrogenic activity. We hypothesized that SPS with high concentration of total fatty acids will significantly decrease LNCaP cell number and Syrian hamster flank organ growth.

Materials and Methods

Ethics statement

The Institutional Animal Care and Use Committee (IACUC) at Kansas State University approved all animal procedures (protocol 3382).

Saw palmetto supplements fatty acids and phytosterols extraction and quantification

Fatty acid and phytosterol profiles of saw palmetto supplements (GNC Herbal Plus SPS, GNC Corporation, Pittsburgh, PA; Jarrow Formulas SPS, Superior Nutrition and Formulation, Los Angeles,

CA; Doctor's Best SPS, All Star Health, Huntington Beach, CA) were analyzed according to previously described method [39] and categorized into high long-chain fatty acids-low phytosterols (HLLP), high long-chain fatty acids-high phytosterols (HLHP), and high medium-chain fatty acids-low phytosterols (HMLP) groups, respectively.

Cell culture and reagents

LNCaP cells [androgen-dependent, prostate adenocarcinoma cells derived from lymph node metastasis (CRL-1740); American Type Culture Collection, Manassas, VA] were grown in Roswell Park Memorial Institute (RPMI)-1640 medium (GIBCO Invitrogen, Carlsband, CA) containing 2 g/L glucose supplemented with 10% fetal bovine serum (Atlanta Biologicals, Inc., Flowery Branch, GA) at 37°C in a 5% CO_2, 95% air-humidified atmosphere incubator. LNCaP cells were maintained in T-75 TPP tissue culture flasks (Midwest Scientific, Inc., Valley Park, MO) with media changed every 72 hours.

Saw palmetto supplements and treatment media for in vitro study

Stock solutions of SPS [GNC Herbal Plus (HLLP), Doctor's Best (HMLP), and Jarrow Formulas (HLHP)] were prepared by dissolving supplements to a total fatty acid concentration of 1 M in dimethyl sulfoxide (DMSO, Sigma-Aldrich, St Louis, MO), and serial dilutions were prepared to concentrations of 0.25 M, 0.5 M and 0.75 M. The SPS concentrations used were based on total fatty acid concentrations that did not cause LNCaP cell death. Fresh dilutions were prepared and stored at 4°C, and used for the 3-day treatment duration of each experiment. SPS treatment media were prepared by dissolving respective saw palmetto stock solutions (0.25 M-1 M) in RPMI-1640 media (0.1% v/v) to concentrations of 250 nM, 500 nM, 750 nM and 1000 nM, and media used once at the beginning of the 72-hour treatment period. SPS with androgen treatment media were prepared daily by dissolving respective saw palmetto stock solutions (0.25 M-1 M) with either testosterone [(10,000 nM) or DHT (1000 nM); both from Steraloids, Inc., Newport, RI)] in media (0.1% v/v for both SPS and androgens) to concentrations

of 250 nM-1000 nM SPS + 10 nM testosterone or 1 nM DHT, respectively, during the 3-day treatment period. Both androgens were dissolved in absolute ethanol and the final ethanol concentration in media was 0.1%. These androgen concentrations maximally stimulate LNCaP cell proliferation [40,41].

A negative control was prepared by dissolving DMSO (0.1% v/v) and/or ethanol (0.1% v/v) in media. Positive controls for SPS with androgen treatments were prepared by dissolving either testosterone or DHT (0.1% v/v) and DMSO (0.1% v/v) in media. In all cell culture treatments, the final DMSO concentration was 0.1%. LNCaP cells (passage number ≤18) were plated at a density of 20,000 cells per well in 96-well plates (Fisher Scientific, Pittsburg, PA) in 6.3 mg/ml penicillin and 10.1 mg/ml streptomycin antibiotic (both from Sigma-Aldrich, St Louis, MO) RPMI-1640 media. Twenty-four hours after plating, LNCaP cells were treated separately with different SPS (250 nM-1000 nM) with and without testosterone (10 nM) or DHT (1 nM) for 72 hours. LNCaP cells were treated with androgens because they stimulate LNCaP cell proliferation [36].

Cell number and cytotoxicity assays

Cell number and cytotoxicity were quantified using the CellTiter 96 AQueous One Solution Assay and Cytotox 96 Non-radioactive Cytotoxicity Assay, respectively (both from Promega Corporation, Madison, WI) with a BioTek Synergy HT Plate reader (BioTek, Winooski, VT) with a reference wavelength of 490 nm. Cell cytotoxicity was calculated as experimental lactate dehydrogenase (LDH) release of the treatment groups divided by control and expressed as a percentage. Cell culture experiments were repeated in three replicates.

Animal study

Five to six-week-old, castrated male Syrian hamsters were purchased (Harlan Laboratories, Inc., Indianapolis, IN) and allowed to acclimate for one week before treatment was initiated. Hamsters were housed individually in plastic cages, had free access to Purina LabDiet 5001 (LabDiet, St Louis, MO)

and water, and were maintained on a 12-h light/12-h dark cycle. The day before treatment begun, the backs of the hamsters were shaved with electric clippers to expose flank organs, a procedure that was repeated weekly during the 21-day study. The study was terminated after 3 weeks. Hamsters were randomized to control (n = 4), high long-chain fatty acids-low phytosterols (n = 6), high long-chain fatty acids-high phytosterols (n = 6), and high medium-chain fatty acids-low phytosterols (n = 6), groups (Table 2.2). To determine if SPS were inhibiting 5α-reductase enzymes, testosterone or DHT (0.5 µg/day) dissolved in 5 µl of ethanol was applied daily to the right hind flank organ using a pipette and disposable tips. The androgens' dosage was used previously and found to stimulate androgen-sensitive flank organ growth moderately to approximately 15–20 mm^2 and exhibited about 50–70% of the maximum stimulation [42]. The left hind flank organ served as the control and was treated with ethanol only. Thirty minutes later, SPS or ethanol (5 µl) were applied to each flank organ in treatment groups and control groups, respectively, using a pipette and disposable tips [43]. Hamsters were euthanized by CO_2-induced asphyxiation. Flank organ area was calculated weekly by taking 2 diameter measurements 90 degrees apart with an electronic, digital, high-precision Mitutoyo caliper (Tokyo, Japan), and using the formula for area of an ellipse: area = π*(length/2)*(width/2), as previously described [44]. The average flank organ area in a group was calculated by summing the individual left or right hind flank organ areas for each hamster in the group, and then dividing by the total number of left or right flank organ sites respectively in the group.

Statistical analysis

Data were analyzed using SAS 9.3 (SAS Institute Inc., Cary, NC) with $p<0.05$ considered statistically significant. Saw palmetto treatments cell number and cytotoxicity data were analyzed using ANOVA with Dunnett's test. Animal study results were analyzed using ANOVA with Fisher's Least Significant Difference (LSD).

Results

Effect of saw palmetto supplements with and without testosterone or DHT stimulation on LNCaP cell number

Doctor's Best SPS had the highest total fatty acid content, followed by GNC Herbal Plus SPS, and then Jarrow Formulas SPS. Doctor's Best SPS contained the highest amount of laurate and myristate, followed by Jarrow Formulas SPS, and then GNC Herbal Plus SPS. Jarrow Formula SPS contained the highest total phytosterol, followed by Doctor's Best SPS, and then GNC Herbal Plus SPS (Table 2.1). Cell number was significantly decreased to 85% of the control with 750 nM of HLLP SPS in testosterone-stimulated LNCaP cells (Figure 2.1B), and significantly decreased to 91%, 92% and 86% of the control with 500 nM, 750 nM and 1000 nM of HLLP SPS, respectively for DHT-stimulated LNCaP cells (Figure 2.1C). Treatment of LNCaP cells with HLHP SPS significantly increased cell number to 112% and 113% of the control with 750 nM and 1000 nM of HLHP SPS, respectively (Figure 2.2A). Cell number was significantly increased to 160% of the control with 250 nM of HLHP SPS for testosterone-stimulated LNCaP cells (Figure 2.2B), and significantly decreased to 88% and 76% of the control with 500 nM and 1,000 nM of HLHP SPS, respectively for DHT-stimulated LNCaP cells (Figure 2.2C). Treatment of LNCaP cells with HMLP SPS significantly decreased cell number to 78% and 64% of the control with 750 nM and 1000 nM of HMLP SPS, respectively (Figure 2.3A). Cell number was significantly decreased to 58% and 72% of the control with 750 nM and 1000 nM of HMLP SPS, respectively, for testosterone-stimulated LNCaP cells (Figure 2.3B), and to 79% and 72% of the control with 750 nM and 1000 nM of HMLP SPS, respectively for DHT-stimulated LNCaP cells (Figure 2.3C). Both HMLP SPS at 750 nM with testosterone stimulation, and 1000 nM HMLP SPS with DHT stimulation inhibited the 50% growth ($ED_{50}S$) of LNCaP cells therefore, a cytotoxicity assay was performed to determine whether this growth inhibition was due to the toxic effect of HMLP SPS at their

respective concentrations with and without androgen treatment. Results showed that HMLP SPS was not cytotoxic to LNCaP cells with and without androgen stimulation (data not shown).

Final body weights, food intake and flank organ areas

There were no significant differences in final body weights, daily food intake, and differences in the left and right flank organ areas between SPS treatment groups (Table 2.3). SPS treatments caused a notable, but nonsignificant reduction in the difference between the left and right flank organ growth in the testosterone-treated SPS groups. The same level of inhibition was not seen in the DHT-treated SPS groups. Right flank organs for controls in both testosterone- and DHT-treated SPS groups were highly pigmented; the left flank organs were not. No pigmentation was seen in either flank organs in the treatment groups (data not shown).

Discussion

We set out to determine the growth-inhibitory effect of SPS with different fatty acid and phytosterol profiles on androgen-sensitive human prostate cancer LNCaP cell number *in vitro* with and without testosterone or DHT stimulation, and the effect of these supplements to inhibit testosterone- or DHT-stimulated growth of androgen-sensitive flank organs in castrated Syrian hamsters.

In LNCaP cells, HMLP SPS significantly decreased cell number at high concentrations with and without testosterone or DHT stimulation. HLLP SPS significantly decreased cell number at high concentrations with testosterone or DHT stimulation. HLHP SPS on the other hand, increased cell number with and without testosterone stimulation, but significantly decreased cell number at high concentrations with DHT stimulation. Overall, SPS' reduced cell number more effectively in the presence of androgens, in comparison to cells that were grown in the presence of SPS only. This may suggest that SPS appear to interfere with testosterone and DHT-mediated growth pathway in LNCaP cells. It is also significant to note that there was no significant difference in LNCaP cell number between

either testosterone or DHT positive controls and the DMSO-control in all the SPS treatment groups. Given that fetal bovine serum used in media preparation lacked androgen, it was expected that there would have been a significant difference in cell number between the androgen-stimulated LNCaP cells and the control. LNCaP cell growth has been found to be inhibited when exogenous androgen is added to 10% fetal calf serum supplemented media. In prostate cancer, androgen receptor operates as a licensing factor for DNA replication required for prostate cancer cell proliferation. At high levels of testosterone, the level of DHT becomes too high preventing androgen receptor degradation during mitosis and thus inhibiting prostate cancer cell growth [45-47]. LNCaP derivative cells that grow in androgen depleted media can also be inhibited by normal levels of DHT (1- l0 nM). Androgen dependent cells that have survived androgen ablation can also acclimate to low levels of androgens and ultimately become androgen insensitive [48].

In animal studies, SPS treatments did not significantly reduce the difference between the left and right flank organ growth in the testosterone- and DHT-treated SPS groups. This is in contrast with results from a previous study which found that γ-linolenic acid inhibited testosterone-stimulated flank organ growth but not DHT-stimulated flank organ growth. Fatty acid compounds with less than 18 carbons have been found to be less effective at inhibiting flank organ growth [22]. HMLP SPS, which had the highest concentration of saturated medium-chain fatty acids, laurate and myristate, did not significantly reduce testosterone- or DHT-stimulated flank organ growth. Although not statistically significant, it is worth noting that HLLP SPS was more effective than HLHP SPS, and the latter more effective than HMLP SPS in both the testosterone and DHT-treated SPS groups in reducing flank organ area. This could mean either laurate or myristate are not the only bioactive components, or that there is a synergistic effect of either specific or all of either fatty acids and/or phytosterols in SPS responsible for their inhibitory effect on the growth of androgen-sensitive flank organs of Syrian hamsters. It might also mean that longer-chain fatty acids are more effective as suggested by a previous publication [22].

SPS treatments caused a notable, but nonsignificant reduction in the difference between the left and right flank organ growth in the testosterone-treated SPS groups. The same level of inhibition was not observed in the DHT-treated SPS groups which may suggest that flank organ growth depends on the local conversion of testosterone to DHT. The right flank organs for controls in both testosterone- and DHT-treated saw palmetto groups were highly pigmented indicating that the androgens were stimulating flank organ growth and causing pigmentation in the hair shaft and near the orifice of the hair follicles [42]. The lack of pigmentation of flank organs in the treatment groups may indicate that SPS were neutralizing the growth stimulation mediated by testosterone and DHT to some extent. Additional studies are required to determine SPS bioactive components and/or their synergistic relationship responsible for their growth-inhibitory effect on the androgen-sensitive flank organs of Syrian hamsters.

Conclusions

The results suggest SPS may be better at inhibiting the conversion of testosterone to DHT to prevent Syrian hamster androgen-sensitive flank organ growth. HLLP and HLHP SPS were more effective than HMLP SPS in reducing flank organ area in both testosterone- and DHT-treated SPS groups suggesting that saw palmetto supplements with longer-chain fatty acids were more effective in decreasing Syrian-hamster androgen-sensitive flank organ growth.

Table 2.1 Fatty acid and phytosterol quantities (mg/g) in saw palmetto supplements

Fatty acid quantities (mg/g) in saw palmetto supplements			
	GNC Herbal Plus	**Jarrow Formulas**	**Doctor's Best**
Laurate (C12:0)	83.3	107.2	274.9
Myristate (C14:0)	31.8	42.5	102.9
Palmitate (C16:0)	97.7	85.7	80.7
Stearate (C18:0)	25.5	32.3	18.0
Oleate (C18:1)	551.8	224.6	296.5
Linoleate (C18:2)	68.9	259.1	48.6
Other fatty acids	59.7	51.2	98.4
Total Fatty Acids	**918.7**	**802.6**	**920.0**
Phytosterol quantities (mg/g) in saw palmetto supplements			
Campesterol	0.2	21.5	0.7
Stigmasterol	0.1	10.1	0.3
β-sitosterol	1.0	33.5	2.3
Total Phytosterols	**1.3**	**65.1**	**3.3**

Table 2.2 Study design

+ Testosterone (0.5 µg/day)	**+ DHT (0.5 µg/day)**
Control (Ethanol only)	Control (Ethanol only)
GNC Herbal Plus (HLLP)	GNC Herbal Plus (HLLP)
Jarrow Formulas (HLHP)	Jarrow Formulas (HLHP)
Doctor's Best (HMLP)	Doctor's Best (HMLP)

Table 2.3. Final body weights, daily food intake, and flank organ area in the testosterone (T) and DHT-treated SPS groups.

Treatment of right flank organ testosterone or DHT; 0.5 µg/5 µl ethanol + saw palmetto supplement	**Final body weights (g)**	**Daily food intake (g)**	**Flank organ area (mm^2)**	
			Left (untreated)	**Right (treated)**
Testosterone + Ethanol (Control)	104.0 ± 2.4	8.7 ± 0.3	19.8 ± 0.7	22.7 ± 2.9
Testosterone + HLHP	106.4 ± 4.4	8.1 ± 0.2	18.0 ± 0.9	20.2 ± 1.3
Testosterone + HLLP	110.7 ± 3.5	8.1 ± 0.2	19.2 ± 1.6	18.9 ± 1.3
Testosterone + HMLP	109.9 ± 4.8	8.3 ± 0.2	17.6 ± 1.4	19.1 ± 1.2
DHT + Ethanol (Control)	103.6 ± 2.5	7.9 ± 0.2	22.4 ± 1.2	23.5 ± 1.6
DHT + HLHP	100.9 ± 5.8	8.4 ± 0.3	18.0 ± 1.4	19.1 ± 1.5
DHT + HLLP	103.9 ± 4.3	8.1 ± 0.3	19.0 ± 2.2	22.3 ± 2.4
DHT + HMLP	108.4 ± 5.2	7.9 ± 0.2	20.4 ± 1.1	21.9 ± 1.9

Table 2.4. Difference between flank organ growth in the left and right flank organs in the testosterone- (T) and DHT-treated SPS groups.

Treatment of right flank organ T or DHT; 0.5 µg/5 µl ethanol + saw palmetto supplement	**Flank organ growth (mm^2)**		**Difference between left and right flank organ growth (mm^2)**
	Left (untreated)	**Right (treated)**	
Testosterone + Ethanol (Control)	1.4 ± 2.7	8.5 ± 1.8	7.1 ± 2.3
Testosterone + HLHP	2.2 ± 1.7	2.8 ± 2.6	0.6 ± 1.5
Testosterone + HLLP	3.2 ± 1.5	2.1 ± 1.2	-1.2 ± 1.9
Testosterone + HMLP	1.8 ± 1.5	3.2 ± 1.8	1.4 ± 2.7
DHT + Ethanol (Control)	0.2 ± 1.7	4.8 ± 3.2	4.6 ± 4.1
DHT + HLHP	0.7 ± 2.0	4.1 ± 2.0	3.4 ± 2.9
DHT + HLLP	5.2 ± 2.2	7.4 ± 1.8	2.1 ± 1.3
DHT + HMLP	4.6 ± 1.9	8.3 ± 3.4	3.7 ± 2.4

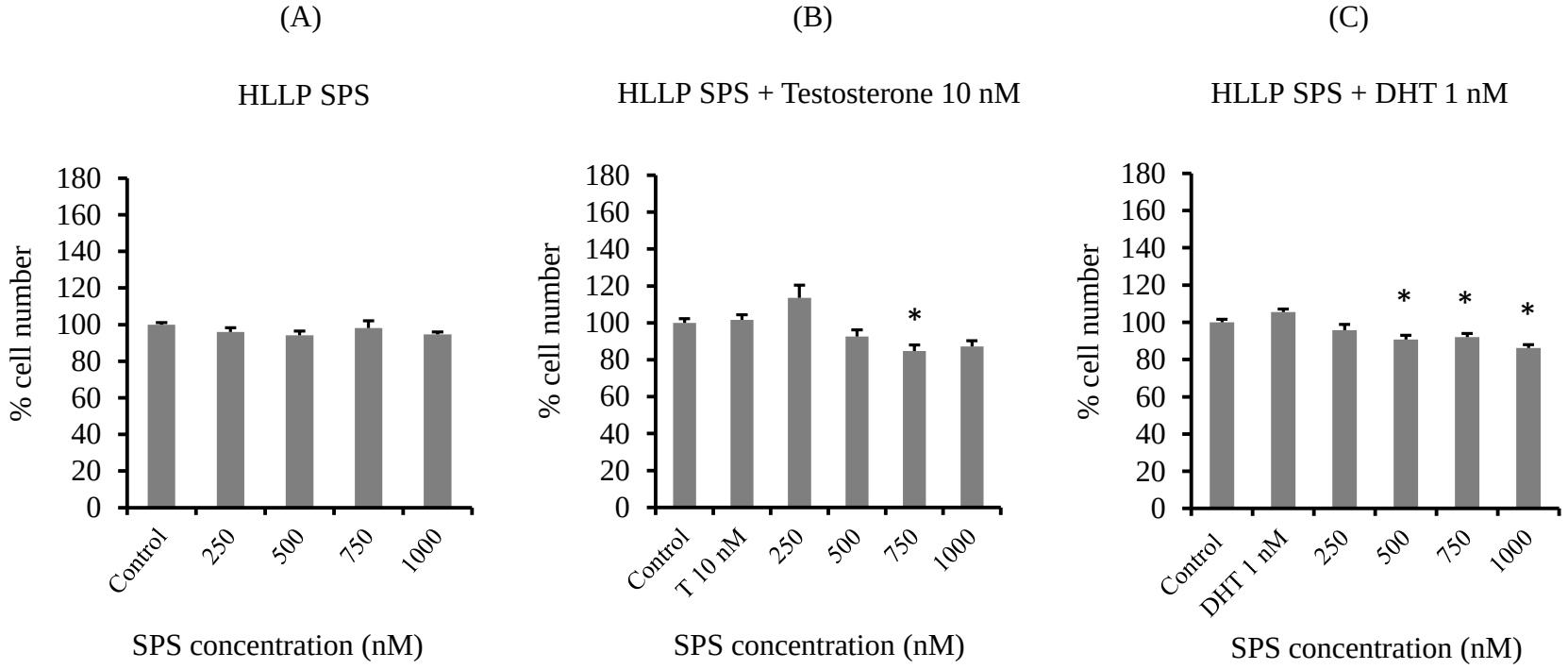

Figure 2.1. LNCaP cell number after dose-dependent treatment with HLLP SPS ± 10 nM testosterone (T) or 1 nM DHT.

(A) MTT assay (cell number) in the absence of testosterone or DHT. (B) MTT assay in the presence of testosterone. (C) MTT assay in the presence of DHT. Data are obtained from three replicates of each experiment, and expressed as mean percentages (± SEM) either in comparison to 0.1% DMSO control (A) or to 10 nM testosterone (B) or 1 nM DHT (C) -corresponding to 100%. P-values (Dunnett's test): $p<0.05$ *vs.* control (Figure 2.1A) or 10 nM testosterone (Figure 2.1B) or 1 nM DHT (Figure 2.1C).

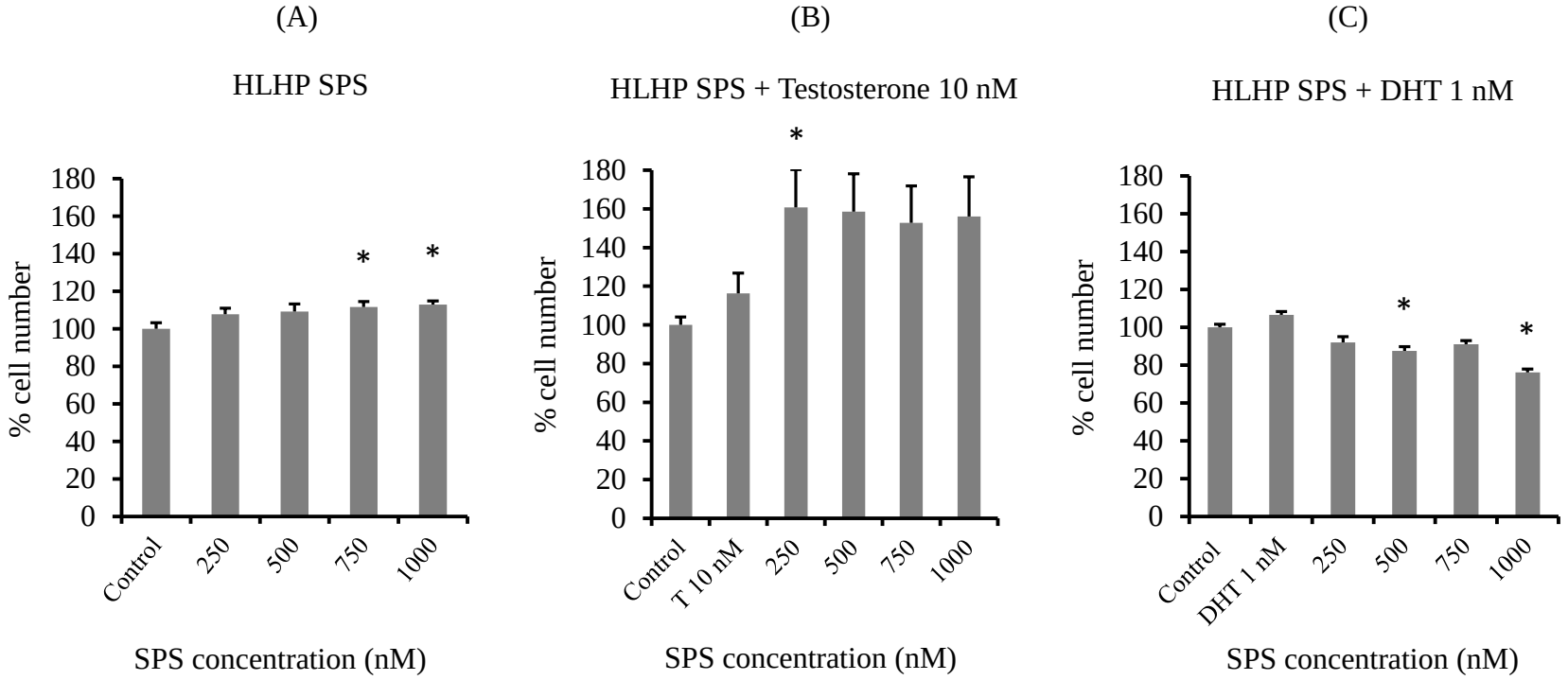

Figure 2.2. LNCaP cell number after dose-dependent treatment with HLHP SPS ± 10 nM testosterone (T) or 1 nM DHT.

(A) MTT assay (cell number) in the absence of testosterone or DHT. (B) MTT assay in the presence of testosterone. (C) MTT assay in the presence of DHT. Data are obtained from three replicates of each experiment, and expressed as mean percentages (± SEM) either in comparison to 0.1% DMSO control (A) or to 10 nM testosterone (B) or 1 nM DHT (C) -corresponding to 100%. P-values (Dunnett's test): $p<0.05$ *vs.* control (Figure 2.2A) or 10 nM testosterone (Figure 2.2B) or 1 nM DHT (Figure 2.2C).

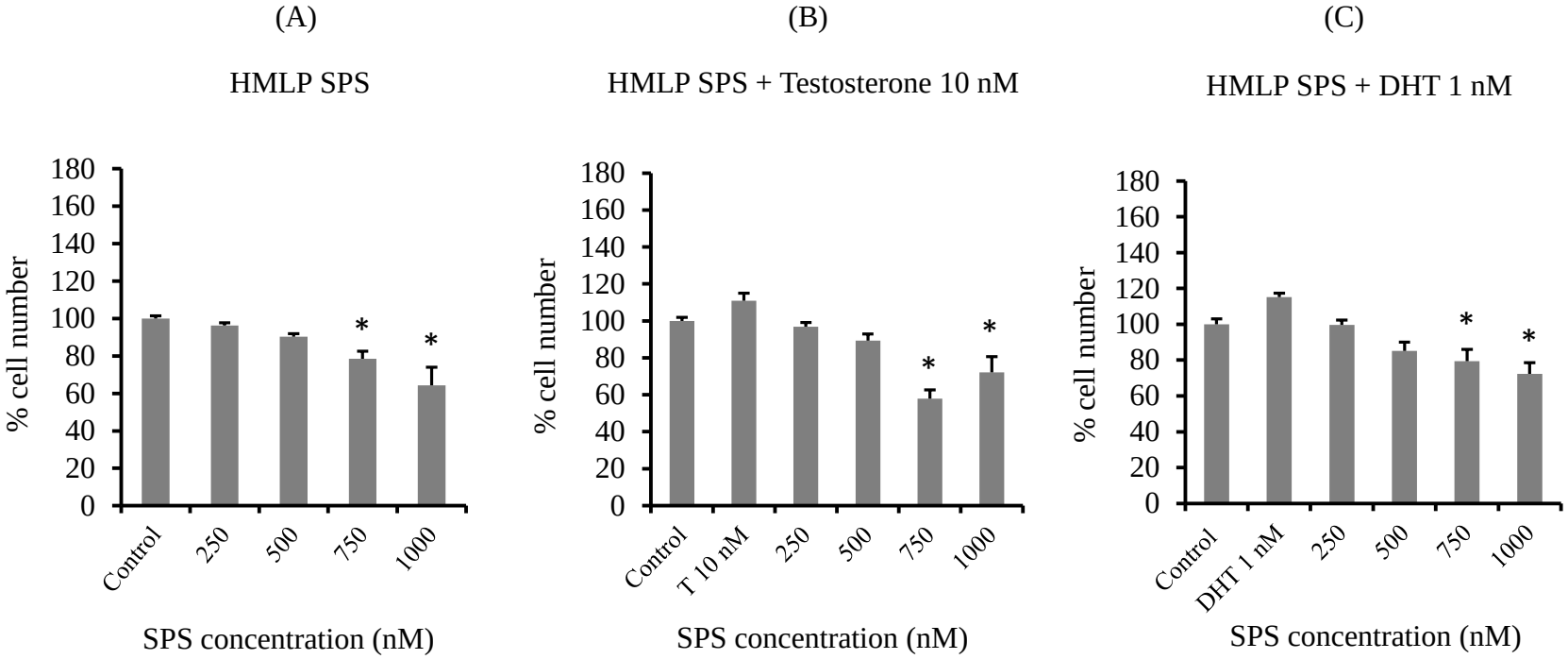

Figure 2.3. LNCaP cell number after dose-dependent treatment with HMLP SPS ± 10 nM testosterone (T) or 1 nM DHT.

(A) MTT assay (cell number) in the absence of testosterone or DHT. (B) MTT assay in the presence of testosterone. (C) MTT assay in the presence of DHT. Data are obtained from three replicates of each experiment, and expressed as mean percentages (± SEM) either in comparison to 0.1% DMSO control (A) or to 10 nM testosterone (B) or 1 nM DHT (C) -corresponding to 100%. P-values (Dunnett's test): $p<0.05$ *vs.* control (Figure 2.3A) or 10 nM testosterone (Figure 2.3B) or 1 nM DHT (Figure 2.3C).

References

1. American Cancer Society. Cancer facts and figures 2015.

2. Grossmann ME, Huang H, Tindall DJ. Androgen receptor signaling in androgen-refractory prostate cancer. J Natl Cancer Inst. 2001;93(22):1687–1697.

3. Andriole GL, Kirby R. Safety and tolerability of the dual 5α-reductase inhibitor dutasteride in the treatment of benign prostatic hyperplasia. Eur Urol. 2003;44(1):82-88.

4. Uemura M, Tamura K, Chung S, Honma S, Okuyama Y, et al. Novel 5α-steroid reductase (SRD5A3, type-3) is overexpressed in hormone-refractory prostate cancer. Cancer Sci. 2008;99(1):81-86.

5. Stiles AR, Russell DW. SRD5A3: A surprising role in glycosylation. Cell. 2010;142(2):196-198.

6. Nickel JC. Comparison of clinical trials with finasteride and dutasteride. Rev Urol. 2004;6 Suppl 9:S31-S39.

7. Andriole GL, Bostwick DG, Brawley OW, Gomella LG, Marberger M, et al. Effect of dutasteride on the risk of prostate cancer. N Engl J Med. 2010;362(13):1192-1202.

8. Thompson IM, Goodman PJ, Tangen CM, Lucia MS, Miller GJ, et al. The influence of finasteride on the development of prostate cancer. N Engl J Med. 2003;349(3):215-224.

9. Anderson ML. A preliminary investigation of the enzymatic inhibition of 5α-reduction and growth of prostatic carcinoma cell line LNCap-FGC by natural astaxanthin and Saw Palmetto lipid extract in vitro. J Herb Pharmacother. 2005;5(1):17-26.

10. Bayne CW, Ross M, Donnelly F, Habib FK. The selectivity and specificity of the actions of the lipido-sterolic extract of Serenoa repens (Permixon) on the prostate. J Urol. 2000;164(3 pt 1):876-881.

11. Bayne CW, Donnelly F, Ross M, Habib FK. Serenoa repens (Permixon): A 5α-reductase types I and II inhibitor-new evidence in a coculture model of BPH. Prostate. 1999;40(4):232-241.

12. Wadsworth TL, Worstell TR, Greenberg NM, Roselli CE. Effects of dietary saw palmetto on the prostate of transgenic adenocarcinoma of the mouse prostate model (TRAMP). Prostate. 2007;67(6):661-673.

13. Van Coppenolle F, Le Bourhis X, Carpentier F, Delaby G, Cousse H, et al. Pharmacological effects of the lipidosterolic extract of Serenoa repens (Permixon) on rat prostate hyperplasia induced by hyperprolactinemia: comparison with finasteride. Prostate. 2000;43(1):49-58.

14. Talpur N, Echard B, Bagchi D, Bagchi M, Preuss HG. Comparison of saw palmetto (extract and whole berry) and cernitin on prostate growth in rats. Mol Cell Biochem. 2003;250(1-2):21-26.

15. de Lourdes Arruzazabala M, Molina V, Más R, Carbajal D, Marrero D, González V, et al. Effects of coconut oil on testosterone-induced prostatic hyperplasia in Sprague-Dawley rats. J Pharm Pharmacol. 2007;59(7):995-999.

16. Olapade EO, Olapade CO, Olapade OC, Olapade EO. Phytomedicines for the treatment of benign prostatic hyperplasia without surgery in Nigeria. In International Conference on Medicinal and Aromatic Plants (Part II). 2001;597:231-234.

17. Hambrock T, Somford DM, Hoeks C, Bouwense SA, Huisman H, et al. Magnetic resonance imaging guided prostate biopsy in men with repeat negative biopsies and increased prostate specific antigen. J Urol. 2010;183(2):520-528.

18. Schantz MM, Bedner M, Long SE, Molloy JL, Murphy KE, et al. Development of saw palmetto (Serenoa repens) fruit and extract standard reference materials. Anal Bioanal Chem. 2008;392(3):427-438.

19. Abe M, Ito Y, Oyunzul L, Oki Fujino T, Yamada S. Pharmacologically relevant receptor binding characteristics and 5α-reductase inhibitory activity of free Fatty acids contained in saw palmetto extract. Biol Pharm Bull. 2009;32(4):646-650.

20. Raynaud JP, Cousse H, Martin PM. Inhibition of type 1 and type 2 5α-reductase activity by free fatty acids, active ingredients of Permixon. J Steroid Biochem Mol Biol. 2002;82(2-3):233-239.

21. Niederprüm HJ, Schweikert HU, Zänker KS. Testosterone 5α-reductase inhibition by free fatty acids from Sabal serrulata fruits. Phytomedicine. 1994;1(2):127-133.

22. Liang T, Liao S. Growth suppression of hamster flank organs by topical application of gamma-linolenic and other fatty acid inhibitors of 5α-reductase. J Invest Dermatol. 1997;109(2):152-157.

23. Abe M, Ito Y, Suzuki A, Onoue S, Noguchi H, et al. Isolation and pharmacological characterization of fatty acids from saw palmetto extract. Anal Sci. 2009;25(4):553-557.

24. Weisser H, Tunn S, Behnke B, Krieg M. Effects of the sabal serrulata extract IDS 89 and its subfractions on 5α-reductase activity in human benign prostatic hyperplasia. Prostate. 1996;28(5):300-306.

25. Cabeza M, Bratoeff E, Heuze I, Ramírez E, Sánchez M, et al.. Effect of beta-sitosterol as inhibitor of 5α-reductase in hamster prostate. Proc West Pharmacol Soc. 2003;46:153-155.

26. Von Holtz RL, Fink CS, Awad AB. beta-Sitosterol activates the sphingomyelin cycle and induces apoptosis in LNCaP human prostate cancer cells. Nutr Cancer. 1998;32(1):8-12.

27. Awad AB, Fink CS, Williams H, Kim U. In vitro and in vivo (SCID mice) effects of phytosterols on the growth and dissemination of human prostate cancer PC-3 cells. Eur J Cancer Prev. 2001;10(6):507-513.

28. Scholtysek C, Krukiewicz AA, Alonso JL, Sharma KP, Sharma PC, et al. Characterizing components of the saw palmetto berry extract (SPBE) on prostate cancer cell growth and traction. Biochem Biophys Res Commun. 2009;379(3):795-798.

29. Berges RR, Windeler J, Trampisch HJ, Senge T. Randomised, placebo-controlled, double-blind clinical trial of beta-sitosterol in patients with benign prostatic hyperplasia. Beta-sitosterol Study Group. Lancet. 1995;345(8964):1529-1532.

30. Nakamura Y, Suzuki T, Nakabayashi M, Endoh M, Sakamoto K, et al. In situ androgen producing enzymes in human prostate cancer. Endocr Relat Cancer. 2005;12(1):101-107.

31. Tien AH, Sadar MD. Androgen-responsive gene expression in prostate cancer progression. In: Androgen-responsive genes in prostate cancer. Springer. 2013;135-153.

32. Feldman BJ, Feldman D. The development of androgen-independent prostate cancer. Nat Rev Cancer. 2001;1(1):34-45.

33. Gann PH. Randomized trials of antioxidant supplementation for cancer prevention: first bias, now chance--next, cause. JAMA. 2009;301(1):102-103.

34. Igawa T, Lin FF, Lee MS, Karan D, Batra SK, et al. Establishment and characterization of androgen-independent human prostate cancer LNCaP cell model. Prostate. 2002;50(4):222-235.

35. Horoszewicz JS, Leong SS, Chu TM, Wajsman ZL, Friedman M, et al. The LNCaP cell line--a new model for studies on human prostatic carcinoma. Prog Clin Biol Res. 1980;37:115-132.

36. Horoszewicz JS, Leong SS, Kawinski E, Karr JP, Rosenthal H, et al. LNCaP model of human prostatic carcinoma. Cancer Res. 1983;43(4):1809-1818.

37. Hamilton JB, Montagna W. The sebaceous glands of the hamster; morphological effects of androgens on integumentary structures. Am J Anat. 1950;86(2):191-233.

38. Takayasu S, Adachi K. Hormonal control of metabolism in hamster costovertebral glands. J Invest Dermatol. 1970;55(1):13-9.

39. Penugonda K, Lindshield BL. Fatty acid and phytosterol profiles of commercial saw palmetto supplements. Nutrients. 2013;5(9):3617-3633.

40. de Launoit Y, Veilleux R, Dufour M, Simard J, Labrie F. Characteristics of the biphasic action of androgens and of the potent antiproliferative effects of the new pure antiestrogen EM-139 on cell cycle kinetic parameters in LNCaP human prostatic cancer cells. Cancer Res. 1991;51(19):5165-5170.

41. Waltering KK, Helenius MA, Sahu B, Manni V, Linja MJ, et al. Increased expression of androgen receptor sensitizes prostate cancer cells to low levels of androgens. Cancer Res. 2009;69(20):8141-8149.

42. Liao S, Lin J, Dang MT, Zhang H, Kao YH, et al. Growth suppression of hamster flank organs by topical application of catechins, alizarin, curcumin, and myristoleic acid. Arch Dermatol Res. 2001;293(4):200-205.

43. Matsuda H, Yamazaki M,, Naruto S, Asanuma Y, Kubo M. Anti-androgenic and hair growth promoting activities of lygodii spora (spore of lygodium japonicum) I. Active constituents inhibiting testosterone 5α-reductase. Biol Pharm Bull. 2002;25(5):622-626.

44. Opoku-Acheampong AB, Nelsen MK, Unis D, Lindshield BL. The effect of finasteride and dutasteride on the growth of WPE1-NA22 prostate cancer xenografts in nude mice. PLoS One. 2012;7(1):e29068.

45. Litvinov IV, Vander Griend DJ, Antony L, Dalrymple S, De Marzo AM, et al. Androgen receptor as a licensing factor for DNA replication in androgen-sensitive prostate cancer cells. Proc Natl Acad Sci U S A. 2006;103(41):15085-15090.

46. Vander Griend DJ, Litvinov IV, Isaacs JT. Stabilizing androgen receptor in mitosis inhibits prostate cancer proliferation. Cell Cycle. 2007;6(6):647-651.

47. D'Antonio JM, Vander Griend DJ, Isaacs JT. DNA licensing as a novel androgen receptor mediated therapeutic target for prostate cancer. Endocr Relat Cancer. 2009;16(2):325-332.

48. Xu YH. The interaction of DHT-receptor with chromatin components of rat prostate. Shi Yan Sheng Wu Xue Bao. 1990;23(3):375-379.

Chapter 3 - Preventive and Therapeutic Efficacy of Finasteride and Dutasteride in TRAMP mice

Abstract

Background: The Prostate Cancer Prevention Trial (PCPT) and Reduction by Dutasteride of Prostate Cancer Events (REDUCE) trial found that 5α-reductase (5α-R) inhibitors finasteride and dutasteride respectively, decreased prostate cancer prevalence but also increased the incidence of high-grade tumors. 5α-R2 is the main isoenzyme in normal prostate tissue; however, most prostate tumors have high 5α-R1 and low 5α-R2 expression. Because finasteride inhibits only 5α-R2, we hypothesized that it would not be as efficacious in preventing prostate cancer development and/or progression in C57BL/6 TRAMP x FVB mice as dutasteride, which inhibits both 5α-R1 and 5α-R2.

Method/Principal findings: Six-week-old C57BL/6 TRAMP x FVB male mice were randomized to AIN93G control or pre- and post- finasteride and dutasteride diet (83.3 mg drug/kg diet) groups (n =30–33) that began at 6 and 12 weeks of age, respectively, and were terminated at 20 weeks of age. The pre- and post- finasteride and dutasteride groups were designed to test the preventive and therapeutic efficacy of the drugs, respectively. Final body weights, genitourinary tract weights, and genitourinary tract weights as percentage of body weights were significantly decreased in the Pre- and Post-Dutasteride groups compared with the control. The Post-Dutasteride group showed the greatest inhibition of prostatic intraepithelial neoplasia progression and prostate cancer development. Surprisingly, the Post-Dutasteride group showed improved outcomes compared with the Pre-Dutasteride group, which had increased incidence of high-grade carcinoma as the most common and most severe lesions in a majority of prostate lobes. Consistent with our hypothesis, we found little benefit from the finasteride diets, and they increased the incidence of high-grade carcinoma.

Conclusion: Our findings have commonalities with previously reported PCPT, REDUCE, and the Reduction by Dutasteride of Clinical Progression Events in Expectant Management (REDEEM) trial results. These results may support the therapeutic use of dutasteride, but not finasteride, for therapeutic or preventive use.

Contributors to study

Conceived and designed the experiments: Brian L. Lindshield. Performed the experiments: Alexander B. Opoku-Acheampong, Dave Unis, Jamie N. Henningson, Amanda P. Beck. Analyzed the data: Alexander B. Opoku-Acheampong, Brian L. Lindshield. Contributed reagents/materials/analysis tools: Alexander B. Opoku-Acheampong, Dave Unis, Brian L. Lindshield. Wrote the manuscript: Alexander B. Opoku-Acheampong, Brian L. Lindshield.

Introduction

Prostate cancer is the most commonly diagnosed non-skin neoplasm in men and is projected to account for 28% of US male cancer cases in 2013 [1]. Most prostate tumor growth is initially androgen-dependent or androgen-sensitive [2]. The main circulating androgen, testosterone, is converted to dihydrotestosterone by the isoenzymes 5α-reductase 1 and 5α-reductase 2. Dihydrotestosterone has up to a ten-fold higher affinity to the androgen receptor than testosterone, making it a more potent androgen [3,4]. 5α-reductase 2 is the major isoenzyme in the prostate [5]; however, multiple [6-9], but not all [10-12], studies have reported increased 5α-reductase 1 and/or decreased 5α-reductase 2 mRNA expression or activity in prostate cancer compared with nonmalignant prostate tissue. Furthermore, 5α-reductase 1 and 5α-reductase 2 were found in 73% and 56%, respectively, of human prostate cancer tissues [11].

Finasteride (5α-reductase 2 inhibitor) and dutasteride (5α-reductase 1 and 5α-reductase 2 inhibitor) are commonly used to treat benign prostatic hyperplasia (BPH), a nonmalignant enlargement of the prostate. The potential of these inhibitors to decrease prostate cancer development and/or progression through their anti-androgen action has been examined in several clinical trials. The Prostate

Cancer Prevention Trial (PCPT) and the Reduction by Dutasteride of Prostate Cancer Events (REDUCE) trial found that finasteride and dutasteride decreased prostate cancer risk by 24.8% and 23%, respectively, but both inhibitors also increased the risk of developing high-grade prostate cancer [13,14]. As a result, the Food and Drug Administration (FDA) amended the safety information for both drugs to state that they increase high-grade prostate cancer in patients [15]. In addition, it has been projected that finasteride and dutasteride in PCPT and REDUCE trials respectively showed no prostate cancer mortality benefit [16]. Another clinical trial, the Reduction by Dutasteride of Clinical Progression Events in Expectant Management (REDEEM) trial found that dutasteride significantly delayed prostate cancer progression with no reported adverse events in men with low-risk, localized prostate cancer [17].

In animal models, dutasteride, but not finasteride, decreased Dunning R-3327H rat prostate tumor weights [18]. Similarly, Canene-Adams and colleagues also reported that finasteride did not alter Dunning R-3327H rat prostate tumor areas or weights despite reducing androgen-sensitive tissue weights [19]. Finasteride also did not decrease prostatic intraepithelial neoplasia (PIN) or adenocarcinoma in 10-week-old transgenic rats bearing the probasin/simian virus 40 T antigen (SV40 Tag) construct but did decrease lesion size in lateral and ventral lobes, but not the dorsal lobe, of the prostate [20]. Both finasteride and dutasteride were effective in reducing LNCaP human prostate cancer xenograft growth in male nude mice [18]. Dutasteride significantly decreased LuCaP 35 tumor growth in Balb/c mice [21]. Previously, we examined the effect of finasteride and dutasteride diets begun 1-2 weeks before or 3 weeks after subcutaneous injection of WPE1-NA22 human prostate cancer cells in male nude mice, but we were unable to answer our research question due to poor tumor growth [22].

Thus, we decided to determine the effect of finasteride and dutasteride in transgenic adenocarcinoma of the mouse prostate (TRAMP) mice since prostate cancer development and progression have been well characterized in this model [23]. TRAMP mice prostate cancer is promoted by the expression of the SV40 large and small T antigen and undergoes progressive stages of cancer development starting from prostatic intraepithelial neoplasia (PIN) to adenocarcinoma and metastasis

[24,25]. In this study, we compared the effect of finasteride- or dutasteride-containing diets begun at 6 weeks or 12 weeks of age on prostate tumor development in C57BL/6 TRAMP x FVB mice. These time points were chosen because 6 weeks is when the mice reach sexual maturity and develop pathologic features similar to low-grade PIN [26]. This would allow us to determine whether finasteride and/or dutasteride can inhibit PIN progression and prostate cancer development. The post- finasteride and dutasteride diets began at 12 weeks of age when mice are expected to have developed PIN and well-differentiated adenocarcinoma [25]. Beginning diets at this age would allow us to determine whether therapeutic finasteride and/or dutasteride can inhibit PIN and/or prostate cancer progression. Because of the increase in 5α-reductase 1 and decrease in 5α-reductase 2 activity and expression that may occur during prostate cancer development, we hypothesized that finasteride diets begun at either time point would not and dutasteride diets begun at either time point would significantly inhibit prostate cancer development and/or progression.

Materials and Methods

Ethics statement

The Institutional Animal Care and Use Committee (IACUC) at Kansas State University approved all animal procedures (protocol 2969).

Study mice, diets, and design

Six-week-old heterozygous C57BL/6-Tg 8247Ng/J TRAMP male and female mice were purchased (The Jackson Laboratory, Bar Harbor, ME) and bred to produce homozygous males. These were bred with female FVB/NJ mice (The Jackson Laboratory, Bar Harbor, ME) to produce C57BL/6 TRAMP x FVB mice. Male C57BL/6 TRAMP x FVB mice were weaned and began consuming the control diet at 3 weeks of age before being randomized into Control, Pre-Finasteride, Post-Finasteride, Pre-Dutasteride, and Post-Dutasteride groups (n = 30–33) at 6 weeks of age. Mice were individually housed, monitored daily, weighed weekly, and provided diets and water ad libitum. AIN93-G treatment

diets (Research Diets, New Brunswick, NJ) contained dutasteride (kindly donated by GlaxoSmithKline Pharmaceuticals, Research Triangle Park, NC) and finasteride (Kemprotec, Middlesbrough, UK) at 83.3 mg/kg of diet, the same dose used in our previous study [22]. These diets were designed to provide ~10mg drug/kg body weight, which was the midrange dutasteride dose provided by Xu and colleagues [18]. Pre- and post-groups began their treatment diets at 6 weeks and 12 weeks of age, respectively (Figure 3.1). Seven mice did not complete the study for health reasons unrelated to tumor growth, leaving the group numbers shown in Figure 1. At 20 weeks of age, mice were anesthetized by CO_2 inhalation and euthanized by exsanguination. The genitourinary tracts, kidneys, and lungs were dissected, and the genitourinary tracts were weighed. Iliac lymph nodes were also collected whenever possible. All tissues were fixed by immersion in 10% neutral buffered formalin for 48 hours, and then moved to 70% alcohol until processing in the Kansas State University Veterinary Diagnostic Laboratory.

Histopathology

The seminal vesicles; anterior, dorsal, lateral, and ventral prostate lobes; ampulla; urinary bladder; and proximal urethra were sampled as one tissue. Orientation was maintained, and the dorsal side was placed down in the cassette for histology processing first. In mice with prostate tumors, distinct prostate lobes were not recognizable, so a section was taken through the center of the mass. Tissues were routinely processed and embedded in paraffin wax. Sections were made at 4 µm, routinely processed, and stained with hematoxylin and eosin. After the dorsal sections were processed, the blocks were melted down and the tissue was flipped and re-embedded for examination of the ventral prostate. Prostate lesions were scored blindly twice by a board-certified veterinary pathologist according to a previously described grading scheme [27]. In short, both the most common and most severe lesions were graded separately, and then adjusted for distribution. If a neoplasm replaced all four prostate lobes, then all lobes received the same score. Select tissues were also blindly scored twice by a second board-certified veterinary pathologist to ensure scoring consistency. Iliac lymph nodes were examined for metastasis by

removal of the kidneys and sublumbar tissue; histological processing was identical to the prostatic tissue. Photomicrographs were taken with an Olympus DP26 digital camera (Olympus America, Center Valley, PA) with a 40X objective, giving 0.75 µm resolution. Images were captured with Olympus cellSens software.

Statistical analysis

Data were analyzed using SAS 9.3 (SAS Institute Inc., Cary, NC) with $p<0.05$ considered statistically significant. Natural logs were used to transform data that did not meet model assumptions. Data were analyzed using ANOVA with Fisher's Least Significant Difference (LSD). Iliac lymph node metastases incidence was analyzed using the Kruskal Wallis non-parametric one-way ANOVA.

Results

Final body weights and genitourinary tract weights

Pre-Dutasteride and Post-Dutasteride groups' final body weights were significantly decreased compared with the control despite no significant difference in daily food intake (Table 3.1); however, both dutasteride diets significantly decreased the weight gain/food intake ratio versus the control and Pre-Finasteride group. While it is a small numerical difference, the Pre-Finasteride group's daily food intake was significantly higher than the control and both dutasteride groups. Genitourinary tract weights for Pre- and Post-Dutasteride groups also were significantly lower than the control (Table 3.1 and Figure 3.2). Genitourinary tract weights as percentage of body weights in the Pre-Dutasteride and Post-Dutasteride groups were also significantly lower than the control and Post-Finasteride group; thus the significant decrease in genitourinary tract weights was not due to the decreased body weights in these groups. Both dutasteride groups' genitourinary tract weights were significantly decreased compared with the Post-Finasteride group; the Pre-Dutasteride group's genitourinary tract weights and genitourinary tract weights as percentage of body weights were also significantly decreased compared with the Pre-

Finasteride group. The Pre-Finasteride group's genitourinary tract weights as percentage of body weights also were significantly decreased compared with the control.

Most severe lesion scores

The raw and adjusted mean most severe lesion scores for the anterior, dorsal, and lateral lobes were significantly decreased in the Post-Dutasteride group versus the control (Table 3.2). Representative images of the different pathological grades used in the grading scheme are shown in Figure 3.3. The adjusted mean most severe lesion score was also significantly decreased for the ventral lobe of the Post-Dutasteride group compared with the control. The raw and adjusted mean most severe lesion scores for the anterior and dorsal lobes of the Post-Dutasteride groups were also significantly decreased compared with the finasteride groups. The raw and adjusted mean most severe lesion scores for the anterior and dorsal lobes of the Pre-Dutasteride group were significantly decreased versus the control. The lateral lobe adjusted mean most severe lesion score was also significantly decreased in the Pre-Dutasteride group compared with the control. There were also no significant differences in raw and adjusted mean most severe lesion scores between the finasteride groups and the control.

Most common lesion scores

The raw mean most common lesion scores for the anterior and dorsal lobes were significantly decreased in both dutasteride groups versus the control (Table 3.3). In addition, for all lobes in the Post-Dutasteride group, the adjusted most common lesion scores were significantly decreased compared with the control. The adjusted most common lesion scores for the anterior, dorsal, and lateral lobes in the Pre-Dutasteride group were significantly decreased versus the control. The Post-Dutasteride group anterior lobe raw and adjusted mean most common lesion scores and both dutasteride groups' dorsal lobe adjusted most common lesion scores were significantly decreased compared with the Post-Finasteride group. The adjusted most common lesion score for the dorsal lobe in the Pre-Finasteride group was significantly decreased versus the control, despite being numerically higher. Transforming the data so

that it would meet assumptions resulted in a transformed adjusted mean score that was significantly lower than the control because the transformed score was not as impacted by the high scores in this group.

Most severe lesion histopathological distribution

Low-grade (LG) and high-grade (HG) PIN incidence as the most severe lesion increased and decreased, respectively, significantly in all lobes in both dutasteride groups versus the control (Table 3.4). Low-grade PIN incidence was increased in the ventral lobe of both finasteride groups compared with the control. Lateral and ventral lobe moderate-grade (MG)-PIN incidence was also significantly decreased in both dutasteride groups versus the control. Compared with the control, there was a significant increase in MG-PIN incidence in the dorsal lobe of the Pre-Finasteride group. Well-differentiated (WD) adenocarcinoma incidence in the anterior lobe was significantly decreased in both finasteride and dutasteride groups compared with the control, and the Pre-Finasteride group had significantly increased moderately differentiated (MD) adenocarcinoma incidence versus the control in the ventral lobe. These differences are, however, based on low incidence levels. The finasteride groups and the Pre-Dutasteride group had significantly increased poorly differentiated (PD) carcinoma and prostate cancer (WD-PD) incidence in the lateral and ventral lobes versus the control. The finasteride groups and the Pre-Dutasteride group also had increased poorly differentiated (PD) carcinoma in the dorsal lobe versus the control. The Pre-Finasteride and Pre-Dutasteride groups had increased prostate cancer (WD-PD) incidence in the dorsal lobe versus the control. The Post-Dutasteride group had significantly decreased and increased PD carcinoma incidence in the anterior and lateral lobes, respectively, compared with the control. Both dutasteride groups had significantly decreased prostate cancer (WD-PD) incidence in the anterior lobe compared with the control.

Most common lesion histopathological distribution

As was observed in the most severe lesion scores, LG-PIN as the most common lesion was significantly increased in all lobes in both dutasteride groups versus the control (Table 3.5). Both finasteride groups also had significantly increased LG-PIN incidence in the dorsal, lateral, and ventral lobes compared with the control. MG-PIN incidence was also significantly decreased for the Pre-Finasteride group and both dutasteride groups in the dorsal, ventral, and lateral lobes versus the control. The Post-Finasteride group had significantly decreased MG-PIN incidence in the ventral and lateral lobes compared with the control. Both dutasteride groups had significantly decreased incidence of HG-PIN versus the control in the anterior, dorsal and lateral lobes. Both finasteride groups had significantly decreased HG-PIN compared with the control in the dorsal and lateral lobes. Both dutasteride groups had significantly decreased incidence of PD carcinoma in the anterior lobe versus the control. Both finasteride groups and the Pre-Dutasteride group had significantly increased PD carcinoma incidence compared with the control in the dorsal, lateral, and ventral lobes. Compared with the control, a significant increase in PD carcinoma incidence was observed in the lateral prostate of the Post-Dutasteride group. Total prostate cancer (WD-PD) was almost entirely composed of PD carcinoma, so the significant differences compared with the control were the same as those seen in PD carcinoma for the anterior, dorsal and lateral lobes.

Iliac lymph node metastases

No significant differences were observed in the incidence of iliac lymph node metastases between groups (Table 3.6); however, a notable difference was found in incidence between Post-Dutasteride (8%) and Post-Finasteride (29%) groups.

Discussion

Although the efficacy of finasteride and dutasteride in inhibiting tumor growth has been compared, we believe we are the first to determine the effectiveness of finasteride and dutasteride on

PIN progression and prostate cancer development in C57BL/6 TRAMP x FVB mice. Overall, we found that the Post-Dutasteride group had the greatest decrease in PIN progression and prostate cancer development. Although not significant, we observed the lowest level of lymph node metastases in this group. We unexpectedly found that the Post-Dutasteride group had better outcomes than the Pre-Dutasteride group, primarily as a result of the higher incidence of PD carcinoma in most lobes in the Pre-Dutasteride group. Both finasteride groups had decreased incidence of HG-PIN, but not to the extent seen in the dutasteride groups. The finasteride groups also had increased incidence of poorly differentiated prostate cancer in most lobes.

Our findings are similar to results in other animal models that found finasteride failed to inhibit prostate cancer progression [20] or tumor growth [18,19] and dutasteride decreased prostate tumor growth [18]. We found the weakest response to dutasteride in the ventral lobe. Another study that used the same scoring system also found fewer statistical differences in the ventral lobe in response to tomato powder and soy germ diets, especially compared with the dorsal and lateral lobes [28]. This decrease in efficacy in the ventral lobe might be explained by the fact that in large probasin-large T antigen mice, dutasteride markedly decreased the dorsolateral prostate weights but had little to no effect on ventral prostate weights [29]. In addition, rat ventral prostate has almost two-fold higher concentrations of testosterone and dihydrotestosterone than the dorsolateral prostate; furthermore, after finasteride administration, ventral prostate lobe concentrations of testosterone are almost twice as high as dorsolateral prostate lobe concentrations [30]. Another possible explanation for reduced sensitivity in the ventral prostate lobes is that the transgene is expressed at much higher levels in the ventral lobe [24].

We were surprised that both dutasteride groups had decreased body weights and weight gain/food intake ratios compared with the control. In our previous study, this diet had no effect on body weights or weight gain/food intake ratios in nude mice despite a longer feeding duration [22]. However, dutasteride has decreased body weight or body weight gain in other studies. For example, dutasteride administration at doses of 2.5 and 5 mg/kg body weight to 8-week-old male Sprague–Dawley rats for 2

weeks led to a significant decrease in their body weights [31], and 4 or 8 weeks of infusion of 2 mg/kg body weight dutasteride treatment led to a significant decrease in body weight gain in large probasin-large T antigen transgenic mice [29]. In our study, the mice were consuming ~8 mg/kg finasteride and dutasteride/day. This is obviously higher than the concentration in previous studies. We did not find an increase in body weights in the Pre-Finasteride group, unlike in our previous study; however, there was a significant increase in food intake versus the control. The lack of an increase in body weights in the Pre-Finasteride group in this study supports our belief that the significant increase in body weights in our previous study was not due to the treatment diet [22].

In our previous study, both finasteride and dutasteride decreased prostate and seminal vesicle weights as percentage of body weights. Dutasteride also significantly decreased seminal vesicle weights compared to finasteride [22]. In the current study, we think prostate tumor development is the reason we did not find significant decreases in genitourinary tract weights in the finasteride groups. The rates of lymph node metastases found in this study are similar to those that have been reported in 18-week-old [28] and 18–24-week-old C57BL/6 TRAMP x FVB mice [32].

We are one of the first to use a new grading scheme for TRAMP mice [27]. When comparing our results to those reported previously, the most notable difference is that we had a lower incidence of PD carcinoma as the most severe lesion compared with 18-week-old C57BL/6 TRAMP x FVB mice [28] and most severe and most common lesions in 18–24-week-old C57BL/6 TRAMP x FVB mice [27]. Instead, we had much higher incidence of PIN as the most severe and most common lesions. Our average most severe lesion scores were also lower than those for 10-week-old C57BL/6 TRAMP x FVB mice, but the average most common lesion scores were similar [27]. It is not clear why our scores were lower using this grading scheme, but variation in the duration and severity of prostate cancer in C57BL/6 TRAMP x FVB mice does exist. Our interpretation of the grading scheme also could have led to scores that were lower than previously reported results. However, we believe that our results from the scoring

scheme have given us tremendous insight into the effect of the treatment diets on PIN progression and prostate cancer development.

Interestingly, there are some similarities between our findings and the outcomes from the finasteride and dutasteride clinical trials. The Pre-Finasteride group was designed to be similar to the participants of PCPT to determine whether finasteride could prevent prostate cancer development. Our findings were similar to PCPT; HG-PIN decreased and incidence of PD carcinoma increased. It is important to note that the effect of finasteride on progression to HG-PIN was weaker than dutasteride. It has been suggested that decreased prostate volume, biopsy density and/or prostate-specific antigen (PSA) performance may have contributed to the detection of more poorly differentiated prostate cancer in PCPT men [33-37], but our findings support that the increased incidence of high-grade prostate tumors seen in PCPT was an adverse effect of finasteride treatment.

The Pre-Dutasteride group was designed to be similar to the REDUCE trial, where the men who received dutasteride were at high risk of developing prostate cancer. Our findings were similar to the REDUCE trial in that the Pre-Dutasteride group had reduced HG-PIN incidence but increased incidence of PD carcinoma. The Post-Dutasteride group was designed to be similar to the REDEEM trial, in which assigned men with low-grade prostate cancer received dutasteride. Similar to the REDEEM trial, in the Post-Dutasteride group, HG-PIN incidence decreased without increasing the incidence of PD carcinoma, except in the lateral prostate.

Some caveats about our study should be considered, especially when interpreting what our findings might mean for the use of these drugs in men. First, the drugs were administered in diet, which differs from how most men take them. Second, the body weight–scaled human oral dose [38] is approximately 80 mg/day, which is much higher than the dutasteride (0.5 mg/day) and finasteride (5 mg/day) doses that most men take. In addition, the significant decrease in body weights in the dutasteride groups might mean that dietary-energy restriction might have contributed to the beneficial effects seen in these groups.

Conclusions

Our results suggest that the timing of dutasteride treatment initiation may be critical to the risk of developing poorly differentiated carcinoma. Our results may support therapeutic, but not preventive, use of dutasteride for this reason. Our results do not support the therapeutic or preventive use of finasteride. We plan to perform immunohistochemistry and *in situ* hybridization on prostates from these mice to elucidate why Post-Dutasteride treatment was effective and why we found a discordant response in the Pre-Dutasteride and both finasteride groups.

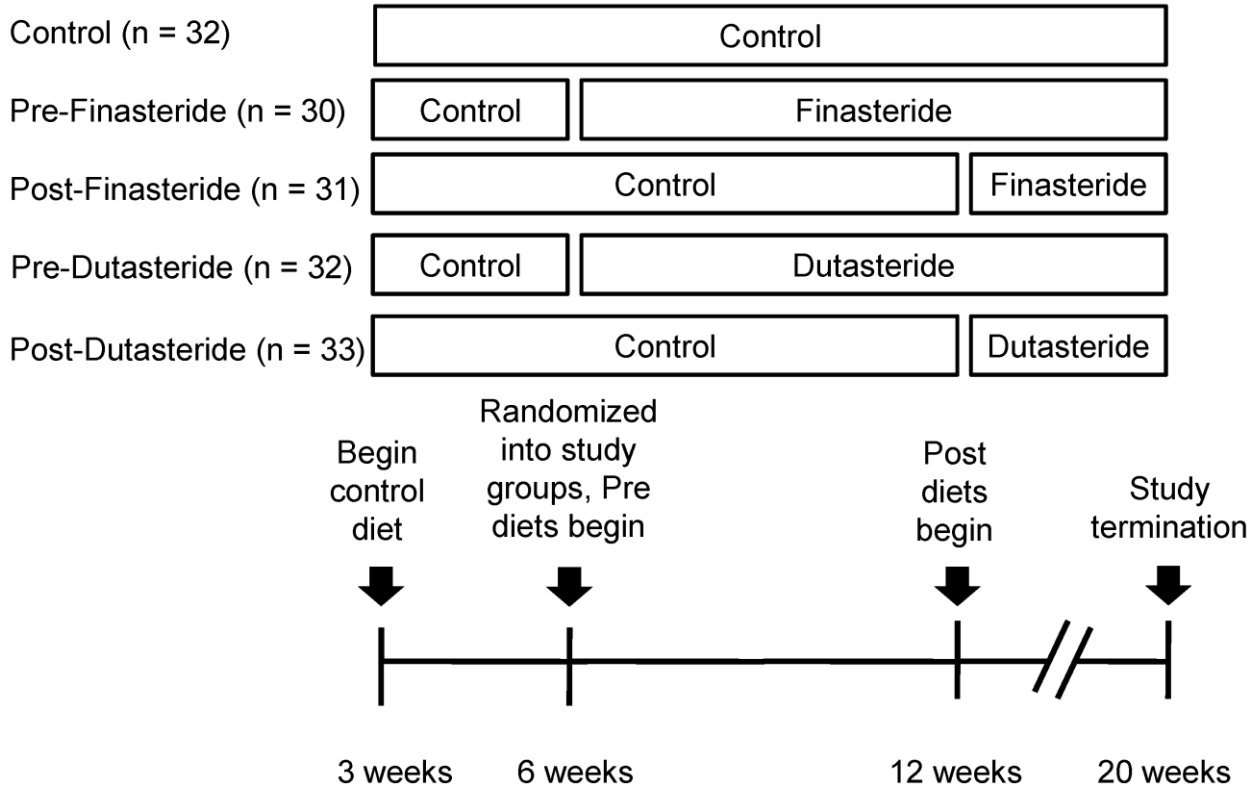

Figure 3.1 Study design

Male C57BL/6 TRAMP x FVB mice were weaned at 3 weeks of age, fed a control diet, and randomized into Control, Pre-Finasteride, Post-Finasteride, Pre-Dutasteride, and Post-Dutasteride groups (n = 30–33) at 6 weeks of age. Pre- and post-groups began their treatment diets at 6 and 12 weeks, respectively, and the study was terminated when mice were 20 weeks of age.

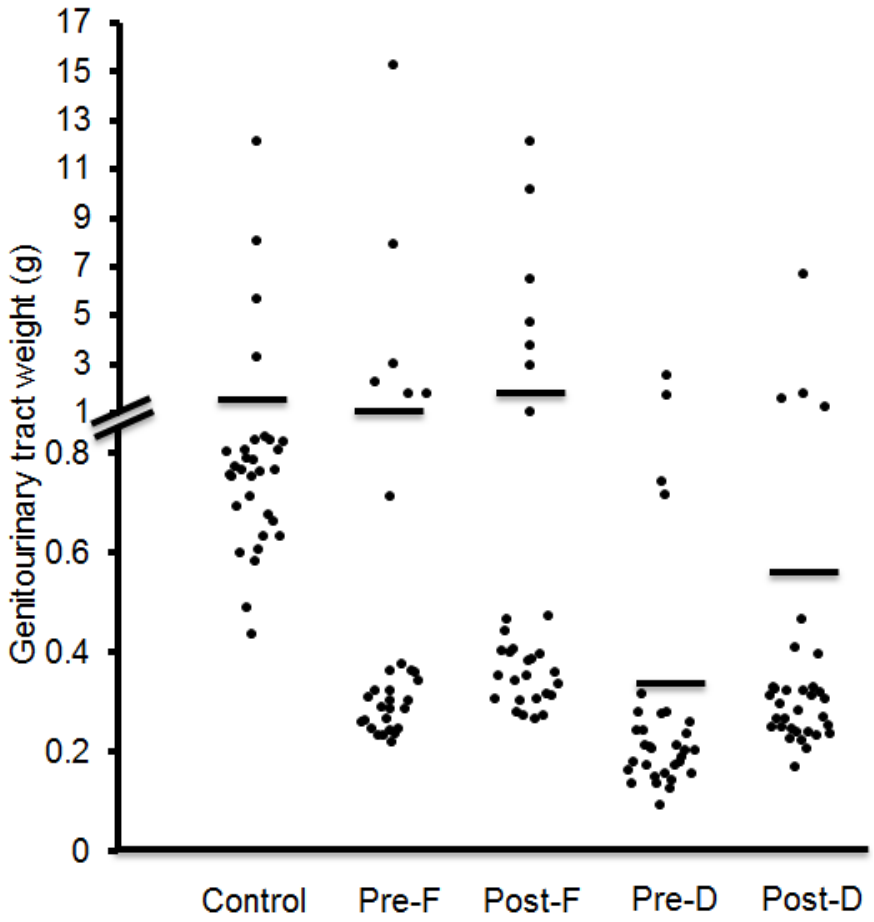

Figure 3.2 Genitourinary tract weights.

Solid lines indicate mean values (n = 30–33). Pre-F = Pre-Finasteride, Post-F = Post-Finasteride, Pre-D = Pre-Dutasteride, Post-D = Post-Dutasteride.

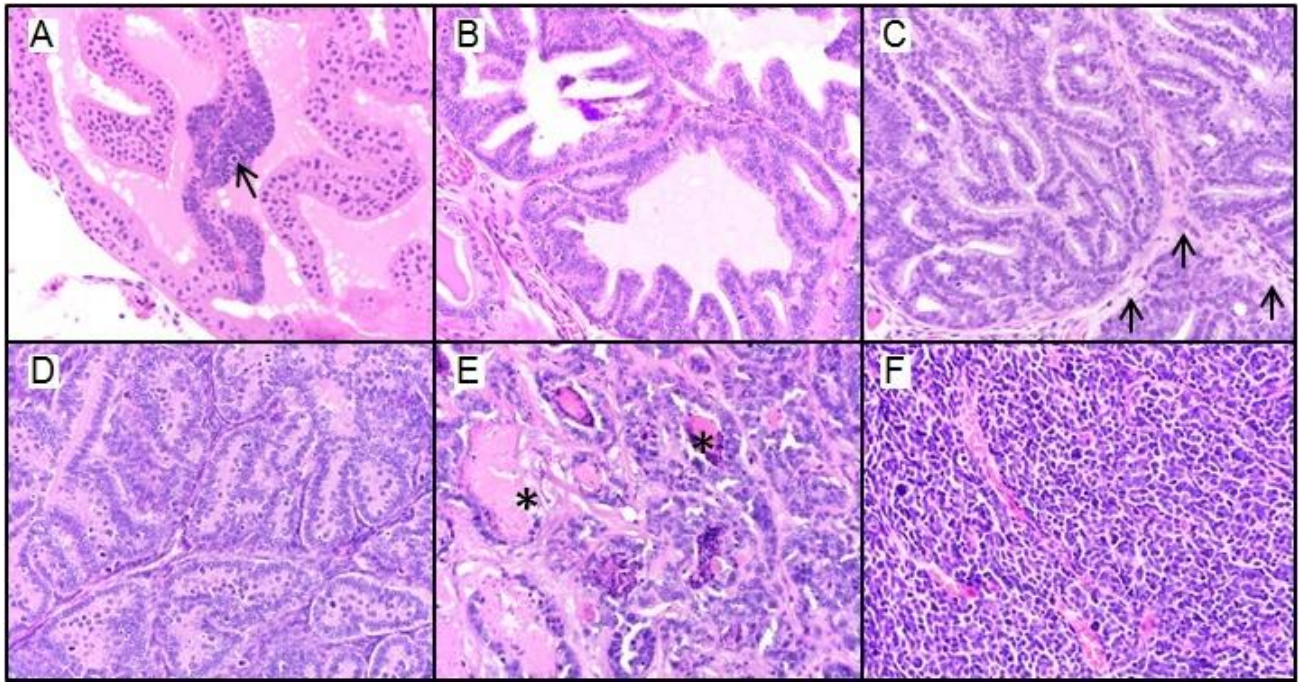

Figure 3.3 Prostate pathology in 20-week-old C57BL/6 TRAMP x FVB male mice captured at 40X magnification.

(A) Grade 1, low-grade PIN. There is focal hyperplasia of prostate epithelial cells resulting in stratification of cells (arrow). Hyperplastic cells have increased basophilia and increased nuclear to cytoplasmic ratios. (B) Grade 2, moderate-grade PIN. Hyperplastic epithelial cells form increased numbers of short and tall papillary projections that extend into the glandular lumen. (C) Grade 3, high-grade PIN. There is loss of prostate glandular lumina due to the presence of numerous hyperplastic prostate epithelial cells that project into the lumen and form a cribriform pattern. Hyperplastic cells do not invade the connective tissue that separates the glands into distinct lobules (arrows). (D) Grade 5, Well-differentiated adenocarcinoma. Well-differentiated neoplastic cells form tubular or glandular like structures that have obliterated lobular architecture by invasion of the connective tissue borders; lobules cannot be observed in this photomicrograph as compared to photomicrograph C. Necrosis of neoplastic cells is absent. (E) Grade 6, Moderately-differentiated adenocarcinoma. Neoplastic prostate epithelial cells are attempting to form glandular structures. Glandular structures vary in size and shape. Cellular atypia is increased and necrosis is present (asterisks).

(F) Grade 7, Poorly differentiated carcinoma. Neoplastic cells have marked atypia and are arranged in sheets with no attempt at forming glandular or tubular structures as compared to figures D and E.

Table 3.1 Final body weights, daily food intake, weight gain/food intake ratio, genitourinary tract weights, and genitourinary tract weights as percentage of body weights (n = 28-33)[1].

Group	Final body weights (g)	Daily food intake (g)	Weight gain/food intake ratio (g gained/g total food intake x 100)	Genitourinary tract weights (g)	Genitourinary tract weights as percentage of body weights
Control	33.3 ± 0.5^{a}	2.99 ± 0.03^{a}	2.8 ± 0.2^{a}	1.56 ± 0.46^{a}	4.91 ± 1.51^{a}
Pre-Finasteride	33.7 ± 0.6^{a}	3.08 ± 0.02^{b}	2.8 ± 0.2^{a}	$1.31 \pm 0.55^{a,b}$	$3.50 \pm 1.32^{b,d}$
Post-Finasteride	$33.0 \pm 0.6^{a,b}$	$3.02 \pm 0.04^{a,b}$	$2.7 \pm 0.2^{a,b}$	1.65 ± 0.55^{a}	$4.87 \pm 1.55^{a,b}$
Pre-Dutasteride	29.9 ± 0.4^{c}	2.96 ± 0.02^{a}	1.6 ± 0.1^{c}	0.35 ± 0.09^{c}	1.19 ± 0.31^{c}
Post-Dutasteride	31.8 ± 0.5^{b}	2.96 ± 0.02^{a}	2.4 ± 0.1^{b}	$0.59 \pm 0.20^{b,c}$	$1.88 \pm 0.63^{c,d}$

[1] Data are mean ± SEM; values with different letters are statistically different from one another ($p<0.05$).

Table 3.2 Raw and adjusted mean most severe lesion scores for the anterior, dorsal, lateral, and ventral prostate lobes (n = 28–33)[1].

	Anterior prostate		Dorsal prostate		Lateral prostate		Ventral prostate	
Group	**Raw**	**Adjusted**	**Raw**	**Adjusted**	**Raw**	**Adjusted**	**Raw**	**Adjusted**
Control	3.36 ± 0.30^{a}	8.69 ± 0.99^{a}	3.56 ± 0.28^{a}	9.52 ± 0.86^{a}	3.45 ± 0.34^{a}	9.45 ± 1.05^{a}	3.03 ± 0.36	8.05 ± 1.13^{a}
Pre-Finasteride	3.20 ± 0.38^{a}	8.92 ± 1.26^{a}	$3.31 \pm 0.44^{a,b}$	$8.74 \pm 1.43^{a,b}$	$3.37 \pm 0.45^{a,b}$	$9.05 \pm 1.46^{a,b}$	3.53 ± 0.49	$9.55 \pm 1.58^{a,b}$
Post-Finasteride	3.03 ± 0.36^{a}	7.69 ± 1.15^{a}	$3.47 \pm 0.37^{a,b}$	9.24 ± 1.20^{a}	$3.32 \pm 0.46^{a,b}$	$8.98 \pm 1.46^{a,b}$	3.26 ± 0.42	$8.73 \pm 1.35^{a,c}$
Pre-Dutasteride	2.09 ± 0.30^{b}	4.84 ± 0.95^{b}	$3.06 \pm 0.45^{b,c}$	$8.03 \pm 1.4^{b,c}$	$3.25 \pm 0.47^{a,b}$	8.52 ± 1.48^{b}	3.11 ± 0.47	$8.05 \pm 1.54^{a,b}$
Post-Dutasteride	2.21 ± 0.26^{b}	5.09 ± 0.82^{b}	2.23 ± 0.33^{c}	5.53 ± 1.04^{c}	2.86 ± 0.43^{b}	7.35 ± 1.34^{b}	2.53 ± 0.40	6.27 ± 1.28^{b}

[1]Data are mean ± SEM; values with different letters are statistically different from one another ($p<0.05$).

Table 3.3 Raw and adjusted mean most common lesion scores for the anterior, dorsal, lateral, and ventral prostate lobes (n = 28–33)[1].

	Anterior prostate		Dorsal prostate		Lateral prostate		Ventral prostate	
Group	**Raw**	**Adjusted**	**Raw**	**Adjusted**	**Raw**	**Adjusted**	**Raw**	**Adjusted**
Control	2.55 ± 0.36^{a}	6.75 ± 1.15^{a}	2.63 ± 0.23^{a}	7.41 ± 0.69^{a}	2.62 ± 0.32	7.42 ± 1.01^{a}	2.72 ± 0.37	7.52 ± 1.19^{a}
Pre-Finasteride	$2.38 \pm 0.41^{a,b}$	$6.23 \pm 1.29^{a,b}$	$2.74 \pm 0.47^{a,b}$	$7.43 \pm 1.49^{b,c}$	2.82 ± 0.47	$7.70 \pm 1.50^{a,b}$	3.16 ± 0.50	$8.64 \pm 1.62^{a,b}$
Post-Finasteride	$2.33 \pm 0.38^{a,c}$	$6.00 \pm 1.19^{a,c}$	$2.82 \pm 0.42^{a,b}$	$7.53 \pm 1.26^{a,b}$	2.88 ± 0.47	$7.95 \pm 1.48^{a,b}$	2.95 ± 0.44	8.11 ± 1.41^{a}
Pre-Dutasteride	$1.63 \pm 0.27^{b,c}$	$3.72 \pm 0.85^{b,c}$	2.32 ± 0.43^{b}	6.06 ± 1.37^{c}	2.69 ± 0.46	7.02 ± 1.44^{b}	2.73 ± 0.46	$7.06 \pm 1.48^{a,b}$
Post-Dutasteride	1.59 ± 0.27^{b}	3.68 ± 0.83^{b}	2.03 ± 0.33^{b}	5.08 ± 1.06^{c}	2.33 ± 0.40	5.95 ± 1.27^{b}	2.28 ± 0.41	5.72 ± 1.30^{b}

[1] Data are mean ± SEM; values with different letters are statistically different from one another ($p<0.05$).

Table 3.4 Histopathological analysis (most severe lesion) of individual prostate lobes in control, finasteride, and dutasteride groups[1, 2].

		Prostatic intraepithelial neoplasia			Adenocarcinoma			Prostate cancer
	n	LG	MG	HG	WD	MD	PD	(WD-PD)
Anterior prostate								
Control	32	2%[a]	30%	50%[a]	3% [a]	0%	16%[a,b]	19%[a]
Pre-Finasteride	30	15%[a,b]	32%	31%[a,b]	0%[b]	2%	20%[a]	22%[a]
Post-Finasteride	29	14%[a]	40%	28%[a,b]	0%[b]	0%	17%[a]	17%[a]
Pre-Dutasteride	32	49%[c]	35%	5%[b]	0%[b]	0%	11%[b,c]	11%[b]
Post-Dutasteride	33	33%[b,c]	48%	9%[b]	0%[b]	0%	9%[c]	9%[b]
Dorsal prostate								
Control	32	2%[a]	11%[a]	69%[a]	2%	2%	16%[a]	19%[a,c]
Pre-Finasteride	29	17%[a]	45%[b]	10%[b,c]	0%	0%	28%[b]	28%[b]
Post-Finasteride	31	5%[a]	40%[a,b]	31%[b]	0%	0%	24%[b]	24%[b,c]
Pre-Dutasteride	31	42%[b]	26%[a,b]	3%[c]	0%	0%	29%[b]	29%[b]
Post-Dutasteride	33	43%[b]	38%[a,b]	6%[c]	0%	0%	12%[a]	12%[a]
Lateral prostate								
Control	28	11%[a]	46%[a]	23%[a]	0%	0%	20%[a]	20%[a]
Pre-Finasteride	30	23%[a]	43%[a]	2%[b]	0%	0%	32%[b]	32%[b]
Post-Finasteride	30	27%[a,b]	35%[a,b]	8%[b]	0%	0%	30%[b,c]	30%[b,c]
Pre-Dutasteride	32	42%[b,c]	22%[b]	3%[b]	0%	0%	33%[b]	33%[b]
Post-Dutasteride	33	48%[c]	20%[b]	6%[b]	0%	0%	26%[c]	26%[c]
Ventral prostate								
Control	30	0%[a]	35%[a]	45%[a]	0%	0%[a]	20%[a]	20%[a]
Pre-Finasteride	28	29%[b]	24%[a,b,c]	9%[b]	0%	4%[b]	35%[b]	38%[b]
Post-Finasteride	30	22%[b]	31%[a,b]	22%[c]	0%	0%[a]	25%[c]	25%[c]
Pre-Dutasteride	31	46%[c]	21%[b,c]	0%[d]	2%	0%[a]	31%[b]	33%[d]
Post-Dutasteride	30	51%[c]	13%[c]	15%[b,c]	0%	0%[a]	20%[a]	20%[a]

[1]Values with different letters are statistically different from one another ($p<0.05$).
[2]LG = low-grade, MG = moderate-grade, HG = high-grade, PIN = prostatic intraepithelial neoplasia, WD = well-differentiated, MD = moderately differentiated, PD = poorly differentiated.

Table 3.5 Histopathological analysis (most common lesion) of individual prostate lobes in control, finasteride, and dutasteride groups[1, 2].

		Prostatic intraepithelial neoplasia			Adenocarcinoma			Prostate cancer
	n	LG	MG	HG	WD	MD	PD	(WD-PD)
Anterior prostate								
Control	32	44%[a]	20%	20%[a]	0%	0%	16%[a]	16%[a]
Pre-Finasteride	30	56%[a]	22%	3%[a,b]	0%	0%	19%[a]	19%[a]
Post-Finasteride	29	50%[a]	29%	5%[a,b]	0%	0%	16%[a]	16%[a]
Pre-Dutasteride	32	76%[b]	16%	0%[b]	0%	0%	8%[b]	8%[b]
Post-Dutasteride	33	79%[b]	14%	0%[b]	0%	0%	8%[b]	8%[b]
Dorsal prostate								
Control	32	5%[a]	59%[a]	28%[a]	0%	0%	8%[a]	8%[a]
Pre-Finasteride	29	55%[b]	19%[b,c]	0%[b]	0%	0%	26%[b]	26%[b]
Post-Finasteride	31	33%[c]	44%[a,d]	2%[b]	0%	0%	21%[b]	21%[b]
Pre-Dutasteride	31	73%[b]	6%[c]	0%[b]	0%	0%	21%[b]	21%[b]
Post-Dutasteride	33	57%[b]	31%[b,d]	0%[b]	0%	0%	12%[a]	12%[a]
Lateral prostate								
Control	28	10%[a]	70%[a]	7%[a]	0%	0%	14%[a]	14%[a]
Pre-Finasteride	30	52%[b]	22%[b]	0%[b]	0%	0%	27%[b]	27%[b]
Post-Finasteride	30	47%[b]	25%[b]	2%[b]	0%	0%	27%[b]	27%[b]
Pre-Dutasteride	32	64%[c]	9%[c]	0%[b]	0%	0%	27%[b]	27%[b]
Post-Dutasteride	33	65%[c]	15%[b,c]	0%[b]	0%	0%	20%[c]	20%[c]
Ventral prostate								
Control	30	14%[a]	68%[a]	2%	0%	0%	16%[a]	16%[a]
Pre-Finasteride	28	45%[b]	20%[b]	0%	0%	0%	35%[b]	35%[b]
Post-Finasteride	30	32%[c]	43%[c]	0%	0%	0%	25%[c]	25%[c,d]
Pre-Dutasteride	31	69%[d]	2%[d]	0%	2%	0%	28%[c]	30%[b,d]
Post-Dutasteride	30	64%[d]	17%[b]	0%	0%	0%	19%[a]	19%[a,c]

[1]Values with different letters are statistically different from one another ($p<0.05$).
[2]LG = low-grade, MG = moderate-grade, HG = high-grade, PIN = prostatic intraepithelial neoplasia, WD = well-differentiated, MD = moderately differentiated, PD = poorly differentiated.

Table 3.6 Iliac lymph node metastases incidence in control, finasteride, and dutasteride groups.

Group	n	Lymph node metastases incidence (%)
Control	21	4 (19)
Pre-Finasteride	26	5 (19)
Post-Finasteride	24	7 (29)
Pre-Dutasteride	22	5 (23)
Post-Dutasteride	24	2 (8)

References

1. American Cancer Society. Cancer facts and figures 2013.

2. Tien AH, Sadar MD. Androgen-responsive gene expression in prostate cancer progression. In: Androgen-responsive genes in prostate cancer. Springer. 2013;135-153.

3. Grossmann ME. Androgen receptor signaling in androgen-refractory prostate cancer. J Natl Cancer Inst. 2001;93(22):1687–1697.

4. Andriole GL, Roehrborn C, Schulman C, Slawin KM, Somerville M, et al. Effect of dutasteride on the detection of prostate cancer in men with benign prostatic hyperplasia. Urology. 2004;64(3):537-541.

5. Russell DW, Wilson JD. Steroid 5α-Reductase: Two genes/two enzymes. Annu Rev Biochem. 1994;63(1):25-61.

6. Luo J, Dunn TA, Ewing CM, Walsh PC, Isaacs WB. Decreased gene expression of steroid 5α-reductase 2 in human prostate cancer: implications for finasteride therapy of prostate carcinoma. Prostate. 2003;57(2):134-139.

7. Titus MA, Gregory CW, Ford OH, Schell MJ, Maygarden SJ, et al. Steroid 5α-reductase isozymes I and II in recurrent prostate cancer. Clin Cancer Res. 2005;11(12):4365-4371.

8. Söderström TG, Bjelfman C, Brekkan E, Ask B, Egevad L, et al. Messenger ribonucleic acid levels of steroid 5α-reductase 2 in human prostate predict the enzyme activity. J Clin Endocrinol Metab. 2001;86(2):855-858.

9. Bjelfman C, Söderström TG, Brekkan E, Norlén BJ, Egevad L, et al. Differential gene expression of steroid 5α-reductase 2 in core needle biopsies from malignant and benign prostatic tissue. J Clin Endocrinol Metab, 1997;82(7):2210-2214.

10. Iehlé C, Radvanyi F, de Medina SGD, Ouafik LH, Gérard H, et al. Differences in steroid 5α-reductase iso-enzymes expression between normal and pathological human prostate tissue. J Steroid Biochem Mol Biol.1999;68(5):189-195.

11. Nakamura Y, Suzuki T, Nakabayashi M, Endoh M, Sakamoto K, et al. In situ androgen producing enzymes in human prostate cancer. Endocr Relat Cancer. 2005;12(1):101-107.

12. Habib FK, Ross M, Bayne CW, Bollina P, Grigor K, et al. The loss of 5α-reductase type I and type II mRNA expression in metastatic prostate cancer to bone and lymph node metastasis. Clin Cancer Res. 2003;9(5):1815-1819.

13. Thompson IM, Goodman PJ, Tangen CM, Lucia MS, Miller GJ, et al. The influence of finasteride on the development of prostate cancer. N Engl J Med. 2003;349(3):215-224.

14. Andriole GL, Bostwick DG, Brawley OW, Gomella LG, Marberger M, et al. Effect of dutasteride on the risk of prostate cancer. N Engl J Med. 2010;362(13):1192-1202.

15. FDA Drug Safety Communication: 5α-reductase inhibitors (5-ARIs) may increase the risk of a more serious form of prostate cancer. Retrieved from http://www.fda.gov/Drugs/DrugSafety/ucm258314.htm. Accessed 2013 September 23.

16. Pinksy PF, Black A, Grubb R, Crawford ED, Andriole G, et al. Projecting prostate cancer mortality in the PCPT and REDUCE chemoprevention trials. Cancer. 2013;119(3):593-601.

17. Fleshner NE. Dutasteride and active surveillance of low-risk prostate cancer. Lancet. 2012;379(9826):1590.

18. Xu Y, Dalrymple SL, Becker RE, Denmeade SR, Isaacs JT. Pharmacologic basis for the enhanced efficacy of dutasteride against prostatic cancers. Clin Cancer Res. 2006;12(13):4072-4079.

19. Canene-Adams K, Lindshield BL, Wang S, Jeffery EH, Clinton SK, et al. Combinations of tomato and broccoli enhance antitumor activity in dunning R3327-H prostate adenocarcinomas. Cancer Res. 2007;67(2):836-843.

20. Cho YM, Takahashi S, Asamoto M, Suzuki S, Tang M, et al. Suppressive effects of antiandrogens, finasteride and flutamide on development of prostatic lesions in a transgenic rat model. Prostate Cancer Prostatic Dis. 2007;10(4):378-383.

21. Schmidt LJ, Regan KM, Anderson SK, Sun Z, Ballman KV, et al. Effects of the 5α-reductase inhibitor dutasteride on gene expression in prostate cancer xenografts. Prostate. 2009;69(16):1730-1743.

22. Opoku-Acheampong AB, Nelsen MK, Unis D, Lindshield BL. The effect of finasteride and dutasteride on the growth of WPE1-NA22 prostate cancer xenografts in nude mice. PLoS One. 2012;7(1):e29068.

23. Costello LC, Franklin RB, Zou J, Feng P, Bok R, et al. Human prostate cancer ZIP1/zinc/citrate genetic/metabolic relationship in the TRAMP prostate cancer animal model. Cancer Biol Ther. 2011;12(12):1078-1084.

24. Greenberg NM, DeMayo F, Finegold MJ, Medina D, Tilley WD, et al. Prostate cancer in a transgenic mouse. Proc Natl Acad Sci U S A. 1995;92(8):3439-3443.

25. Kaplan-Lefko PJ, Chen TM, Ittmann MM, Barrios RJ, Ayala GE, et al. Pathobiology of autochthonous prostate cancer in a pre-clinical transgenic mouse model. Prostate. 2003;55(3):219-237.

26. Gingrich JR, Barrios RJ, Foster BA, Greenberg NM. Pathologic progression of autochthonous prostate cancer in the TRAMP model. Prostate Cancer Prostatic Dis. 1999;2(2):70-75.

27. Berman-Booty LD, Sargeant AM, Rosol TJ, Rengel RC, Clinton SK, et al. A review of the existing grading schemes and a proposal for a modified grading scheme for prostatic lesions in TRAMP mice. Toxicol Pathol. 2012;40(1):5–17.

28. Zuniga KE, Clinton SK, Erdman JW Jr. The interactions of dietary tomato powder and soy germ on prostate carcinogenesis in the TRAMP model. Cancer Prev Res (Phila). 2013;6(6):548-557.

29. Shao TC, Li H, Ittmann M, Cunningham GR. Effects of dutasteride on prostate growth in the large probasin-large T antigen mouse model of prostate cancer. J Urol. 2007;178(4 pt 1):1521-1527.

30. Prahalada S, Rhodes L, Grossman SJ, Heggan D, Keenan KP, et al. Morphological and hormonal changes in the ventral and dorsolateral prostatic lobes of rats treated with finasteride, a 5α-reductase inhibitor. Prostate. 1998;35(3):157-164.

31. Ku JH, Shin JK, Cho MC, Myung JK, Moon KC, et al. Effect of dutasteride on the expression of hyposia-inducible factor 1α, vascular endothelial growth factor and microvessel density in rat and human prostate tissue. Scand J Urol Nephrol. 2009;43(6):445-453.

32. Gingrich JR, Barrios RJ, Kattan MW, Nahm HS, Finegold MJ, et al. Androgen-independent prostate cancer progression in the TRAMP model. Cancer Res. 1997;57(21):4687-4691.

33. Elliott CS, Shinghal R, Presti JC Jr. The influence of prostate volume on prostate-specific antigen performance: implications for the prostrate cancer prevention trial outcomes. Clin Cancer Res. 2009;15(14):4694-4699.

34. Pinsky P, Parnes H, Ford L. Estimating rates of true high-grade disease in the Prostate Cancer Prevention Trial. Cancer Prev Res (Phila). 2008;1(3):182-186.

35. Redman MW, Tangen CM, Goodman PJ, Lucia MS, Coltman CA Jr, et al. Finasteride does not increase the risk of high-grade prostate cancer: A bias-adjusted modeling approach. Cancer Prev Res (Phila). 2008;1(3):174-181.

36. Lucia MS, Epstein JI, Goodman PJ, Darke AK, Reuter VE, et al. Finasteride and high-grade prostate cancer in the Prostate Cancer Prevention Trial. J Natl Cancer Inst. 2007;99(18):1375-1383.

37. Kaplan SA, Roehrborn CG, Meehan AG, Liu KS, Carides AD, et al. PCPT: Evidence that finasteride reduces risk of most frequently detected intermediate- and high-grade (Gleason Score 6 and 7) cancer. Urology. 2009;73(5):935-939.

38. US Environmental Protection Agency Recommended use of body weight 3/4 as the default method in derivation of the oral reference dose. Retrieved from http://www.epa.gov/raf/publications/interspecies-extrapolation.htm. Accessed 2013 September 23.

Chapter 4 - Characterization of Molecular Changes due to Finasteride and Dutasteride treatment in TRAMP Mice Prostate Cancer; and in 8, 12, 16 and 20-week-old AIN-93G-fed TRAMP Mice Prostate Cancer −A Histopathological Study using Immunohistochemistry and *In Situ* Hybridization

Abstract

Background: Previously, we studied the effect of finasteride- or dutasteride-containing diets begun at 6 weeks (Pre) or 12 weeks (Post) of age on prostate cancer development in C57BL/6 TRAMP x FVB mice. Pre and post groups received drugs before and after mice were expected to develop prostate cancer, respectively. Post-Dutasteride treatment was more effective than Pre-Dutasteride; and both dutasteride treatments better than both finasteride treatments in decreasing prostatic intraepithelial neoplasia (PIN) progression and prostate cancer development. Pre-Finasteride, Post-Finasteride and Pre-Dutasteride treatments significantly decreased incidence of high-grade PIN, but increased incidence of poorly differentiated prostate cancer. In this study, we characterized the molecular changes in prostate cancer in these mice to elucidate the discordant response in the Pre-Dutasteride and both finasteride groups and determine why Post-Dutasteride treatment was more effective. We also determined molecular changes in prostate cancer with increasing age in C57BL/6 TRAMP x FVB mice.

Method/Principal findings: The expression levels of androgen receptor and Ki-67 protein, DNA fragmentation from apoptosis were measured using immunohistochemistry; and 5α-reductase 1 and 5α-reductase 2 mRNA were measured using *in situ* hybridization in formalin-fixed, paraffin-embedded prostate tissue of AIN-93G control, Pre-Finasteride, Post-Finasteride, Pre-Dutasteride, and Post-Dutasteride (n = 5) treated male TRAMP mice with genitourinary weight less than 1 gram; and AIN-93G control, Pre-Finasteride, Post-Finasteride (n = 4), Pre-Dutasteride (n = 2), and Post-Dutasteride (n

= 4) treated male TRAMP mice with genitourinary weight greater than 1 gram; and also in 8 (n = 5), 12 (n = 8), 16 (n = 9) and 20 (n = 12)-week-old AIN-93G-fed male TRAMP mice. Pre-Finasteride treatment significantly decreased androgen receptor expression in small tumors. Pre-Finasteride, Post-Finasteride, and Post-Dutasteride treatments significantly increased hyperplastic apoptosis in small tumors. Pre-Finasteride treatment significantly increased hyperplastic apoptosis in large tumors. Post-Finasteride and Post-Dutasteride treatments significantly reduced proliferation in large tumors.

Conclusion: Our results suggest the difference in genitourinary weights is influenced more by proliferation, rather than androgen receptor and apoptosis in tumor, indicating that in large lesions, proliferation is most crucial and this imbalance between proliferation, apoptosis and androgen receptor may be responsible for the development of large tumors. Mice age may not be significantly important in regulating proliferation, androgen receptor and apoptosis to promote tumor growth.

Contributors to study

Conceived and designed the experiments: Brian L. Lindshield. Performed the experiments: Alexander B. Opoku-Acheampong, Jamie N. Henningson. Analyzed the data: Alexander B. Opoku-Acheampong, Jamie N. Henningson, Brian L. Lindshield. Contributed reagents/materials/analysis tools: Alexander B. Opoku-Acheampong, Jamie N. Henningson. Wrote the manuscript: Alexander B. Opoku-Acheampong.

Introduction

Prostate cancer is the most commonly diagnosed male cancer in the US and the second leading cause of male cancer death [1]. Most prostate cancer growth is initially androgen-dependent or sensitive [2]. In prostate stromal cells, testosterone, the main plasma androgen is converted by 5α-reductase 1 and 5α-reductase 2 isoenzymes to the more potent dihydrotestosterone (DHT), which has up to a 10-fold higher affinity to the androgen receptor than testosterone [3,4]. 5α-reductase 2 is predominantly expressed in the epithelial and stromal cells in normal prostate tissue, however, multiple studies [5-8], although not all [9,10], have reported increased or unchanged 5α-reductase 1 and/or decreased or lost

5α-reductase 2 mRNA expression or activity in prostate cancer compared to nonmalignant prostate tissue. Recently, 5α-reductase 3 has been identified as a new isoenzyme and found to be overexpressed in hormone-refractory prostate cancer cells and tissues [11].

In transgenic mice, it has been shown that androgen receptor levels in prostate epithelium are a major factor controlling proliferation and that increased AR expression results in a higher proliferative rate and increased risk for prostate cancer [12], and the progression of prostate cancer to castrate-resistant prostate cancer [13]. In fact, some authors have reported that androgen receptor is expressed in almost all primary prostate cancers and most castration-resistant prostate cancers [14,15]. However, evidence of loss of androgen receptor expression in tumor cells exists [16].

In the adult prostate, androgens are thought to contribute to the maintenance of homeostasis between cell proliferation and apoptosis [17,18]. Inside the prostatic luminal epithelium, DHT binds to androgen receptors to trigger the transcription of genes that control cellular proliferation and apoptosis by regulating the expression and secretion of growth factors. Animal studies have shown that growth factors secreted by prostatic stromal cells can act on epithelial cells to affect proliferation and apoptosis [17,19,20]. In humans, DHT may induce the production of epidermal growth factor (EGF), keratinocyte growth factor (KGF), and insulinlike growth factors (IGFs)—all of which control cellular proliferation [17]. Similarly, DHT affects the activity of transforming growth factor-β (TGF-β) which controls apoptosis [20,21]. In prostate cancer, there is a loss of constraints on cell proliferation along with dysregulation of apoptosis which leads to an imbalance between cell division and cell death [22]. Increased prostate cell proliferation [23,24] and decreased apoptosis [25,26] have both been implicated in increasing the risk of prostate cancer.

Since cell proliferation and apoptosis are androgen-dependent mechanisms [17,18], decreasing DHT production via 5α-reductase inhibition is an approach that may be effective in preventing or delaying the growth of prostate cancer [27]. Finasteride (5α-reductase 2 inhibitor) and dutasteride (5α-reductase 1 and 5α-reductase 2 inhibitor) are two pharmaceuticals commonly used to treat benign

prostatic hyperplasia (BPH), a nonmalignant enlargement of the prostate. The potential of these inhibitors to decrease prostate cancer development and/or progression through their antiandrogen action has been studied in several clinical trials [28-30]. Previously, we studied the effect of finasteride- or dutasteride-containing diets at 6 weeks (Pre) or 12 weeks (Post) of age on prostate tumor development in C57BL/6 TRAMP x FVB mice. Post-Dutasteride treatment was more effective than Pre-Dutasteride; and both dutasteride treatments better than both finasteride treatments in decreasing prostatic intraepithelial neoplasia (PIN) progression and prostate cancer development. The finasteride groups and the Pre-Dutasteride group also had increased incidence of poorly differentiated prostate cancer in most lobes compared to the control [31]. Thus, we were interested in characterizing the molecular changes in these mice to elucidate the discordant response in the Pre-Dutasteride and both finasteride groups and determine why Post-Dutasteride treatment was more effective.

The cell-type specific expression patterns of 5α-reductase 1 and 5α-reductase 2 mRNA, androgen receptor and Ki-67 protein, DNA fragmentation from apoptosis were determined in formalin-fixed, paraffin-embedded prostate tissue sections of finasteride and dutasteride treated male C57BL/6 TRAMP x FVB mice. We compared expression levels in mice with genitourinary weight (GU) less than 1 gram (mainly associated with lower most common and most severe lesion scores, and PIN) to levels in mice with GU weight greater than 1 gram (mainly associated with higher most common and most severe lesion scores, and poorly differentiated carcinoma) to understand the discordant response seen previously within the treatment groups. The expression levels of biomarkers were also determined and compared in 8, 12, 16 and 20-week-old male AIN-93G-fed male C57BL/6 TRAMP x FVB mice to better understand how their levels vary at different ages and stages of prostate carcinogenesis. These time points were selected because C57BL/6 TRAMP x FVB mice develop epithelial hyperplasia by 8 weeks [32], and PIN and well-differentiated adenocarcinoma by 12 weeks [33]. Sixteen weeks is intermediate between 12 and 20 weeks when TRAMP mice would have developed poorly differentiated and invasive carcinoma [33]. Kaplan and colleagues used the above stated time points previously to study the

incidence and distribution of pathologic changes within each lobe of C57BL/6 TRAMP x FVB mice prostate as a function of time [33]. This will enable us to measure the expression of these prostate cancer biomarkers at different stages of growth and development of prostate cancer in TRAMP mice.

These prostate cancer biomarkers were selected because their expression levels in C57BL/6 TRAMP x FVB mice prostate will provide an objective evaluation of the molecular response to mice age, and finasteride and dutasteride intervention, beyond the most severe and most common lesion scores. Determining androgen receptor and 5α-reductase isoenzyme expression is important because both age, and finasteride and dutasteride inhibiting 5α-reductase isoenzymes and reducing DHT levels to alter the expression profile of 5α-reductase isoenzymes and androgen receptor, respectively, change cytologic and architectural features of TRAMP mice prostate. Although 5α-reductase has been quantified in human and animal models, to the best of our knowledge, we believe we are the first to quantify 5α-reductase levels in TRAMP mice.

Materials and Methods

Tissues

Sections of prostate tissue from male C57BL/6 TRAMP X FVB mice in AIN-93G control, Pre-Finasteride and Post-Finasteride, and Pre-Dutasteride and Post-Dutasteride diet groups from our previous study [31] were used for immunohistochemical (IHC) and *in situ* hybridization (ISH) analysis in this study. Additionally, 6-week-old heterozygous C57BL/6-Tg 8247Ng/J TRAMP male and female mice were purchased (The Jackson Laboratory, Bar Harbor, ME) and bred to produce homozygous males. These were bred with female FVB/NJ mice (The Jackson Laboratory, Bar Harbor, ME) to produce C57BL/6 TRAMP x FVB mice. Male C57BL/6 TRAMP x FVB mice were weaned and began consuming AIN-93G diet at 3 weeks of age before being randomized to 8 (n = 5), 12 (n = 8), 16 (n = 9) and 20 (n = 12)-week groups. Mice were individually housed, monitored daily, weighed weekly, and provided AIN-93G diet and water ad libitum. Mice were terminated at their respective time points, anesthetized by CO_2 inhalation and euthanized by exsanguination. The genitourinary tracts, kidneys, and

lungs were dissected, and the genitourinary tracts were weighed. Iliac lymph nodes were also collected whenever possible. All tissues were fixed by immersion in 10% neutral buffered formalin (NBF) for 48 hours, and then moved to 70% alcohol until processing in the Kansas State University Veterinary Diagnostic Laboratory.

Histopathology

Histological processing of prostate tissues, sectioning, scoring for most common and most severe lesions, and adjusting for distribution, were performed as described previously [31,34]. The anterior, dorsal, lateral and ventral lobes of C57BL/6 TRAMP × FVB mice were assigned two grades each between 0-7. The first grade is the most severe lesion within the lobe [normal prostate as least severe (grade 0), and poorly differentiated as most severe (grade 7)]. The second grade is the most common lesion within the lobe [normal prostate as least common (grade 0), and poorly differentiated as most common (grade 7). The most severe and most common lesions within a lobe were adjusted for distribution, either as focal, multifocal, or diffuse. With focal, there are fewer than three foci within the lobe. Multifocal indicates there are three or more foci within the lobe, with less than 50% of the lobe containing the lesion of interest. Diffuse indicates greater than 50% of the lobe is affected [34]. The expression levels of androgen receptor and Ki-67 protein, DNA fragmentation from apoptosis were measured using immunohistochemistry; and 5α-reductase 1 and 5α-reductase 2 mRNA were measured using *in situ* hybridization in formalin-fixed, paraffin-embedded prostate tissue of AIN-93G control, Pre-Finasteride, Post-Finasteride, Pre-Dutasteride, and Post-Dutasteride (n = 5) treated male TRAMP mice with genitourinary weight less than 1 gram; and AIN-93G control, Pre-Finasteride, Post-Finasteride (n = 4), Pre-Dutasteride (n = 2), and Post-Dutasteride (n = 4) treated male TRAMP mice with genitourinary weight greater than 1 gram; and also in 8 (n = 5), 12 (n = 8), 16 (n = 9) and 20 (n = 12)-week-old AIN-93G-fed male TRAMP mice.

Ki-67 immunohistochemistry

Prostate sections (4 µm) were deparaffinized in Leica Bond Dewax Solution (Leica Microsystems Inc., Buffalo Grove, USA) at 72°C, and then rehydrated in 100% ethanol, followed by 3 washes in Tris-buffered saline. Antigen retrieval was carried out with Novocastra Bond Epitope Retrieval Solution 1 (citrate buffer, pH 6) (AR9961; Leica Microsystems Inc., Buffalo Grove, IL) for 20 minutes at 100°C. The sections were stained with a prediluted rabbit monoclonal antibody to Ki-67 (CPRM325AA; Biocare Medicals, Concord, CA) for 15 minutes at room temperature. The anti-rabbit poly-HRP-IgG polymer from the Bond Polymer Refine Detection System (Leica Microsystems Inc., Buffalo Grove, IL) was used for the enhancement of the signal. The substrate chromogen, 3,3′-diaminobenzidine (DAB), was used for the detection of the complex. Sections were counterstained with Gill's hematoxylin, and processed back to xylene through an increasing ethanol gradient [95% (1X) and 100% (2X)], and then mounted. Tissue from a canine mast cell tumor was used as a positive control.

TUNEL staining

Terminal deoxynucleotidyl transferase dUTP nick end labeling (TUNEL) staining was performed using the Apoptag Peroxidase *In Situ* Apoptosis Detection kit (S7100; Millipore, Temecula, CA). Prostate sections (4 µm) were baked in a Fisher Scientific Isotemp (model 281A) vacuum oven preheated to 60°C for 30 minutes. After baking, sections were deparaffinized in xylene, rehydrated through a graded ethanol series [100% (2X), 95% and 70% (both 1X)] and treated with ready-to-use proteinase K (S302080-2; Dako North America, Inc., Carpinteria, CA) for 15 minutes at room temperature. Sections were washed with 2 changes of distilled water for 5 minutes each. Endogenous peroxidases were blocked with 3% hydrogen peroxide in phosphate buffered saline (PBS, pH 7.4), for 5 minutes and washed with 2 changes of PBS. Equilibration buffer containing digoxigenin-conjugated nucleotides was placed directly onto the section for 10 seconds. Sections were then incubated with terminal deoxynucleotide transferase (TdT) enzyme (1:15 dilution) in a humidified chamber at 37°C for 1 hour. Sections were then incubated for 10 minutes at room temperature in stop-wash buffer, rinsed in

3 changes of PBS for 1 minute each, and then incubated with anti-digoxigenin conjugate for 30 minutes at room temperature. Sections were washed in 4 changes of PBS for 2 minutes each, and then incubated with the substrate chromogen, 3,3′-diaminobenzidine (DAB) for 3 minutes. Sections were then stained with 0.5% (w/v) methyl green counterstain, dehydrated through 100% N-butanol (3X) and xylene and then mounted.

Androgen receptor immunohistochemistry

Prostate sections (4 µm) were baked in a Fisher Scientific Isotemp (model 281A) vacuum oven preheated to 60°C for 30 minutes. After baking, sections were deparaffinized in xylene and rehydrated using a decreasing ethanol gradient [100% (2X), 95% and 80% (both 1X)]. Endogenous alkaline phosphatase was blocked using 3% hydrogen peroxide in methanol. Antigen retrieval was carried out by microwaving at 540W in 10 mM Tris/EDTA buffer, pH 9, four times for 5 minutes. Sections were blocked with 2.5% normal horse serum (Vector Laboratories, Inc., Burlingame, CA) before incubation for 1 hour at 37°C with a rabbit polyclonal antibody (1:50 dilution; N-20, sc-816; Santa Cruz Biotechnology, Santa Cruz, CA). After washing, sections were incubated with ImmPRESS-AP anti-rabbit IgG (alkaline phosphatase) polymer detection reagent (MP-5401; Vector Laboratories, Inc., Burlingame, CA) for 30 minutes at room temperature. Colors were developed with a Vector Red alkaline phosphatase substrate kit (SK-5100; Vector Laboratories, Inc., Burlingame, CA). Slides were subsequently counterstained with hematoxylin (Vector Laboratories, Inc., Burlingame, CA), and processed back to xylene through an increasing ethanol gradient [80%, 95% (both 1X) and 100% (2X)] and then mounted. Normal rabbit IgG (1:100; sc-2027: Santa Cruz Biotechnology, Santa Cruz, CA, USA) was used as a negative control.

5α-reductase 1 and 5α-reductase 2 in situ hybridization

5α-reductase 1 and 5α-reductase 2 accessions NM 175283.3 and NM 053188.2, respectively, obtained from National Center for Biotechnology Information (NCBI) website were submitted to Advanced Cell Diagnostics, Inc., [(ACD), Hayward, CA)] for custom probe design and synthesis.

Prostate sections (4 µm) were baked in a Fisher Scientific (model 77) slide warmer preheated to 55°C for 25 minutes. Sections were deparaffinized in xylene, rehydrated in 100% ethanol, and air-dried for 5 minutes at room temperature. Sections were then treated serially with: Pre-Treatment 1 solution (endogenous hydrogen peroxidase block with Pretreat 1 solution for 10 minutes at room temperature); Pre-Treatment 2 (100-104°C, 25 minutes immersion in Pretreat 2 solution); and, Pre-Treatment 3 (protease digestion, 40°C for 28 minutes); rinses with distilled water (2X) were performed after each Pre-Treatment step. Sections were then hybridized in 5α-reductase 1 or 5α-reductase 2 probes, without a cover slip, at 40°C for 2 hours in a HybEZ Oven (ACD). After wash buffer steps, signal amplification from the hybridized probes were performed by the serial application of Amp 1, 40°C for 30 minutes (PreAmplifier step), Amp 2, 40°C for 15 minutes (signal enhancer step), Amp 3, 40°C for 30 minutes (amplifier step), Amp 4, 40°C for 15 minutes (Label Probe step), Amp 5, ambient temperature for 30 minutes, and Amp 6, ambient temperature for 15 minutes (signal amplifications steps); wash buffer steps with Wash Buffer (ACD, proprietary) were performed after each Amp step. Horseradish peroxidase (HRP) activity was then observed by the application of 3,3′-diaminobenzidine (DAB) for 10 minutes at ambient temperature. Sections were then counterstained with Gill's hematoxylin, dehydrated through graded ethanol [95% (1X), 100% (2X)] and xylene and then mounted. Sections were quality controlled for RNA integrity with an RNAscope probe for cyclophilin B (*Mm-Ppib*) RNA (positive control) and for nonspecific background with a probe for bacterial *dap*B RNA (negative control). Specific RNA staining signal was identified as brown, punctate dots.

Quantification of prostate cancer biomarkers

A board-certified pathologist identified areas of epithelium that were composed of a single layer of cells as normal epithelium; hyperplastic regions as where cells lost polarity and piled up on one another; and tumor as diffuse sheets of cells with no organization characterized by neoplastic cellular characteristics, using an Olympus DP26 digital camera (Olympus America, Center Valley, PA). These areas were scanned using a Pannoramic Midi scanner (3D Histech, Budapest, Hungary) with a 20X

objective, giving 2 megapixel resolution. Images were captured using the 3D Histech software. Scanned images were then annotated using Halo software (Indica Laboratory, Coralles, NM). Androgen receptor and Ki-67 protein, and DNA fragmentation from apoptosis were quantitated using the double stain cytoplasmic and nuclear stain algorithm (Indica Laboratory), which was set to identify a single positive nuclear stain. Data were quantified for Ki-67, androgen receptor and apoptosis in normal prostate, hyperplasia and tumor sections of prostate sections.

The total positive cells per area was calculated as:

$$\text{Total positive cells per area } (\mu m^2) = \frac{\text{Total positive cells}}{\text{Tissue area } (\mu m \wedge 2)}$$

Data for 5α-reductase 1 and 5α-reductase 2 in normal prostate, hyperplasia, tumor, epithelium and stroma of prostate section were evaluated by a board-certified veterinary pathologist for cell type positivity in samples. Immunohistochemistry and *in situ* hybridization data are from a single experiment for each biomarker.

Statistical Analysis

Data were analyzed using SAS 9.3 (SAS Institute Inc., Cary, NC) with $p<0.05$ considered statistically significant. Ki-67, androgen receptor and apoptosis expression in normal prostate, hyperplasia and tumor, most common and most severe lesion scores were analyzed using ANOVA with Fisher's Least Significant Difference (LSD).

Results

Cell proliferation in prostates of finasteride and dutasteride treated TRAMP mice

Representative staining for Ki-67 in normal prostate, hyperplasia and tumor, and their annotated images are shown in Figure 4.1. There were no significant differences in Ki-67 expression in normal prostate, hyperplasia or tumor across treatment groups both with GU weight less than 1 gram and greater than 1 gram (Table 4.1). In mice with GU weight greater than 1 gram, there was a significant increase in Ki-67 expression in hyperplasia compared to normal prostate and tumor of the Post-Finasteride and

Post-Dutasteride groups (Table 4.1). There was a significant increase in Ki-67 expression in hyperplasia of the control and Post-Dutasteride groups with GU weight greater than 1 gram compared to respective groups of mice with GU weight less than 1 gram (Table 4.1).

Apoptosis in prostates of finasteride and dutasteride treated TRAMP mice

Representative staining for apoptosis in normal prostate, hyperplasia and tumor, and their annotated images are shown in Figure 4.2. There was a significant increase in apoptosis in normal prostate of the control compared to Pre-Finasteride, Post-Finasteride, and Pre-Dutasteride groups of mice with GU weight less than 1 gram (Table 4.2). Apoptosis was significantly increased in tumor of the Pre-Dutasteride group compared to the control, Post-Finasteride and Post-Dutasteride groups with GU weight less than 1 gram. In mice with GU weight less than 1 gram, there was a significantly higher rate of apoptosis in hyperplasia compared to normal prostate of the Pre-Finasteride, Post-Finasteride and Post-Dutasteride groups (Table 4.2). A significant increase in apoptosis was observed in tumor compared to normal prostate and hyperplasia of the Pre-Finasteride group of mice with GU weight greater than 1 gram. Apoptosis was significantly increased in normal prostate and hyperplasia of the Pre-Dutasteride group with GU weight greater than 1 gram compared to mice with GU weight less than 1 gram (Table 4.2). There was also a significant increase in apoptosis of the Pre-Finasteride and Post-Finasteride groups with GU weight greater than 1 gram compared to respective groups of mice with GU weight less than 1 gram.

Androgen receptor expression in prostates of finasteride and dutasteride treated TRAMP mice

Representative staining for androgen receptor in normal prostate, hyperplasia and tumor, and their annotated images are shown in Figure 4.3. Androgen receptor expression was significantly increased in hyperplasia compared to normal prostate of the control and Pre-Dutasteride groups with GU weight less than 1 gram (Table 4.3). There was a significant increase in androgen receptor expression in hyperplasia compared to tumor of the control, Pre-Finasteride and Post-Finasteride, and Pre-Dutasteride

groups with GU weight less than 1 gram. A significant increase in androgen receptor expression was seen in hyperplasia compared to normal prostate of the Post-Finasteride group with GU weight greater than 1 gram. There was a significant increase in androgen receptor expression in normal prostate compared to tumor of the Pre-Finasteride, Post-Finasteride and Post-Dutasteride groups with GU weight greater than 1 gram. In mice with GU weight greater than 1 gram, there was a significant increase in androgen receptor expression in hyperplasia compared to tumor of the control, Pre-Finasteride, Post-Finasteride, and Post-Dutasteride groups. There was also a significant decrease in androgen receptor expression in hyperplasia of the Pre-Finasteride group compared to other treatment groups (Table 4.3). A significant increase in androgen receptor expression in hyperplasia and a significant decrease in expression in tumor were observed in the Post-Dutasteride group with GU weight greater than 1 gram compared to mice with GU weight less than 1 gram (Table 4.3).

5α-reductase 1 and 5α-reductase 2 in prostates of finasteride and dutasteride treated TRAMP mice

Representative staining for 5α-reductase 1 and 5α-reductase 2 in normal prostate, hyperplasia and tumor, and their annotated images are shown in Figure 4.4. The percent positive for 5α-reductase 1 and 5α-reductase 2 was high and expressed similarly in normal prostate and hyperplasia, but higher than the percent positive in tumor of mice with GU weight less than 1 gram, and lower than the percent positive in tumor of mice with GU weight greater than 1 gram (Table 4.4). 5α-reductase 1 was more frequently expressed in prostate epithelium compared to stroma. 5α-reductase 2 was expressed equally in prostate epithelium and stroma.

Most severe and most common lesion scores in 8 to 20-week-old TRAMP mice

The raw and adjusted mean most severe and most common lesion scores for the anterior and dorsal lobes were significantly increased in 20-week-old mice versus 8, 12 and 16-week-old mice (Table 4.5 and 4.6). The raw and adjusted mean most severe and most common lesion scores for the lateral and ventral lobes were significantly increased in 16 and 20-week-old mice versus 8 and 12-week-old mice.

The adjusted mean most common lesion score for the dorsal lobe was significantly increased in 16-week-old mice versus 12-week-old mice.

Most common lesion histopathological distribution in 8 to 20-week-old TRAMP mice

Low-grade PIN as the most common lesion was significantly increased in the anterior lobe in 8-week-old mice versus 12 and 20-week-old mice (Table 4.7). Moderate-grade PIN as the most common lesion was significantly increased in the anterior lobe in 12-week-old mice versus 8, 16 and 20-week-old mice. Moderate-grade PIN as the most common lesion was significantly increased in the dorsal lobe in 8 and 12-week-old mice versus 16 and 20-week-old mice. Moderate-grade PIN as the most common lesion was significantly increased in the ventral lobe in 8,12 and 16-week-old mice versus 20-week-old mice. High-grade PIN as the most common lesion was significantly increased in the dorsal lobe in 16 and 20-week-old mice versus 8 and 12-week-old mice. Poorly differentiated carcinoma and prostate cancer as the most common lesions were significantly increased in the anterior and dorsal lobes in 20-week-old mice versus 8, 12 and 16-week-old mice. Poorly differentiated carcinoma and prostate cancer as the most common lesions were significantly increased in the lateral and ventral lobes in 20-week-old mice versus 16-week-old mice. Poorly differentiated carcinoma and prostate cancer as the most common lesions were significantly increased in the lateral and ventral lobes in 16 and 20-week-old mice versus 8 and 12-week-old mice.

Most severe lesion histopathological distribution in 8 to 20-week-old TRAMP mice

Low-grade PIN as the most severe lesion was significantly increased in the anterior lobe in 8-week-old mice versus 12 and 20-week-old mice (Table 4.8). Low-grade PIN as the most severe lesion was significantly increased in the ventral lobe in 8-week-old mice versus 16 and 20-week-old mice. Moderate-grade PIN as the most severe lesion was significantly increased in the lateral lobe in 8 and 12-week-old mice versus 16 and 20-week-old mice. Moderate-grade PIN as the most severe lesion was significantly increased in the ventral lobe in 8-week-old mice versus 12, 16 and 20-week-old mice. High-grade PIN as the most severe lesion was significantly increased in the lateral lobe in 12 and 16-week-

old mice versus 8 and 20-week-old mice. High-grade PIN as the most severe lesion was significantly increased in the ventral lobe in 12-week-old mice versus 8 and 20-week-old mice. High-grade PIN as the most severe lesion was significantly increased in the dorsal lobe in 12 and 16-week-old mice versus 20-week-old mice. Poorly differentiated carcinoma and prostate cancer as the most severe lesions were significantly increased in the anterior lobe in 20-week-old mice versus 8, 12 and 16-week-old mice. Poorly differentiated carcinoma and prostate cancer as the most severe lesions were significantly increased in the dorsal lobe in 20-week-old mice versus 8, 12 and 16-week-old mice. Poorly differentiated carcinoma and prostate cancer as the most severe lesions were significantly increased in the dorsal lobe in 16-week-old mice versus 8 and 12-week-old mice. Poorly differentiated carcinoma and prostate cancer as the most severe lesions were significantly increased in the lateral and ventral lobe in 16 and 20-week-old mice versus 8 and 12-week-old mice.

Cell proliferation in prostates of 8 to 20-week-old TRAMP mice

There was a significant increase in Ki-67 expression in hyperplasia compared to normal prostate and tumor of 20-week-old mice (Table 4.9). There was a significant decrease in Ki-67 expression in normal prostate and hyperplasia in 16 and 20-week-old mice compared to 8-week-old mice (Table 4.9).

Apoptosis in prostates of 8 to 20-week-old TRAMP mice

There was a significant increase in apoptosis in hyperplasia compared to normal prostate in 8-week-old mice (Table 4.9). There was a significant increase in apoptosis in tumor compared to normal prostate in 20-week-old mice.

Androgen receptor expression in prostates of 8 to 20-week-old TRAMP mice

There was a significant increase in androgen receptor expression in normal prostate and hyperplasia compared to tumor in 12 and 20-week-old mice (Table 4.9). There was a significant increase in androgen receptor expression in hyperplasia compared to normal prostate and tumor in 16-week-old mice.

5α-reductase 1 and 5α-reductase 2 expression in prostates of 8 to 20-week-old TRAMP mice

The percent positive for 5α-reductase 1 and 5α-reductase 2 was higher in hyperplasia compared to normal prostate and tumor, and higher in normal prostate compared to tumor (Table 4.10). 5α-reductase 1 was predominantly expressed in prostate epithelium compared to stroma while 5α-reductase 2 was highly expressed in both prostate epithelium and stroma.

Discussion

TRAMP mice with GU weight less than 1 gram had mostly low to high-grade PIN and may represent men at the early stages of prostate cancer development, while mice with GU weight greater than 1 gram had mostly poorly differentiated carcinoma and may represent men with advanced stage prostate cancer. Cell proliferation in normal prostate, hyperplasia and tumor were not significantly different from each other in all groups with GU weight less than 1 gram, which may suggest that for this study, proliferation was not out of control in the GU weight less than 1 gram groups. The significantly higher apoptosis in hyperplasia compared to normal prostate and tumor of Post-Finasteride and Post-Dutasteride groups with GU weight greater than 1 gram suggests that post-treatments may not be effective in inhibiting proliferation in hyperplasia, and may rather facilitate large tumor formation. The significant increase in Ki-67 expression in hyperplasia of the control and Post-Dutasteride groups with GU weight greater than 1 gram compared to respective groups with GU weight less than 1 gram suggests that a loss of proliferation control in hyperplasia may lead to large tumors in these groups. In previous research, finasteride did not increase proliferative changes in rat prostate [35], or had no effect on proliferation in human prostate [36], and dutasteride increased proliferation in human prostate cancer [37].

Apoptosis was generally low, or almost nonexistent, in majority of prostates in treatment groups. Finasteride and dutasteride treatments decreased apoptosis, mostly nonsignificantly in mice tumors compared to normal prostate or hyperplasia. The significant increase in apoptosis in tumor compared to normal prostate and hyperplasia of the Pre-Finasteride group with GU weight greater than 1 gram

suggests Pre-Finasteride treatment could slow cancer development by increasing apoptosis in hyperplastic cells. Also, the significant increase in apoptosis in tumor of the Pre-Dutasteride group compared to the control, Post-Finasteride and Post-Dutasteride groups with GU weight less than 1 gram suggests Pre-Dutasteride treatment could slow the progression of cancer by inducing apoptosis in tumor of mice with GU weight less than 1 gram. Other studies found finasteride decreased apoptosis in Dunning prostate R3327-H rat tumor [38] while dutasteride increased apoptosis in LPB-Tag mice dorsolateral [39] and human [40] prostate.

The high expression of androgen receptor in normal prostate and hyperplasia may promote large tumor formation, and once tumor is established, androgen receptor expression is downregulated and may not be very critical in tumor development. Androgen receptor expression was decreased in tumor compared to hyperplasia in most groups. This observation is consistent with previous research that found androgen receptor expression to be seldom increased in primary prostate cancer [41,42]. The weak androgen receptor expression in tumors is consistent with weak androgen receptor staining in majority of human mild differentiated and poorly differentiated prostate cancer [43,44]. This may suggest that androgen receptor is not primarily required to stimulate growth and development of prostate at this stage, and that prostate cancer may bypass the androgen receptor pathway partially or entirely via other cellular pathways. Finasteride treatments significantly reduced androgen receptor expression in small tumors. In large tumors, finasteride and Post-Dutasteride treatments significantly reduced androgen receptor expression. In other studies, finasteride significantly decreased epithelial androgen receptor expression but stromal androgen receptor expression was unchanged in human prostate tissues [45]. Amplification of androgen receptor gene following finasteride treatment has also been reported in androgen independent human prostate cancer [46].

To the best of our knowledge, we are the first to determine 5α-reductase 1 and 5α-reductase 2 mRNA expression in TRAMP mice. 5α-reductase 1 was predominantly expressed in prostate epithelium, while 5α-reductase 2 was highly expressed in both prostate epithelium and stroma as has been previously

reported in human prostate [47]. Though qualitative, results suggest that there is a loss of 5α-reductase expression in small tumors, while tumors with increased expression might be more prone to becoming large and poorly differentiated carcinoma. Both finasteride and dutasteride treatments may decrease 5α-reductase enzymes in mice with smaller tumors, and prove ineffective in mice with larger tumors. The results in mice tumor with GU weight less than 1 gram cancer are similar to studies that found finasteride reduced 5α-reductase activity in rat ventral prostate [48], while dutasteride decreased 5α-reductase 1 and 5α-reductase 2 activities in LPB-Tag mice dorsolateral prostate [39].

In the AIN-93G-fed TRAMP mice, most mice at 8 weeks of age had developed low- to high-grade PIN as the most common and most severe lesions in all lobes, as was also observed in 8-week-old TRAMP mice in a study by Kaplan-Lefko and colleagues [33]. TRAMP mice are known to develop pathological features similar to low-grade PIN as early as 4 to 6 weeks of age [49]. Most mice had developed moderate- and high-grade PIN as the most common and most severe lesions at 12 and 16 weeks, as has been previously reported [33]. Phyllodes-like tumor was not detected in any lobe between 8 to 20 weeks of age. Moderately differentiated adenocarcinoma was observed at 20 weeks in all lobes and presented only a low percentage (0-4%) of the total pathology of the prostate, both observations seen previously [33]. The low incidence of moderately differentiated adenocarcinoma may suggest that it was the transitional stage between PIN and prostate cancer development. Most mice had developed poorly differentiated carcinoma at 20 weeks as the most common and most severe lesion as has been reported previously [49]. In addition, poorly differentiated carcinoma was not observed in any lobe until 12 weeks of age, and incidence of prostate cancer was higher in 20-week-old mice compared to 16-week-old mice. Overall, there was a low incidence of PIN, and a high incidence of poorly differentiated carcinoma and prostate cancer as the most severe and most common lesions in 20-week-old TRAMP mice, similar to results seen previously [34,50]. These results in addition to those from this study, differ with the high incidence of PIN, and low incidence of poorly differentiated carcinoma and prostate cancer

as the most severe and most common lesions in 20-week-old TRAMP mice reported previously [31], and this discrepancy could be due to the small sample size used in this study.

Cell proliferation increased with age in normal prostate and hyperplasia of TRAMP mice. Similarly, in another study, the proliferation index in the AH tumors of 3FloxT mice increased incrementally as age increased. On the contrary, the percentage of Ki-67 positive cells in the AH tumor regions in 3PEKOT mice was not significantly changed at 8 and 12 weeks of age, but was significantly decreased at 18 and 24 weeks of age [51]. Cell proliferation may increase in hyperplasia with increasing age to promote cancer formation, as was observed in 16 and 20-week-old mice. The low rate of cell proliferation in tumors could be due to cells having become necrotic and thus limiting blood supply to cells to stimulate proliferation.

Apoptosis in normal prostate, hyperplasia or tumor in TRAMP mice was not significantly affected by age. Others have reported that apoptotic index did not significantly change at different ages in 4-5, 7-9, and 10-14 month-old PSA-Cre;Pten-loxP/+ mice prostate [52]. This, in addition to our results, suggest that increased apoptosis occurred at the early stages of tumor development. On the contrary, others found ageing in mice induced apoptosis in ventral prostate [53]. The higher apoptosis in hyperplasia compared to tumor in our study, is consistent with elevated apoptosis in preneoplastic lesions in a previous study [54], and this may prevent prostate cancer development.

There was a marked decrease in androgen receptor expression in all tumors compared to normal prostate and hyperplasia. In other studies, there was a decrease in androgen receptor staining intensity as a function of age in rat ventral lobe, but the staining intensity increased in the dorsal and lateral lobes with age [55]. The loss of androgen receptor expression in tumors may be due to them bypassing androgen receptor pathway for growth, or a reduction in the stability of androgen receptor protein that decreases the androgen receptor protein level to one difficult to detect immunohistologically [16]. In humans, epigenetic silencing of androgen receptor expression by methylation has been observed in 8% of primary prostate cancers [56]. In our study, the increase in androgen receptor expression in

hyperplasia could promote prostate cancer development. Androgen receptor expression in normal prostate, hyperplasia and tumor did not increase with age in 8 to 20-week-old mice which suggests that androgen receptor levels do not vary during the different stages of PIN and prostate cancer development.

The decreased 5α-reductase 1 and 5α-reductase 2 expression in 8 to 20-week-old mice tumor suggests that in this age group, both isoenzymes may be downregulated by age or during prostate cancer development. The decreased 5α-reductase 1 expression in tumor contrasts with what has been reported previously [5-8], where 5α-reductase 1 was increased in prostate cancer. It is too early to draw any conclusions from 5α-reductase qualitative results, hence quantifying expression levels will help determine how age, and finasteride and dutasteride treatments changed the expression prolife of 5α-reductase isoenzymes to alter cytologic and architectural features of TRAMP mice prostate.

Conclusions

Our results suggest that formation of large genitourinary tract is influenced more by cell proliferation, rather than androgen receptor or apoptosis in tumor, indicating that in large lesions, proliferation is most crucial and this imbalance between proliferation, apoptosis and androgen receptor may be responsible for the development of large tumors. The timing of finasteride and dutasteride treatments may be critical in decreasing proliferation and androgen receptor expression, and increasing apoptosis in normal prostate, hyperplasia and tumor to prevent prostate cancer in TRAMP mice. Mice age may not be significantly important in regulating proliferation, androgen receptor and apoptosis to promote tumor growth.

Table 4.1 Quantitative immunohistochemical expression of Ki-67 in finasteride and dutasteride treated TRAMP mice. The values are the mean total Ki-67 positive cells per tissue area (μm^2) ± SEM in normal prostate, hyperplasia or tumor.

TRAMP mice with genitourinary weight less than 1 gram				
Group	n	Prostate	Hyperplasia	Tumor
Control	5	0.2 ± 0.2	0.2 ± 0.1	0.07 ± 0.05
Pre-Finasteride	5	0.4 ± 0.2	1.2 ± 0.9	0.2 ± 0.2
Post-Finasteride	5	0.3 ± 0.2	1.1 ± 0.5	0.2 ± 0.2
Pre-Dutasteride	5	0.5 ± 0.3	1.4 ± 0.7	0.01 ± 0.0
Post-Dutasteride	5	1.1 ± 0.7	0.7 ± 0.3	0.07 ± 0.07
TRAMP mice with genitourinary weight greater than 1 gram				
Control	4	0.6 ± 0.6	2.1 ± 0.5*	0.6 ± 0.4
Pre-Finasteride	4	0.7 ± 0.7	1.9 ± 1.0	0.4 ± 0.1
Post-Finasteride	4	0.0 ± 0.0[1]	2.2 ± 0.0[2]	0.4 ± 0.1[1]
Pre-Dutasteride	2	0.0 ± 0.0	0.0 ± 0.0	0.5 ± 0.4
Post-Dutasteride	4	0.0 ± 0.0[1]	2.7 ± 0.5*,[2]	0.6 ± 0.3[1]

$p<0.05$ *vs.* normal prostate, hyperplasia and tumor within group (numbers), and genitourinary weight less than 1 gram compared to greater than 1 gram (asterisk).

Table 4.2 Quantitative immunohistochemical expression of apoptosis in finasteride and dutasteride treated TRAMP mice. The values are the mean total apoptosis positive cells per tissue area (μm^2) ± SEM in normal prostate, hyperplasia or tumor.

TRAMP mice with genitourinary weight less than 1 gram				
Group	n	Prostate	Hyperplasia	Tumor
Control	5	0.4 ± 0.3^{a}	0.3 ± 0.06	0.1 ± 0.08^{a}
Pre-Finasteride	5	$0.0 \pm 0.0^{b,1}$	0.4 ± 0.06^{1}	$0.2 \pm 0.2^{a,b,1,2}$
Post-Finasteride	5	$0.0 \pm 0.0^{b,1}$	0.3 ± 0.1^{2}	$0.01 \pm 0.01^{a,1}$
Pre-Dutasteride	5	0.0 ± 0.0^{b}	0.5 ± 0.2	1.0 ± 0.7^{b}
Post-Dutasteride	5	$0.05 \pm 0.05^{a,b,1}$	0.5 ± 0.2^{2}	$0.1 \pm 0.1^{a,1,2}$
TRAMP mice with genitourinary weight greater than 1 gram				
Control	4	0.0 ± 0.0^{a}	0.7 ± 0.3^{a}	0.9 ± 0.4
Pre-Finasteride	4	$0.0 \pm 0.0^{a,1}$	$0.2 \pm 0.1^{a,1}$	$1.1 \pm 0.3^{*,2}$
Post-Finasteride	4	0.0 ± 0.0^{a}	0.0 ± 0.0^{a}	$0.3 \pm 0.1^{*}$
Pre-Dutasteride	2	$0.5 \pm 0.0^{b*}$	$3.5 \pm 0.0^{b*}$	0.9 ± 0.2
Post-Dutasteride	4	0.08 ± 0.08^{a}	0.4 ± 0.4^{a}	0.4 ± 0.1

$p<0.05$ *vs.* normal prostate, hyperplasia and tumor within group (numbers), across groups (letters), and genitourinary weight less than 1 gram compared to greater than 1 gram (asterisk).

Table 4.3 Quantitative immunohistochemical expression of androgen receptor in finasteride and dutasteride treated TRAMP mice. The values are the mean total androgen receptor positive cells per tissue area (μm^2) ± SEM in normal prostate, hyperplasia or tumor.

TRAMP mice with genitourinary weight less than 1 gram				
Group	n	Prostate	Hyperplasia	Tumor
Control	5	5.2 ± 0.5^{1}	$9.6 \pm 0.4^{a,2}$	4.4 ± 4.4^{1}
Pre-Finasteride	5	6.8 ± 0.5^{1}	$7.0 \pm 0.7^{b,1}$	1.7 ± 1.5^{2}
Post-Finasteride	5	7.5 ± 1.2^{1}	$9.1 \pm 0.8^{a,1}$	0.01 ± 0.01^{2}
Pre-Dutasteride	5	5.7 ± 0.8^{1}	$9.1 \pm 0.9^{a,2}$	2.9 ± 2.9^{1}
Post-Dutasteride	5	5.7 ± 1.4	$7.9 \pm 0.3^{a,b}$	5.4 ± 0.0
TRAMP mice with genitourinary weight greater than 1 gram				
Control	4	$8.3 \pm 2.2^{1,2}$	8.8 ± 1.5^{2}	2.1 ± 1.5^{1}
Pre-Finasteride	4	7.3 ± 0.9^{1}	8.8 ± 0.9^{1}	0.4 ± 0.2^{2}
Post-Finasteride	4	6.8 ± 0.0^{1}	9.4 ± 0.0^{2}	0.2 ± 0.1^{3}
Pre-Dutasteride	2	9.8 ± 0.0	8.9 ± 0.0	1.5 ± 1.4
Post-Dutasteride	4	8.8 ± 0.7^{1}	$9.9 \pm 0.7^{*,1}$	$0.7 \pm 0.5^{*,2}$

$p<0.05$ *vs.* normal prostate, hyperplasia and tumor within group (numbers), across groups (letters), and genitourinary weight less than 1 gram compared to greater than 1 gram (asterisk).

Table 4.4 Qualitative *in situ* hybridization expression of 5α-reductase 1 and 5α-reductase 2 in finasteride and dutasteride treated TRAMP mice. The values are the number of prostate sections from the total number of prostate sections within that group positive for 5α-reductase 1 or 5α-reductase 2 in normal prostate, hyperplasia, tumor, prostate epithelia or stroma, and expressed as a percent in parenthesis.

TRAMP mice with genitourinary weight less than 1 gram											
		5α-reductase 1					5α-reductase 2				
Group	n	Prostate (%)	Hyperplasia (%)	Tumor (%)	Prostate epithelia (%)	Prostate stroma (%)	Prostate (%)	Hyperplasia (%)	Tumor (%)	Prostate epithelia (%)	Prostate stroma (%)
Control	5	5 (100%)	5 (100%)	1 (20%)	5 (100%)	0 (0%)	5 (100%)	5 (100%)	1 (20%)	5 (100%)	5 (100%)
Pre-Finasteride	5	4 (80%)	4 (80%)	2 (40%)	4 (80%)	0 (0%)	3 (60%)	4 (80%)	2 (40%)	5 (100%)	5 (100%)
Post-Finasteride	5	5 (100%)	4 (80%)	2 (40%)	3 (60%)	0 (0%)	4 (80%)	3 (60%)	0 (0%)	5 (100%)	5 (100%)
Pre-Dutasteride	5	3 (60%)	3 (60%)	2 (40%)	2 (40%)	0 (0%)	3 (60%)	3 (60%)	3 (60%)	4 (100%)	4 (100%)
Post-Dutasteride	5	4 (80%)	5 (100%)	0 (0%)	5 (100%)	0 (0%)	3 (60%)	3 (60%)	0 (0%)	3 (60%)	4 (80%)
TRAMP mice with genitourinary weight greater than 1 gram											
Control	4	3 (75%)	3 (75%)	4 (100%)	3 (75%)	0 (0%)	2 (50%)	2 (50%)	4 (100%)	2 (50%)	2 (50%)
Pre-Finasteride	4	3 (75%)	3 (75%)	4 (100%)	3 (75%)	0 (0%)	3 (75%)	3 (75%)	4 (100%)	3 (75%)	3 (75%)
Post-Finasteride	4	1 (25%)	1 (25%)	4 (100%)	1 (25%)	0 (0%)	1 (25%)	1 (25%)	4 (100%)	1 (25%)	1 (25%)
Pre-Dutasteride	2	1 (50%)	2 (100%)	2 (100%)	2 (100%)	1 (50%)	2 (100%)	2 (50%)	2 (100%)	2 (100%)	2 (100%)
Post-Dutasteride	4	3 (75%)	3 (75%)	4 (100%)	3 (75%)	1 (25%)	2 (50%)	2 (50%)	4 (100%)	2 (50%)	2 (50%)

Table 4.5 Raw and adjusted mean most severe lesion scores for the anterior, dorsal, lateral, and ventral prostate lobes (n = 5–12)[1].

	Anterior prostate		Dorsal prostate		Lateral prostate		Ventral prostate	
Group	**Raw**	**Adjusted**	**Raw**	**Adjusted**	**Raw**	**Adjusted**	**Raw**	**Adjusted**
8-weeks	2.10 ± 0.28[a]	4.10 ± 0.86[a]	2.50 ± 0.17[a]	6.10 ± 0.38[a]	1.90 ± 0.10[a]	4.80 ± 0.47[a]	1.60 ± 0.16[a]	4.30 ± 0.63[a]
12-weeks	2.56 ± 0.13[a]	6.13 ± 0.30[a]	3.00 ± 0.29[a]	7.38 ± 0.81[a]	3.00 ± 0.41[a]	7.50 ± 1.15[a]	1.56 ± 0.27[a]	3.56 ± 0.67[a]
16-weeks	2.39 ± 0.31[a]	5.78 ± 0.95[a]	3.78 ± 0.42[a]	10.17 ± 1.39[a]	5.17 ± 0.50[b]	14.44 ± 1.62[b]	4.83 ± 0.59[b]	13.66 ± 1.87[b]
20-weeks	4.92 ± 0.51[b]	14.21 ± 1.65[b]	5.63 ± 0.43[b]	16.33 ± 1.38[b]	5.42 ± 0.51[b]	15.88 ± 1.62[b]	4.86 ± 0.61[b]	14.18 ± 1.93[b]

[1]Data are mean ± SEM; values with different letters are statistically different from one another (p<0.05).

Table 4.6 Raw and adjusted mean most common lesion scores for the anterior, dorsal, lateral, and ventral prostate lobes (n = 5–12)[1].

	Anterior prostate		Dorsal prostate		Lateral prostate		Ventral prostate	
Group	**Raw**	**Adjusted**	**Raw**	**Adjusted**	**Raw**	**Adjusted**	**Raw**	**Adjusted**
8-weeks	1.30 ± 0.21[a]	2.70 ± 0.58[a]	2.00 ± 0.00[a]	5.20 ± 0.13[a,b]	1.50 ± 0.17[a]	3.70 ± 0.65[a]	1.60 ± 0.16[a]	4.30 ± 0.63[a]
12-weeks	1.81 ± 0.14[a]	4.44 ± 0.41[a]	2.00 ± 0.00[a]	5.50 ± 0.26[a]	1.63 ± 0.13[a]	4.25 ± 0.46[a]	1.25 ± 0.21[a]	3.13 ± 0.62[a]
16-weeks	1.83 ± 0.34[a]	4.56 ± 1.01[a]	3.22 ± 0.50[a]	9.39 ± 1.49[b]	4.11 ± 0.63[b]	11.94 ± 1.93[b]	4.22 ± 0.60[b]	12.28 ± 1.87[b]
20-weeks	4.83 ± 0.53[b]	14.04 ± 1.69[b]	4.75 ± 0.50[b]	14.00 ± 1.55[c]	5.21 ± 0.52[b]	15.25 ± 1.67[b]	4.77 ± 0.63[b]	14.09 ± 1.96[b]

[1]Data are mean ± SEM; values with different letters are statistically different from one another (p<0.05).

Table 4.7 Histopathological analysis (most common lesion) of individual prostate lobes in 8-20-week-old AIN-93G-fed TRAMP mice[1, 2].

		Prostatic intraepithelial neoplasia			Adenocarcinoma			Prostate cancer
	n	**LG**	**MG**	**HG**	**WD**	**MD**	**PD**	**(WD-PD)**
Anterior prostate								
8-weeks	5	80%^{a}	10%^{a}	10%	0%	0%	0%^{a}	0%^{a}
12-weeks	8	25%^{b,c}	69%^{b}	6%	0%	0%	0%^{a}	0%^{a}
16-weeks	9	50%^{a,b}	39%^{a}	6%	0%	0%	6%^{a}	6%^{a}
20-weeks	12	13%^{c}	21%^{a}	8%	0%	4%	54%^{b}	58%^{b}
Dorsal prostate								
8-weeks	5	0%	100%^{a}	0%^{a}	0%	0%	0%^{a}	0%^{a}
12-weeks	8	0%	100%^{a}	0%^{a}	0%	0%	0%^{a}	0%^{a}
16-weeks	9	0%	67%^{b}	11%^{b}	0%	0%	22%^{b}	22%^{a}
20-weeks	12	0%	38%^{b}	8%^{c}	0%	4%	50%^{c}	54%^{b}
Lateral prostate								
8-weeks	5	50%	50%	0%	0%	0%	0%^{a}	0%^{a}
12-weeks	8	38%	63%	0%	0%	0%	0%^{a}	0%^{a}
16-weeks	9	11%	44%	0%	0%	0%	44%^{b}	44%^{b}
20-weeks	12	17%	8%	8%	0%	4%	63%^{c}	67%^{c}
Ventral prostate								
8-weeks	5	40%	60%^{a}	0%	0%	0%	0%^{a}	0%^{a}
12-weeks	8	25%	50%^{a}	0%	0%	0%	0%^{a}	0%^{a}
16-weeks	9	0%	56%^{a}	0%	0%	0%	44%^{b}	44%^{b}
20-weeks	12	17%	8%^{b}	0%	0%	4%	54%^{c}	58%^{c}

[1]Values with different letters are statistically different from one another (p<0.05).
[2]LG = low-grade, MG = moderate-grade, HG = high-grade, PIN = prostatic intraepithelial neoplasia, WD = well-differentiated, MD = moderately differentiated, PD = poorly differentiated.

Table 4.8 Histopathological analysis (most severe lesion) of individual prostate lobes in 8-20-week-old AIN-93G-fed TRAMP mice[1, 2].

		Prostatic intraepithelial neoplasia			Adenocarcinoma			Prostate cancer
	n	**LG**	**MG**	**HG**	**WD**	**MD**	**PD**	**(WD-PD)**
Anterior prostate								
8-weeks	5	30%^{a}	30%	40%	0%	0%	0%^{a}	0%^{a}
12-weeks	8	0%^{b}	44%	56%	0%	0%	0%^{a}	0%^{a}
16-weeks	9	17%^{a,b}	50%	28%	0%	0%	6%^{a}	6%^{a}
20-weeks	12	8%^{b}	8%	17%	0%	4%	54%^{b}	58%^{b}
Dorsal prostate								
8-weeks	5	0%	50%	50%^{a,b}	0%	0%	0%^{a}	0%^{a}
12-weeks	8	0%	25%	69%^{a}	0%	0%	6%^{a}	6%^{a}
16-weeks	9	0%	11%	67%^{a}	0%	0%	22%^{b}	22%^{b}
20-weeks	12	0%	17%	13%^{b}	0%	4%	67%^{c}	71%^{c}
Lateral prostate								
8-weeks	5	10%	90%^{a}	0%^{a}	0%	0%	0%^{a}	0%^{a}
12-weeks	8	0%	50%^{b}	38%^{b}	0%	0%	13%^{a}	13%^{b}
16-weeks	9	0%	6%^{c}	39%^{b}	0%	0%	56%^{b}	56%^{c}
20-weeks	12	17%	4%^{c}	8%^{a}	0%	4%	67%^{b}	71%^{d}
Ventral prostate								
8-weeks	5	40%^{a}	60%^{a}	0%^{a}	0%	0%	0%^{a}	0%^{a}
12-weeks	8	13%^{a,b}	44%^{b}	18.75%^{b}	0%	0%	0%^{a}	0%^{a}
16-weeks	9	0%^{b}	39%^{b}	5.6%^{a,b}	0%	0%	56%^{b}	56%^{b}
20-weeks	12	8%^{b}	17%^{c}	0%^{a}	0%	4%	54%^{b}	58%^{c}

[1]Values with different letters are statistically different from one another (p<0.05).
[2]LG = low-grade, MG = moderate-grade, HG = high-grade, PIN = prostatic intraepithelial neoplasia, WD = well-differentiated, MD = moderately differentiated, PD = poorly differentiated.

Table 4.9 Quantitative immunohistochemical expression of Ki-67, apoptosis and androgen receptor in 8, 12, 16 and 20-week-old TRAMP mice. The values are the mean total androgen receptor, Ki-67 or apoptosis positive cells per tissue area (μm^2) ± SEM in normal prostate, hyperplasia or tumor.

Genitourinary weight from 8 to 20 weeks										
		Cell proliferation (Ki-67)			Apoptosis			Androgen receptor		
Group	n	Prostate	Hyperplasia	Tumor	Prostate	Hyperplasia	Tumor	Prostate	Hyperplasia	Tumor
8-weeks	5	1.6 ± 0.5^{a}	3.3 ± 0.9^{a}	---	0.0 ± 0.0^{1}	0.4 ± 0.1^{2}	---	5.9 ± 1.1	7.1 ± 0.7	---
12-weeks	5	$1.1 \pm 0.4^{a,b}$	$1.6 \pm 0.6^{a,b}$	0.5 ± 0.0	0.0 ± 0.0	0.8 ± 0.5	0.1 ± 0.0	7.9 ± 0.6^{1}	8.5 ± 0.2^{1}	0.1 ± 0.0^{2}
16-weeks	5	0.3 ± 0.3^{b}	0.5 ± 0.4^{b}	0.2 ± 0.1	0.0 ± 0.0	0.5 ± 0.2	0.2 ± 0.02	6.7 ± 0.5^{1}	9.3 ± 0.9^{2}	3.9 ± 0.2^{1}
20-weeks	5	$0.3 \pm 0.2^{b,1}$	$1.2 \pm 0.2^{b,2}$	0.2 ± 0.09^{1}	0.0 ± 0.0^{1}	$0.1 \pm 0.05^{1,2}$	0.2 ± 0.07^{2}	7.5 ± 1.2^{1}	9.2 ± 1.3^{1}	1.5 ± 0.8^{2}

$p<0.05$ *vs.* normal prostate, hyperplasia and tumor within group (numbers) and across groups (letters).

Table 4.10 Qualitative *in situ* hybridization expression of 5α-reductase 1 and 5α-reductase 2 in 8, 12, 16 and 20-week-old TRAMP mice. The values are the number of prostate sections from the total number of prostate sections within that group positive for 5α-reductase 1 or 5α-reductase 2 in normal prostate, hyperplasia, tumor, prostate epithelia or stroma, and expressed as a percent in parenthesis.

		5α-reductase 1					**5α-reductase 2**				
Group	n	Prostate (%)	Hyperplasia (%)	Tumor (%)	Prostate epithelia (%)	Prostate stroma (%)	Prostate (%)	Hyperplasia (%)	Tumor (%)	Prostate epithelia (%)	Prostate stroma (%)
8-weeks	5	3 (60%)	5 (100%)	1 (20%)	5 (100%)	0 (0%)	4 (80%)	4 (80%)	0 (0%)	4 (80%)	4 (80%)
12-weeks	5	4 (80%)	5 (100%)	4 (80%)	5 (100%)	0 (0%)	4 (80%)	5 (100%)	3 (60%)	5 (100%)	5 (100%)
16-weeks	5	2 (40%)	4 (80%)	1 (20%)	5 (100%)	0 (0%)	1 (20%)	4 (80%)	2 (40%)	5 (100%)	5 (100%)
20-weeks	5	3 (60%)	3 (60%)	3 (60%)	3 (60%)	1 (20%)	3 (60%)	3 (60%)	4 (80%)	3 (60%)	3 (60%)

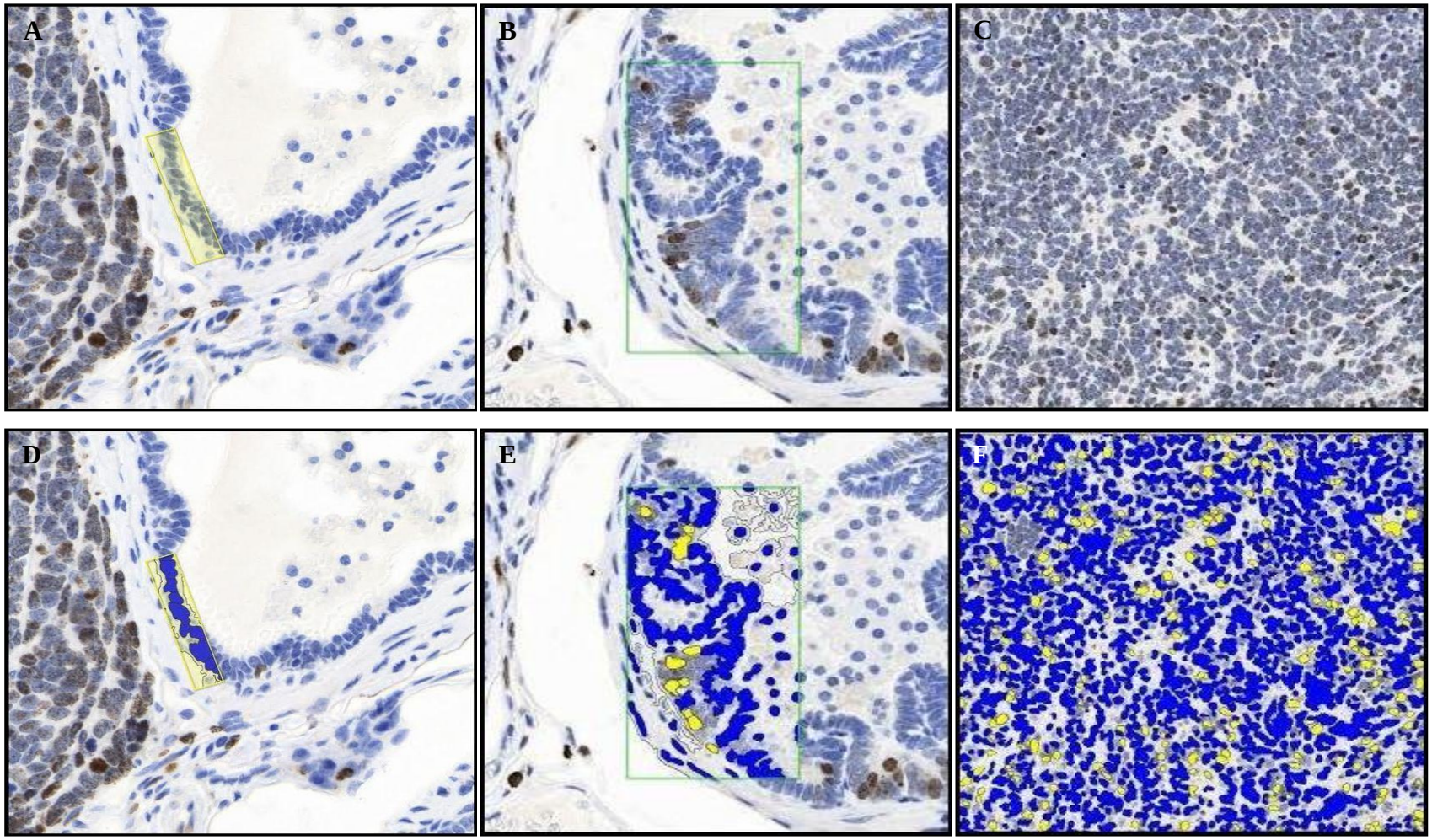

Figure 4.1 Representative staining for Ki-67 in (A) normal prostate showing single layer of cells, (B) hyperplasia showing cells with lost polarity and piled up on one another, and (C) tumor showing diffuse sheets of cells with no organization and characterized by neoplastic cellular characteristics. The rectangular boxes within the different tissue specific cell types are representative sections that were selected by a board-certified veterinary pathologist and digitized (annotated) with Halo software to identify and quantify Ki-67 immunopositive staining in (E) normal prostate, (F) hyperplasia and (G) tumor.

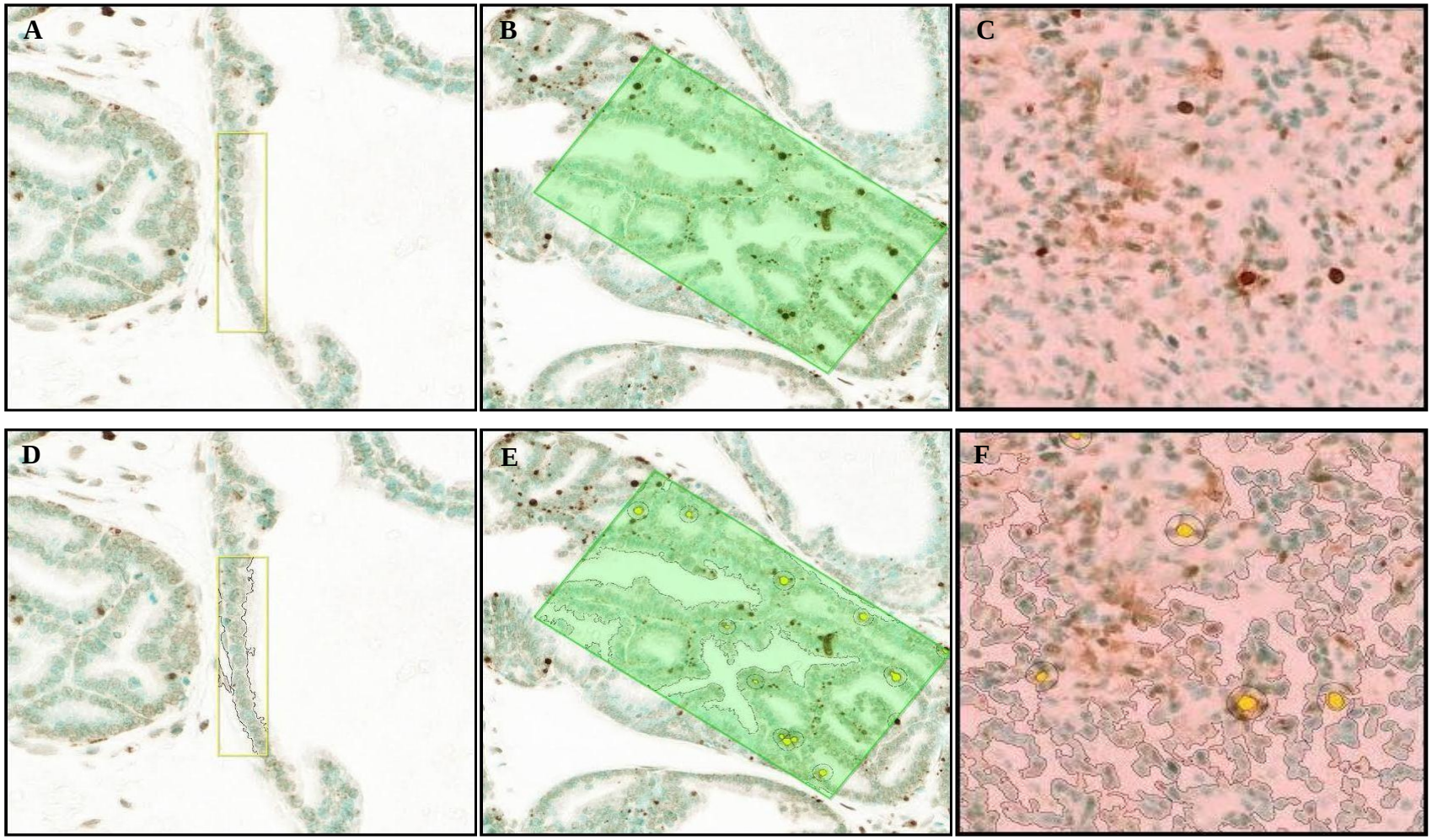

Figure 4.2 Representative TUNEL staining in (A) normal prostate showing single layer of cells, (B) hyperplasia showing cells with lost polarity and piled up on one another, and (C) tumor showing diffuse sheets of cells with no organization and characterized by neoplastic cellular characteristics. The rectangular boxes within the different tissue specific cell types are representative sections that were selected by a board-certified veterinary pathologist and digitized (annotated) with Halo software to identify and quantify TUNEL immunopositive staining in (E) normal prostate, (F) hyperplasia and (G) tumor.

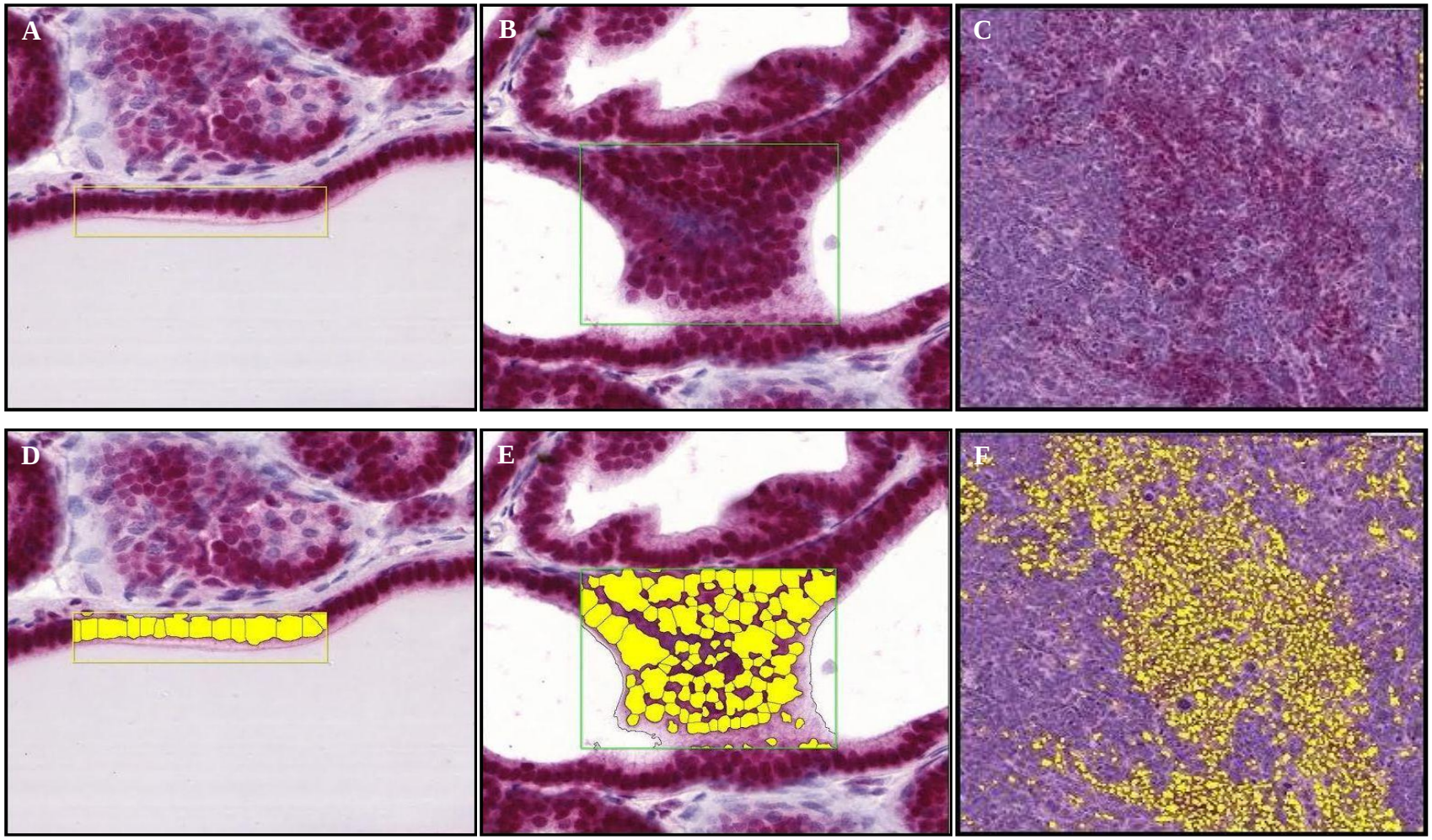

Figure 4.3 Representative staining for androgen receptor in (A) normal prostate showing single layer of cells, (B) hyperplasia showing cells with lost polarity and piled up on one another, and (C) tumor showing diffuse sheets of cells with no organization and characterized by neoplastic cellular characteristics. The rectangular boxes within the different tissue specific cell types are representative sections that were selected by a board-certified veterinary pathologist and digitized (annotated) with Halo software to identify and quantify androgen receptor immunopositive staining in (E) normal prostate, (F) hyperplasia and (G) tumor.

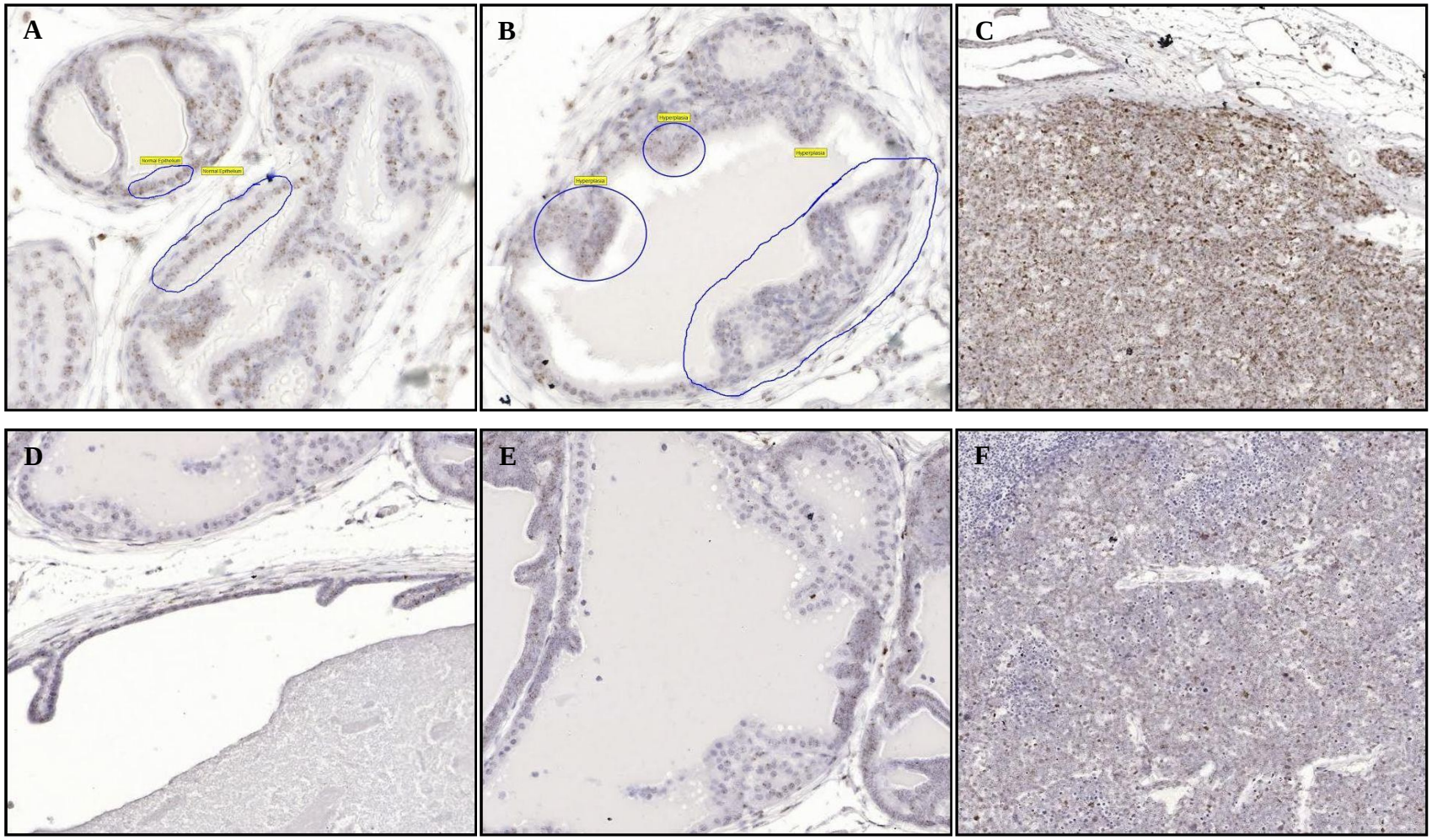

Figure 4.4 Representative staining for 5α-reductase 1 mRNA and for 5α-reductase 2 mRNA (A and D, respectively) in normal prostate showing single layer of cells, (B and E, respectively) hyperplasia showing cells with lost polarity and piled up on one another, and (C and F, respectively) tumor showing diffuse sheets of cells with no organization and characterized by neoplastic cellular characteristics. The circles and ovals within select tissues are representative sections showing 5α-reductase 1 mRNA staining.

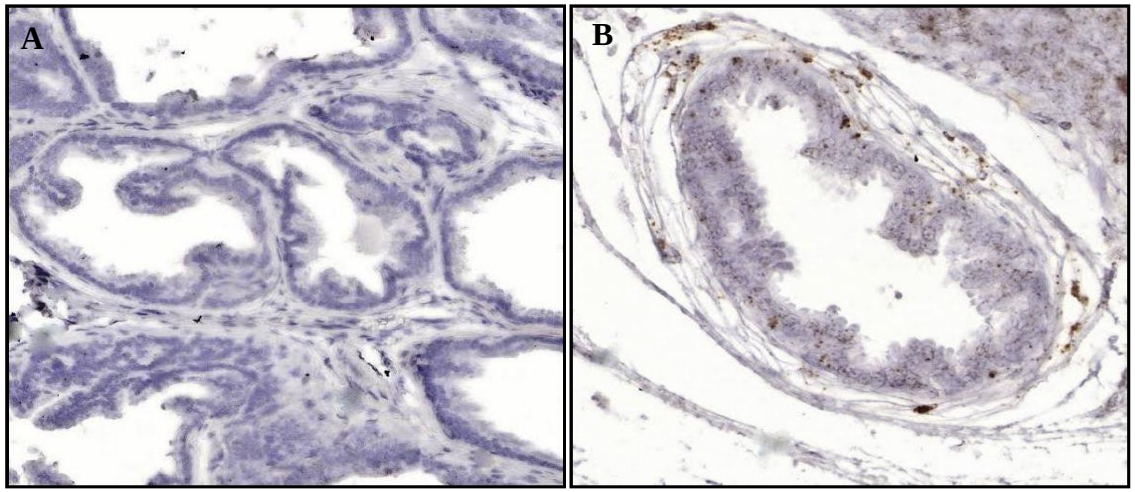

Figure 4.5 Representative staining for 5α-reductase 1 (A) and 5α-reductase 2 (B) mRNA in prostate stroma which is composed of smooth muscle cells, fibroblasts, myofibroblasts, endothelial cells and immune cells.

References

1. American Cancer Society. Cancer facts and figures 2015.

2. Tien AH, Sadar MD. Androgen-responsive gene expression in prostate cancer progression. In: Androgen-responsive genes in prostate cancer. Springer. 2013;135-153.

3. Andriole GL, Roehrborn C, Schulman C, Slawin KM, Somerville M et al. Effect of dutasteride on the detection of prostate cancer in men with benign prostatic hyperplasia. Urology. 2004;64(3):537-541.

4. Grossmann ME, Huang H, Tindall DJ. Androgen receptor signaling in androgen-refractory prostate cancer. J Natl Cancer Inst. 2001;93(22):1687–1697.

5. Luo J, Dunn TA, Ewing CM, Walsh PC, Isaacs WB. Decreased gene expression of steroid 5α-reductase 2 in human prostate cancer: implications for finasteride therapy of prostate carcinoma. Prostate. 2003;57(2):134-139.

6. Titus MA, Gregory CW, Ford OH, Schell MJ, Maygarden SJ, et al. Steroid 5α-reductase isozymes I and II in recurrent prostate cancer. Clin Cancer Res. 2005;11(12):4365-4371.

7. Söderström TG, Bjelfman C, Brekkan E, Ask B, Egevad L, et al. Messenger ribonucleic acid levels of steroid 5α-reductase 2 in human prostate predict the enzyme activity. J Clin Endocrinol Metab. 2001;86(2):855-858.

8. Bjelfman C, Söderström TG, Brekkan E, Norlén BJ, Egevad L, et al. Differential gene expression of steroid 5α-reductase 2 in core needle biopsies from malignant and benign prostatic tissue. J Clin Endocrinol Metab, 1997;82(7):2210-2214.

9. Iehlé C, Radvanyi F, de Medina SGD, Ouafik LH, Gérard H, et al. Differences in steroid 5α-reductase iso-enzymes expression between normal and pathological human prostate tissue. J Steroid Biochem Mol Biol.1999;68(5):189-195.

10. Nakamura Y, Suzuki T, Nakabayashi M, Endoh M, Sakamoto K, et al. In situ androgen producing enzymes in human prostate cancer. Endocr Relat Cancer. 2005;12(1):101-107.

11. Uemura M, Tamura K, Chung S, Honma S, Okuyama A, et al. Novel 5α-steroid reductase (SRD5A3, type-3) is overexpressed in hormone-refractory prostate cancer. Cancer Sci. 2008;99(1):81-86.

12. Stanbrough M, Leav I, Kwan PW, Bubley GJ, Balk SP. Prostatic intraepithelial neoplasia in mice expressing an androgen receptor transgene in prostate epithelium. Proc Natl Acad Sci U S A. 2001;98(19):10823-10828.

13. Dahlman KB, Parker JS, Shamu T, Hieronymus H, Chapinski C, et al. Modulators of prostate cancer cell proliferation and viability identified by short-hairpin RNA library screening. PLoS One. 2012;7(4):e34414.

14. Culig Z, Hobisch A, Bartsch G, Klocker H. Androgen receptor - an update of mechanisms of action in prostate cancer. Urol Res. 2000;28(4):211-219.

15. Koivisto P, Kolmer M, Visakorpi T, Kallioniemi OP. Androgen receptor gene and hormonal therapy failure of prostate cancer. Am J Pathol. 1998;152(1):1-9.

16. Heinlein CA, Chang C. Androgen receptor in prostate cancer. Endocr Rev. 2004;25(2):276-308.

17. Dicker AP, Merrick G, Gomella L, Valicenti RK, Waterman F. Basic and advanced techniques in prostate brachytherapy. CRC Press. 2005.

18. Isaacs JT. Antagonistic effect of androgen on prostatic cell death. Prostate. 1984;5(5):545-557.

19. Balk SP. AR, the cell cycle, and prostate cancer. Nucl Recept Signal. 2008;6:e001.

20. Niu Y, Xu Y, Zhang J, Bai J, Yang H, et al. Proliferation and differentiation of prostatic stromal cells. BJU Int. 2001;87(4):386-393.

21. Kim IY, Zelner DJ, Sensibar JA, Ahn HJ, Park L, et al. Modulation of sensitivity to transforming growth factor-beta 1 (TGF-beta 1) and the level of type II TGF-beta receptor in LNCaP cells by dihydrotestosterone. Exp Cell Res. 1996;222(1):103-110.

22. Andreeff M, Goodrich DW, Pardee AB. Cell proliferation, differentiation, and apoptosis. Holland-Frei Cancer Medicine. 2000:17-32.

23. Heber D. Prostate enlargement: the canary in the coal mine? Am J Clin Nutr. 2002;75(4):605-606.

24. Sellers K, Fox MP, Bousamra M, Slone SP, Higashi RM, et al. Pyruvate carboxylase is critical for non-small-cell lung cancer proliferation. J Clin Invest. 2015;125(2):687-698.

25. Wong RS. Apoptosis in cancer: from pathogenesis to treatment. J Exp Clin Cancer Res. 2011;30(1):87.

26. Khan N, Adhami VM, Mukhtar H. Apoptosis by dietary agents for prevention and treatment of prostate cancer. Endocr Relat Cancer. 2010;17(1):R39-R52.

27. Bayraktar S. The Mechanism of androgen deprivation and the androgen receptor. Open Prost Cancer J. 2010;3:47-56.

28. Thompson IM, Goodman PJ, Tangen CM, Lucia MS, Miller GJ, et al. The influence of finasteride on the development of prostate cancer. N Engl J Med. 2003;349(3):215-224.

29. Andriole GL, Bostwick DG, Brawley OW, Gomella LG, Marberger M, et al. Effect of dutasteride on the risk of prostate cancer. N Engl J Med. 2010;362(13):1192-1202.

30. Fleshner NE. Dutasteride and active surveillance of low-risk prostate cancer. Lancet. 2012;379(9826):1590.

31. Opoku-Acheampong AB, Unis D, Henningson JN, Beck AP, Lindshield BL. Preventive and therapeutic efficacy of finasteride and dutasteride in TRAMP mice. 2013;8:e77738.

32. Gingrich JR, Barrios RJ, Kattan MW, Nahm HS, Finegold MJ, et al. Androgen-independent prostate cancer progression in the TRAMP model. Cancer Res. 1997;57(21):4687-4691.

33. Kaplan-Lefko PJ, Chen TM, Ittmann MM, Barrios RJ, Ayala GE, et al. Pathobiology of autochthonous prostate cancer in a pre-clinical transgenic mouse model. Prostate. 2003;55(3):219-237.

34. Berman-Booty LD, Sargeant AM, Rosol TJ, Rengel RC, Clinton SK, et al. A review of the existing grading schemes and a proposal for a modified grading scheme for prostatic lesions in TRAMP mice. Toxicol Pathol. 2012;40(1):5–17.

35. Prahalada SR, Keenan KP, Hertzog PR, Gordon LR, Peter CP, et al. Qualitative and quantitative evaluation of prostatic histomorphology in rats following chronic treatment with finasteride, a 5-alpha reductase inhibitor. Urology. 1994;43(5):680-685.

36. Glassman DT, Chon JK, Borkowski A, Jacobs SC, Kyprianou N. Combined effect of terazosin and finasteride on apoptosis, cell proliferation, and transforming growth factor-beta expression in benign prostatic hyperplasia. Prostate. 2001;46:45-51.

37. Gleave M, Qian J, Andreou C, Pommerville P, Chin J, Casey R, et al. The effects of the dual 5α-reductase inhibitor dutasteride on localized prostate cancer–results from a 4-month pre-radical prostatectomy study. Prostate. 2006 66(15):1674–1685.

38. Canene-Adams K, Lindshield BL, Wang S, Jeffery EH, Clinton SK, et al. Combinations of tomato and broccoli enhance antitumor activity in Dunning R3327-H prostate adenocarcinomas. Cancer Res. 2007;67(2):836-843.

39. Shao TC, Li H, Ittmann M, Cunningham GR. Effects of dutasteride on prostate growth in the large probasin-large T antigen mouse model of prostate cancer. J Urol. 2007;178(4 pt 1):1521-1527.

40. Andriole GL, Humphrey P, Ray P, Gleave ME, Trachtenberg J, et al. Effect of the dual 5α-reductase inhibitor dutasteride on markers of tumor regression in prostate cancer. J Urol. 2004;172(3):915-919.

41. Visakorpi T, Hyytinen E, Koivisto P, Tanner M, Keinänen R, et al. In vivo amplification of the androgen receptor gene and progression of human prostate cancer. Nat Genet. 1995;9(4):401-406.

42. Koivisto P, Kononen J, Palmberg C, Tammela T, Hyytinen E, et al. Androgen receptor gene amplification: a possible molecular mechanism for androgen deprivation therapy failure in prostate cancer. Cancer Res. 1997;57(2):314-319.

43. Pienta KJ, Abate-Shen C, Agus DB, Attar RM, Chung LW, et al. The current state of preclinical prostate cancer animal models. Prostate. 2008;68(6):629-639.

44. Morgenbesser S, McLaren R, Richards B, Zhang M, Akmaev V, Winter S, et al. Identification of genes potentially involved in the acquisition of androgen-independent and metastatic tumor growth in an autochthonous genetically engineered mouse prostate cancer model. Prostate. 2007;67:83-106.

45. Bauman TM, Sehgal PD, Johnson KA, Pier T, Bruskewitz RC, et al. Finasteride treatment alters tissue specific androgen receptor expression in prostate tissues. Prostate. 2014;74(9):923–932.

46. Palmberg C, Koivisto P, Hyytinen E, Isola J, Visakorpi T, et al. Androgen receptor gene amplification in a recurrent prostate cancer after monotherapy with the nonsteroidal potent antiandrogen Casodex (bicalutamide) with a subsequent favorable response to maximal androgen blockade. Eur Urol. 1997;31(2):216-219.

47. Shirakawa T, Okada H, Acharya B, Zhang Z, Hinata N, et al. Messenger RNA levels and enzyme activities of 5 alpha-reductase types 1 and 2 in human benign prostatic hyperplasia (BPH) tissue. Prostate. 2004;58(1):33-40.

48. George FW, Russell DW, Wilson JD. Feed-forward control of prostate growth: dihydrotestosterone induces expression of its own biosynthetic enzyme, steroid 5α-reductase. Proc Natl Acad Sci U S A. 1991;88(18):8044-8047.

49. Gingrich JR, Barrios RJ, Foster BA, Greenberg NM. Pathologic progression of autochthonous prostate cancer in the TRAMP model. Prostate Cancer Prostatic Dis. 1999;2(2):70-75.

50. Zuniga KE, Clinton SK, Erdman JW Jr. The interactions of dietary tomato powder and soy germ on prostate carcinogenesis in the TRAMP model. Cancer Prev Res (Phila). 2013;6(6):548-557.

51. Tien JC, Liao L, Liu Y, Liu Z, Lee DK, et al. The steroid receptor coactivator-3 is required for developing neuroendocrine tumor in the mouse prostate. Int J Biol Sci. 2014 ;10(10):1116-1127.

52. Ma X, Ziel-van der Made AC, Autar B, van der Korput HA, Vermeij M, et al. Targeted biallelic inactivation of Pten in the mouse prostate leads to prostate cancer accompanied by increased epithelial cell proliferation but not by reduced apoptosis. Cancer Res. 2005;65(13):5730-5739.

53. Jara M, Carballada R, Esponda P. Age-induced apoptosis in the male genital tract of the mouse. Reproduction. 2004;127(3):359-366.

54. James SJ, Muskhelishvili L, Gaylor DW, Turturro A, Hart R. Upregulation of apoptosis with dietary restriction: implications for carcinogenesis and aging. Environ Health Perspect. 1998;106 Suppl 1:307-312.

55. Banerjee PP, Banerjee S, Brown TR. Increased androgen receptor expression correlates with development of age-dependent, lobe-specific spontaneous hyperplasia of the brown Norway rat prostate. Endocrinology. 2001 Sep;142(9):4066-4075.

56. Sasaki M, Tanaka Y, Perinchery G, Dharia A, Kotcherguina I, et al. Methylation and inactivation of estrogen, progesterone, and androgen receptors in prostate cancer. J Natl Cancer Inst. 2002;94(5):384-390.

Chapter 5-Summary and future directions

In Chapter 2, saw palmetto supplements treatments caused a notable, but nonsignificant reduction in the difference between the left and right flank organ areas in the testosterone-treated SPS groups. The same level of inhibition was not seen in the dihydrotestosterone-treated SPS groups. This study was unable to answer the question about which fatty acid or phytosterol compounds and their concentrations are responsible for the growth-inhibitory effect of saw palmetto supplements in androgen-sensitive LNCaP cells and Syrian hamster flank organs. *In vitro* results suggest the high medium-chain fatty acids-low phytosterols was most effective in decreasing LNCaP cell number, while *in vivo* results suggest the high long-chain fatty acids-low phytosterols saw palmetto supplement may be the most promising supplement for inhibiting the growth of androgen-sensitive flank organ of Syrian hamsters in response to androgen treatment. Future studies should determine which saw palmetto supplements bioactive components and/or their synergistic relationship are responsible for the supplements growth-inhibitory potential on Syrian hamster androgen-sensitive flank organs. This could be done by basing the saw palmetto supplement concentration not only on total fatty acids, but on total phytosterols only, and on both fatty acids and phytosterols, and then test their efficacy on androgen-sensitive prostate cancer cells and prostate cancer animal model. Additionally, increasing the sample size of saw palmetto supplement groups, and animals could lead to outcomes of the study becoming significant. Immunohistochemistry and *in situ* hybridization should be performed on the flank organs of the Syrian hamsters to determine cancer biomarkers (5α-reductase 1, 5α-reductase 2, androgen receptor, Ki-67 and apoptosis) to determine why saw palmetto supplements reduced the difference between the left and right flank organ growth more in the testosterone-treated SPS groups more than the dihydrotestosterone (DHT)-treated SPS groups. Results from these studies would provide knowledge on the efficacy of fatty acids and phytosterols, and whether they are better at inhibiting the conversion of testosterone to DHT, or preventing binding of DHT to androgen receptors in androgen-sensitive tissues. If the efficacy of SPS is established in hamster models, supplements could be administered through diet to a more reliable prostate cancer model like the

transgenic adenocarcinoma of the mouse prostate (TRAMP) mice to determine their efficacy in inhibiting prostate cancer development. Since TRAMP mice mimic the progressive development of prostate cancer in humans, results from this study will provide evidence about the potential of saw palmetto supplements in decreasing prostate cancer growth in humans.

In Chapter 3, the Post-Dutasteride group showed the greatest inhibition of prostatic intraepithelial neoplasia progression and prostate cancer development. The Post-Dutasteride group showed improved outcomes compared with the Pre-Dutasteride group, which had increased incidence of high-grade adenocarcinoma as the most common and most severe lesions in a majority of prostate lobes. There was little benefit from the finasteride diets, and they increased the incidence of high-grade adenocarcinoma. Future studies should determine the effect of finasteride and dutasteride on TRAMP mice prostate cancer beyond the 20-week termination to determine the effect on prostate cancer metastasis. This study will simulate the effect of these 5α-reductase inhibitors on growth of metastasized prostate cancer in men. Also, the body weight–scaled human oral dose of finasteride and dutasteride was approximately 80 mg/day, which is higher than the dutasteride (0.5 mg/day) and finasteride (5 mg/day) doses that most men take. Scaling down these doses used in animal studies to levels administered in men should mimic the effect of these drugs in men.

In Chapter 4, this study determined the molecular changes in TRAMP mice from a previous study [1] to elucidate the discordant response in the Pre-Dutasteride and both finasteride groups and determine why Post-Dutasteride treatment was more effective. The cell-type specific expression patterns of 5α-reductase 1 and 5α-reductase 2 using *in situ* hybridization; and androgen receptor, cell proliferation and apoptosis using immunohistochemistry were determined in formalin-fixed, paraffin-embedded tissue sections of finasteride and dutasteride treated TRAMP mice prostates. . The percent positive for 5α-reductase 1 and 5α-reductase 2 was high and expressed similarly in normal prostate and hyperplasia, but higher than the percent positive in tumor of mice with GU weight less than 1 gram, and lower than the percent positive in tumor of mice with GU weight greater than 1 gram. There was a decrease in 5α-

reductase 1 and 5α-reductase mRNA expression in tumor compared to normal prostate and hyperplasia in 8 to 20-week-old TRAMP mice. These are qualitative results, therefore future studies should focus on annotating and quantifying 5α-reductase 1 and 5α-reductase mRNA expression in these mice to better understand how their levels vary in finasteride- and dutasteride-treated TRAMP mice, and at different ages and stages of prostate carcinogenesis. These results could provide evidence on the efficacy of finasteride and dutasteride in decreasing early stage prostate cancer (GU weights less than 1 gram), and advanced stage prostate cancer (GU weights greater than 1 gram). Quantifying expression in 8 to 20-week-old TRAMP mice would establish the levels to which 5α-reductase isoenzymes are expressed in tumors as mice age, and this knowledge could be used to develop 5α-reductase inhibitors to preventively or therapeutically inhibit prostate cancer growth in men at various ages and stages of prostate cancer development. Also, studying the effect of 5α-reductase inhibitors in a model (e.g. PSP94/tag mouse model) in which prostate cancer originates from an epithelial origin [2,3] rather than neuroendocrine (e.g. TRAMP mice) [4-6] will provide results replicable to that seen in the epithelial regions of human prostate cancer.

References

1. Opoku-Acheampong AB, Unis D, Henningson JN, Beck AP, Lindshield BL. Preventive and therapeutic efficacy of finasteride and dutasteride in TRAMP mice. 2013;8:e77738.

2. Kas K, Finger E, Grall F, Gu X, Akbarali Y, et al. ESE-3, a novel member of an epithelium-specific ets transcription factor subfamily, demonstrates different target gene specificity from ESE-1. J Biol Chem. 2000;275(4):2986-2998.

3. Oettgen P, Kas K, Dube A, Gu X, Grall F, et al. Characterization of ESE-2, a novel ESE-1-related Ets transcription factor that is restricted to glandular epithelium and differentiated keratinocytes. J Biol Chem. 1999;274(41):29439-29452.

4. Ahmad I, Sansom OJ, Leung HY. Advances in mouse models of prostate cancer. Expert Rev Mol Med. 2008;10:e16.

5. Kasper S, Smth JA Jr. Genetically modified mice and their use in developing therapeutic strategies for prostate cancer. J Urol. 2004;172(1):12-19.

6. Klein RD. The use of genetically engineered mouse models of prostate cancer for nutrition and cancer chemoprevention research. Mutat Res. 2005;576(1-2):111-119.